Evaluation of the Impact of Large-Scale Taxiway Maintenance on the Task Load of Ground Controllers

Master of Science Thesis

Sander Poelstra

TU Delft

Evaluation of the Impact of Large-Scale Taxiway Maintenance on the Task Load of Ground Controllers

Master of Science Thesis

by

Sander Poelstra

to obtain the degree of Master of Science
at the Delft University of Technology,
to be defended publicly on Tuesday 25 February 2025 at 13:00.

Student number:	4719573	
Project duration:	March 2024 – February 2025	
Thesis committee:	Dr.ir. C. Borst	(TU Delft, Chairman)
	Dr. O.A. Sharpanskykh	(TU Delft, Supervisor)
	M.F. von der Burg	(TU Delft, Supervisor)
	Ir. O. Stroosma	(TU Delft, External examiner)
	F. Dijkstra	(LVNL, Company supervisor)

Cover: Sunset at Schiphol Airport by Photography Air Traffic Control the Netherlands (LVNL)

An electronic version of this thesis is available at http://repository.tudelft.nl/.

TU Delft

Acknowledgements

This master thesis marks the end of my student time at the Delft University of Technology. I experienced this time as an challenging yet rewarding experience, and I'm very grateful for the development I made throughout the years.
For this master thesis, I would like to pay my gratitude to my thesis supervisors Alexei Sharpanskykh and Malte von der Burg. I really appreciated their continuous support and valuable insights for my project. Furthermore, I would like to pay my gratitude to my company supervisor Ferdinand Dijkstra. His expertise in the Air Traffic Management field, and his provision of fast support has really helped me throughout this research. Also, I would like to pay my gratitude to Steven Kempen for being my company supervisor for the first part of my thesis, and for making me familiar with taxiway maintenance. Additionally, I would like to pay my gratitude to Marco van der Park and Martijn Potuijt for their insights and advice regarding controller decision-making. Their help have been really appreciated.
Lastly, I want to express my appreciation to my parents, sister and friends for supporting me throughout this study. I'm grateful that I have received the chance to work on this project, and I have enjoyed it very much. I'm excited for the new challenges to come.

Sander Poelstra
Delft, January 2025

Contents

List of Figures

List of Tables

List of Abbreviations

A-CDM	Airport Collaborative Decision Making
AAS	Amsterdam Airport Schiphol
ACC	Area Control Center
ACGT	Actual Commence of Ground Handling
ADEP	Aerodrome Of Departure
AIBT	Actual In-Block Time
ALCMS	Airfield Lighting Control & Monitoring System
ALDT	Actual Landing Time
AOBT	Actual Off-Block Time
APC	Apron Planning & Control
APP	Approach
ARDT	Actual Ready for Departure Time
ASDE	Airport Surface Detection Equipment
ASRT	Actual Start-Up Request Time
ASTRA	Airport Surveillance Tracker
ATC	Air Traffic Control
ATM	Air Traffic Management
ATOT	Actual Take Off Time
BOS	Baanonderhoudsstrategie (Runway Maintenance Strategy)
CAT	Category
CTOT	Calculated Take Off Time
CTR	Controlled Traffic Region
DC	Declared Capacity
EDD	Electronic Data Display
EFSS	Electronic Flight Strip System
EOBT	Estimated Off-Block Time
FAA	Federal Aviation Administration
FIR	Flight Information Region
FMA	Flow Manager Aircraft
GA	General Aviation

GC	Ground Control
GU	Guidance Unit
ICAO	International Civil Aviation Organisation
IFR	Instrument Flight Rules
KNMI	Koninklijk Nederlands Meteorologisch Instituut (Royal Netherlands Meteorological Institute)
LVNL	Luchtverkeersleiding Nederland (Air Traffic Control the Netherlands)
MAASMO-sim	Multi-Agent Airport Surface Movement Operations simulator
MAPF	Multi-Agent Path Finding
MAS	Multi-Agent System
MTOW	Maximum Take Off Weight
OPL	Outbound Planner
R/T	Radio Telephony
RC	Runway Controller
RMO	Runway Mode of Operation
ROT	Runway Occupancy Time
RSG	Royal Schiphol Group
RVR	Runway Visual Range
RWY	Runway
SID	Standard Instrument Departures
SIMP	Safe Interval Motion Planning
SIPP	Safe Interval Path Planning
SUP	Tower Supervisor
TAR	Terminal Area Surveillance Radar
TMA	Terminal Manoeuvring Area
TOBT	Target Off-Block Time
TSAT	Target Start Up Approval Time
TWR	Tower
TWR-C	Schiphol Tower Centre
TWR-W	Schiphol Tower West
TWY	Taxiway
UFMC	Unmanned Follow-Me Cars

Introduction

At Royal Schiphol Group, maintenance strategies are being developed to plan maintenance more optimally and efficiently for the longer term. Such a strategy has already been drawn up for the runways, but not yet for the taxiway network at Schiphol [13]. Normally, taxiway maintenance is conducted based on technical necessity, meaning that only the performance of the taxiway itself is included. Now, when drawing up a taxiway maintenance strategy, the impact on ground operations is also considered to ensure more optimal and efficient maintenance plans. To include these ground operations when planning taxiway maintenance, the impact of taxiway maintenance on different operational indicators is investigated first. There are different operational indicators that could potentially be affected by taxiway maintenance, including taxi time and taxi distance. Another important indicator that is also of interest is the workload experienced by ground controllers, which could potentially be impacted by resulting changes in flows because of taxiway maintenance. It is essential to study these operational indicators to prevent shifting of maintenance works. Therefore, several operational indicators have already been studied in relation to taxiway maintenance, including taxi time and taxi distance [57]. However, no research has yet been done on the relation between taxiway maintenance and workload experienced by ground controllers.

This master thesis was set-up to research the missing insight of the impact of taxiway maintenance on the workload of ground controllers. Furthermore, this research was done at the Knowledge & Development Center Mainport Schiphol, where data and resources from both Royal Schiphol Group and Air Traffic Control the Netherlands were provided. This was beneficial for the project, as both maintenance specialists and operational experts were involved, making the project multidisciplinary. Although both parties have interest in this project, the interests go beyond those of the specialists, as the improved understanding of the relationship between maintenance and workload could lead to more efficient ground operations, benefiting all involved.

This report contains all components of the master thesis, structured into three parts. In part I, the scientific paper of this master thesis is presented. Then, in part II, the supporting Literature Study for this research is presented. Lastly, in part III, additional supporting work for this report is presented.

I

Scientific Paper

Evaluation of the Impact of Large-Scale Taxiway Maintenance on the Task Load of Ground Controllers

Sander Poelstra*

Delft University of Technology, Delft, The Netherlands

Abstract

At airports, taxiway maintenance is a complex task affecting airport ground operations, specifically airport surface movement operations managed by ground controllers. It is expected that taxiway maintenance also affects the task load experienced by ground controllers. However, to our best knowledge, no studies were performed so far to quantify and assess this influence. To fill this gap, this research studies the impact of taxiway maintenance on the task load of ground controllers. It is essential to develop this understanding to ensure that taxiway maintenance is planned safely, efficiently, and robustly. This research uses Schiphol Airport as a use case, for which an existing airport surface movement simulator was used to model the ground traffic with a single-agent trajectory planning algorithm. To realistically represent the traffic patterns at Amsterdam Schiphol Airport, the simulated model was calibrated using real trajectory data and expert opinion. To quantify the task load of ground controllers, the well-known Dynamic Density model and a novel measure, based on controller's mental re-plannings, were used and compared to each other. Based on a maintenance scenario, simulations were performed for two runway configurations, with the aim to study the differences in task load between the nominal and maintenance scenario for different flight schedules. The main outcome of this analysis is that conflicting flows, resulting from taxiway maintenance, have a significant contribution to the task load of ground controllers. It was further found that the effects of these conflicts on the task load are localized and do not propagate further to other areas, and other ground controllers who do not have responsibility over the specific area in question do not experience this impact in task load.

1 Introduction

At airports, surface movement operations are constantly exposed to various disturbances. Such events include runway reconfigurations, gate re-plannings, and technical failures of taxiing aircraft [1]. A particular event type that occurs regularly and affects movements at the airport is taxiway maintenance. This event causes aircraft to follow routes different from standard taxiway routes, depending on runway configurations. There are different types of taxiway maintenance, with large-scale maintenance being the most impactful because ground movements are affected for the longest period compared to other types of maintenance. Adopting changed ground movements for this duration affects several operational indicators, such as aircraft taxi speed, aircraft taxi distance, and aircraft taxi time. Another important indicator affected by these changes in ground movements is the workload of ground controllers [2] because the emergence of different traffic flows results in controllers responding differently on these flows, which is expected to have an impact on the task load on these controllers. A ground controller is an air traffic controller responsible for all movements on the manoeuvring area, excluding available and inoperable runways and exits [3]. This includes providing Aerodrome control service, Flight information service and alerting service for aircraft, towing and vehicle movements [4]. Furthermore, one of the most important tasks of this controller is to prevent collisions involving aircraft on the airside surface, excluding the runways [5]. In addition, ground controllers are responsible for their own geographical region, called sectors [3]. Although this workload indicator is

*MSc Student, Sustainable Air Transport, Faculty of Aerospace Engineering, Delft University of Technology

considered relevant for planning maintenance, no maintenance models yet exist that take into account this indicator. Understanding the impact of taxiway maintenance on the workload of ground controllers is important because this indicator is strongly related to safety and ground capacity and these factors deteriorate if the workload becomes too high. Furthermore, a clear understanding of the relationship between workload and taxiway maintenance is essential for creating efficient and robust maintenance plannings [2].

In general, several studies have been done to accurately describe workload. From these studies, workload can be considered as a combination of task load and performer-based characteristics [6] [7] [8]. Performer-based characteristics include the effort and strategies applied to solve tasks, and can be considered subjective [9]. On the other hand, task load is expressed as the number of tasks that someone needs to complete [10], and can be considered objective [7]. In the context of taxiway maintenance, task load is mainly of interest as the changes in aircraft flows, because of taxiway maintenance, directly impact the tasks of the ground controller, but not directly the performer-based characteristics. This was obtained based on discussions with operational experts. Furthermore, nominal and maintenance scenarios can be compared objectively without performer interference, and this measure is more manageable than performer-based characteristics, which provides a better measure to be used for maintenance plannings. Limited studies have been conducted on modelling and evaluating air traffic controllers' task load, including for ground control, where research on assessing the task load is limited. One of the few examples is the study on the impact of sector splitting and merging on the task load of ground controllers [11]. Overall, no research has yet been done on the impact of taxiway maintenance on the ground controllers' task load.

The task load of a ground controller is largely determined by the traffic flows. These flows, in their turn, are strongly dependent on the runway configurations used [12]. Therefore, it is essential to study the impact of taxiway maintenance on the task load of ground controllers per runway configuration. As a result, the following research objective has been established for this study:
To model and evaluate the impact of large-scale taxiway maintenance on the task load of ground controllers for different runway configurations.
In the literature, different methods are used to model task load. These methods include administering questionnaires after human-in-the-loop experiments with controllers [13] and applying machine learning techniques based on historical data [11]. As these include having intensive sessions with controllers, they do not provide the flexibility and robustness necessary to simulate maintenance scenarios. Therefore, in this research, an approach based on fast-time simulations of airport surface movement operations was employed. The simulated model is based on a single-agent trajectory planning algorithm that plans individual paths for each aircraft on a graph representing the taxiway network of an airport. This method is considered flexible and robust, as it is able to simulate a great variety of operational and maintenance scenarios. The planning algorithm used is Single-Agent Motion Planning (SIMP) [14]. This algorithm is developed at the TU Delft, and is an extension on the Safe Interval Path Planning (SIPP) algorithm, which takes into account kinodynamic and shapes of aircraft and other ground vehicles and has proven to be most efficient compared to other planning algorithms [15] [16]. Based on the individual trajectories generated by SIMP, the task load is determined using two task load metrics. The first one is based on a variant of the Dynamic Density model created for Ground Control, which is a Linear Regression model consisting of multiple independent variables related to Dynamic Density, and is calibrated using Radio Telephony (RT) load [11]. Furthermore, this model is optimized to better represent real operations. The second metric is a new metric introduced in this research based on expert opinion, which aims to capture the number of re-plannings a ground controller makes to solve potential conflicts in a certain period of time. This metric is considered to measure qualitative aspects of task load, as the complexity of problem solving is considered. Furthermore, this metric aims to quantify cognitive task load, as this metric captures mental decision-making. On the other hand, Dynamic Density includes mainly quantitative aspects of task load, as this indicator better captures the management of multiple aircraft and situational monitoring [11]. Therefore, both metrics are used to provide a better overall indication of task load. In a nutshell, the re-planning metric quantifies the task load by considering the number of separation violations between aircraft in a certain period of time, as ground controllers should have solved these violations by re-planning them. The airport that is considered for evaluation is Amsterdam Airport Schiphol for a relevant taxiway maintenance scenario chosen based on discussions with taxiway maintenance experts. For this scenario, the task load of ground controllers was evaluated using the metrics introduced above.

This research paper has the following structure. First, in section 2, the case study of this research is presented. Hereafter, in section 3, the methodology of this research is described. Then, in section 4, verification of the implementation of the tool that measures re-plannings of ground controllers and the Dynamic Density model, and two validation steps are presented. In the first validation step, the paths generated by the SIMP algorithm are compared with real operational paths from ASTRA data, and in the second validation step, both task load measures are compared with each other. Next, in section 5, the experimental set-up for the simulations is provided. Then, in section 6, the results of this research are provided and discussed. Hereafter, in section 7, the overall discussion of this research is presented. Finally, in section 8, the conclusions of this research are presented, and recommendations are given for future work.

2 Case Study

In this research, the surface movement operation system that is under investigation is Amsterdam Airport Schiphol. This airport is considered as it contains a complex taxiway and runway layout [17], and has large traffic volumes [18]. Therefore, previous studies discussed that Schiphol Airport is a relevant airport to study task load, especially when conducting maintenance on key parts of the infrastructure [2] [11] [19].
At this airport, the part of the infrastructure where the impact of its closure is being studied is intersection A21B till taxiway C3, and is shown in Figure 1a together with the layout and main taxiway network. This main taxiway network consists of the taxiways Alpha, Bravo, Charlie, Delta, Quebec, Victor, Yankee, and Zulu. In Figure 1a, the main taxiways are coloured and the maintenance location is marked by a grey shaded area. Concerning the maintenance area, intersection A21B till taxiway C3 is considered as maintenance scenario because maintenance experts from Schiphol Airport indicated this as most interesting for their maintenance planning because this part is pushed forward to a later period each time for maintenance due to it being operationally infeasible. In Figure 1b, a close-up of this maintenance area is given by the purple transparent area including the surrounding and concerning taxiway names.

Furthermore, task load is measured per Ground Control sector. In this case, sectors are managed by ground controllers who are responsible for the traffic moving through them. These sectors are operationally flexible, meaning that the configuration of these sectors are dynamic [20]. However, for this research, the sectors are assumed static, meaning that these do not change throughout the research. This is done to disregard sector dynamics and primarily focus on the impact as a consequence of taxiway maintenance. These static sectors are given in Figure A.1 in Appendix A. In this research, only sectors Center, North and South are considered because sector West is not seen as a constraining sector regarding task load.

As the surface movement operations at Schiphol Airport are dynamic, large and complex [1], simplifications were made. The first simplification is that only movements of aircraft are considered in this research, as the used agent-based simulation model considered only aircraft. Secondly, aircraft depart and arrive based on the Actual Off-Block Time and Actual Landing Time given in the flight schedules to accurately model historical events. Thirdly, aircraft follow standard taxiway directions as much as possible to accurately model representative surface movement operations. Lastly, aircraft departing from and arriving at gates above the black dotted flow split line given in Figure 1a travel via the north to and from the Polder (36L/18R) and Zwanenburg (36C/18C) Runway, and aircraft departing from and arriving at gates below the black dotted flow split line travel via the south to and from the Polder and Zwanenburg Runway. This last simplification is made based on discussions with operational experts.

3 Methodology

In this part, the methodology of this research is provided. This is done by first giving an overview in subsection 3.1. Then, in the following parts, the different methods used in this research are discussed.

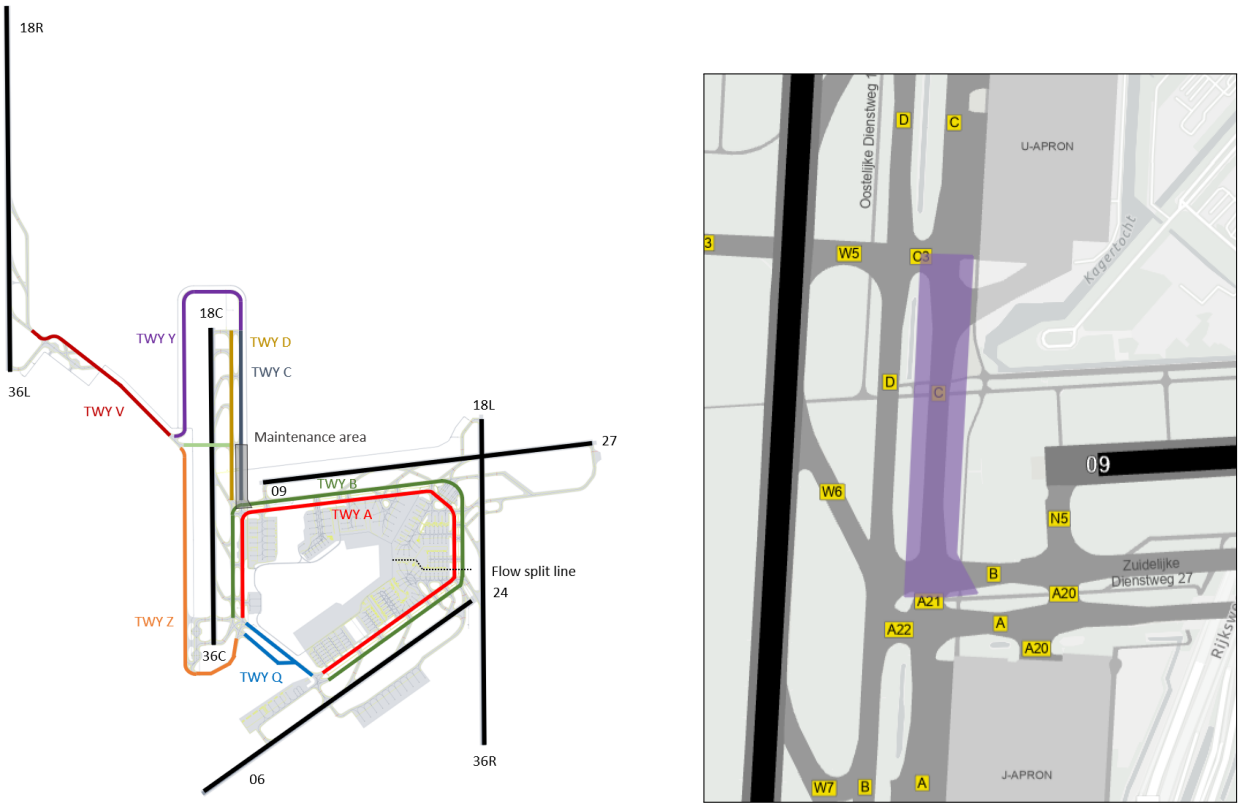

(a) Layout of Schiphol **(b)** Maintenance area

Figure 1: Layout of Amsterdam Airport Schiphol and the considered maintenance area. In Figure 1a, the main taxiways (TWYs) are coloured and the maintenance location is marked by a grey shaded area. Furthermore, in this figure, the flow split line indicates the boundary for aircraft moving via the north or south when making use of runways 36L/18R and 36C/18C. In Figure 1b, a close-up of the maintenance area given by the purple transparent area is shown including the surrounding and concerning taxiway names

3.1 Overview

The basis of this research is the existing Single-Agent Motion Planning (SIMP) algorithm implemented in the Multi-Agent Airport Surface Movement Operations simulator (MAASMO-sim). The SIMP algorithm is a single-agent path planning algorithm that computes the optimal paths for agents by taking into account heterogeneous, non-holonomic agent properties. Furthermore, the MAASMO-sim provides a flexible environment to test and simulate various operational ground movements at airports [14]. To make sure the paths generated by SIMP correspond to realistic traffic flows representative for the given maintenance scenario and runway configurations, the SIMP was customized by calibrating its parameters and adding additional constraints. This is initially done based on advise from operational experts. The resulting paths are used to calculate both task load metrics. To determine the first metric named the Dynamic Density-based task load metric, the Dynamic Density model was used, which reflects the Radio Telephony load. The second task load metric named the violation-based task load metric was calculated by the developed Violation Tool, which determined the number of times the minimum separation between aircraft was violated based on the overlaps of shapes, called protected zones, around aircraft. To validate the developed agent-based model, as the first step, the routes generated by SIMP and historical routes extracted from the real Airport Surveillance Tracker (ASTRA) database of LVNL were compared with each other using the Dynamic Density model. This was done to make sure the biased paths generated by SIMP are comparable with paths from real operations. If the paths were not comparable, re-calibration of the SIMP algorithm was necessary. Hereafter, the second validation step was done to compare the Dynamic Density-based and violation-based task load metrics with each other. This was done to inspect whether both metrics contain properties that are similar to each other.

The different components are given in Figure 2, where the arrows indicate which components influence which components. After the validation, the developed model was used to determine the task load in the selected taxiway maintenance scenarios. Simulations were run per runway configuration to understand what the impact is of the considered maintenance scenario on the task load of ground controllers. These results were analyzed and conclusions were drawn. The calibration of the used path planning algorithm is discussed in subsection 3.2, the Dynamic Density model in subsection 3.3, and the violation-based task load metric in subsection 3.4. The validation steps are considered in more detail in section 4.

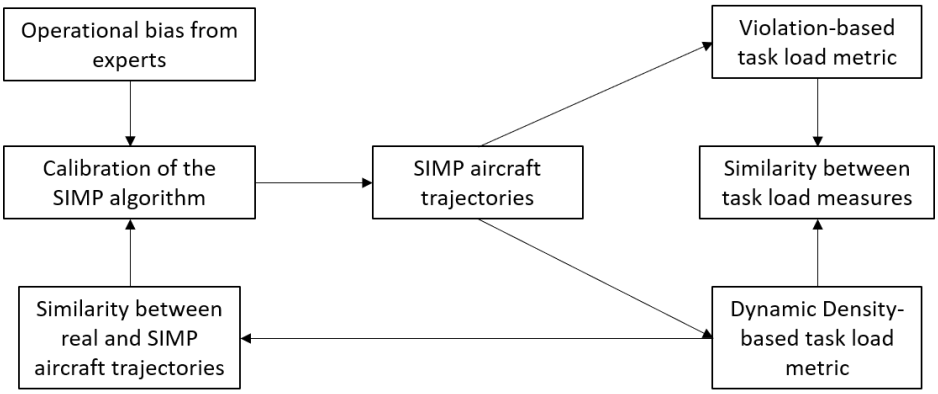

Figure 2: Diagram of components, with the arrows indicating which components influence which components

3.2 Calibration of the SIMP Algorithm

In this part, the calibration of the existing SIMP algorithm is discussed. The SIMP algorithm was developed at the TU Delft [14], and is an augmented version of the SIPP algorithm, which is a single-agent path planning algorithm that uses safe time intervals to compute the optimal path for an agent. A safe time interval is defined as an interval in time in which an agent does not conflict with other agents, based on feasible motions. Using these safe time intervals, SIPP searches in a state space that consists of configuration and interval pairs rather than location and time step pairs, as is the case for A* and Dijkstra. More explanations on the SIPP algorithm are provided in [21]. SIMP builds further on the SIPP algorithm by taking heterogeneous, non-holonomic agent properties, including their dimensions, into account. This algorithm uses motions in continuous time and space along a graph representing the taxiway network of an airport. Such a graph consists of edges and vertices, and its application for the layout of Schiphol airport is presented in [22]. Further explanations on the SIMP algorithm are provided in [14].
The existing SIMP algorithm was calibrated to ensure that the aircraft traffic flows on the airport surface are similar to the flows observed in reality. To make sure aircraft follow preferred taxiway directions, cost factors associated with the corresponding taxiway segments are introduced in the SIMP algorithm to bias the aircraft routes in these directions [23]. The bias of paths is achieved by changing the associated cost of traversing a taxiway segment during path planning. In this research, the cost factor is set to 5, meaning that it is five-times more expensive to traverse taxiway segments that are not part of the standard taxiway directions in comparison with those taxiway segment that are part of the standard taxiway directions for identical taxi time and distance.
To take into account maintenance during planning, and to make sure aircraft follow the right taxiway directions when making use of certain gates, additional layout constraints were implemented. Regarding the maintenance case, the taxiway segments that are situated at the location of the maintenance intervention, and those that are directly connected to the maintenance intervention were constrained, meaning that the agent-based simulation model would plan the paths for aircraft such that these taxiway segments are not used. Furthermore, the taxiway segments located at the black dotted flow split line shown in Figure 1a were also constrained, making sure that aircraft follow the correct standard taxiway directions for both the nominal and maintenance case.

3.3 Dynamic Density Model

In this research, the Dynamic Density-based task load metric is calculated using the Dynamic Density model developed by Stijn Brunia for his Master thesis. A full explanation on this model is presented in [11]. In a nutshell, the Dynamic Density model is a Linear Regression model consisting of different independent variables related to Dynamic Density, and predicts the RT load as its dependent variable. In this research, certain properties of this model were modified. First, the model was adjusted such that the aircraft route data used to calculate the task load does not only come from historical route data, such as ASTRA database of LVNL, but also from route data from the MAASMO-sim. In such a way, a seamless integration between the agent-based model and the Dynamic Density model was established. Therefore, the Dynamic Density model can now be applied for cases that do not necessarily relate to real-life historic scenarios, creating more flexibility and robustness for the usage of this model. When simulating historic scenarios, the Tower flight schedules are now also added as an additional input. From these flight schedules, the time of landing of the different aircraft was set to be equal to the Actual Landing Time (ALDT), and the time of push-back equal to the Actual Off-Block Time (AOBT), meaning that the actual intended landing and push-back times can be better approximated, and the task load for historic scenarios can now be better predicted.

3.4 Violation-Based Task Load Metric

In this part, the calculation of the violation-based task load metric using the developed Violation Tool is explained. To this end, first it is explained how the shape and dimensions of the protected zones are defined in subsubsection 3.4.1. Then, in subsubsection 3.4.2, it is explained how a violation is defined using these protected zones. Hereafter, in subsubsection 3.4.3, it is explained how these violations are detected and interpreted.

3.4.1 Shape and Dimensions of the Protected Zones

The number of violations is dependent on the shape and dimensions of the protected zones. Based on previous research and discussions with operational experts, it was concluded that the shape of the protected zones are elliptical, and that the dimensions of the protected zones are dependent on the weight class, speed of the aircraft and aircraft dimensions to include minimum separations between aircraft [24] [25]. To dynamically account for these factors, expressions for the semi-major axis "a" and semi-minor axis "b" of the elliptical protected zones are defined. For these expressions, it is assumed that the center of the aircraft is the center of the ellipse, and that the semi-major axis runs along the length of the aircraft. The expressions for the semi-major axis "a" and semi-minor axis "b" are given in Equation 1.

$$a = \frac{l_{aircraft} * k_{weight} + v_{aircraft} * c}{2} \qquad b = \frac{w_{aircraft}}{2} \tag{1}$$

In Equation 1, $l_{aircraft}$ is the length of the aircraft in meters, $w_{aircraft}$ is the wingspan of the aircraft in meters, $v_{aircraft}$ is the speed of the aircraft in meters per second, and k_{weight} is a parameter that is dependent on the separation distances defined by Van Oosterom et al. (2023) [25]. This k_{weight} parameter is equal to the minimal separation defined for the weight class of the concerning aircraft, divided by the minimal separation defined for narrow-body aircraft. In this research, the k_{weight} parameter is equal to 1 for narrow-body aircraft, 1.25 for wide-body aircraft and 1.5 for heavy-wide-body aircraft. Furthermore, the factor c is introduced, which is equal to one second to make sure the addition in the expression for the semi-major axis can be performed.
For both axes, the speed of the aircraft is added to create the linear relation between aircraft speed and separation, which was included based on discussions with operational experts. It may be noticed that when the speed is low, aircraft are able to move closer along and behind each other, which relates to the ground movement operations on the apron.

3.4.2 Violation Definition

A violation is defined as the overlapping of two protected zones, meaning that two protected zones share the same spatial coordinates in a certain period of time. The principle of a violation is shown in Figure 3.

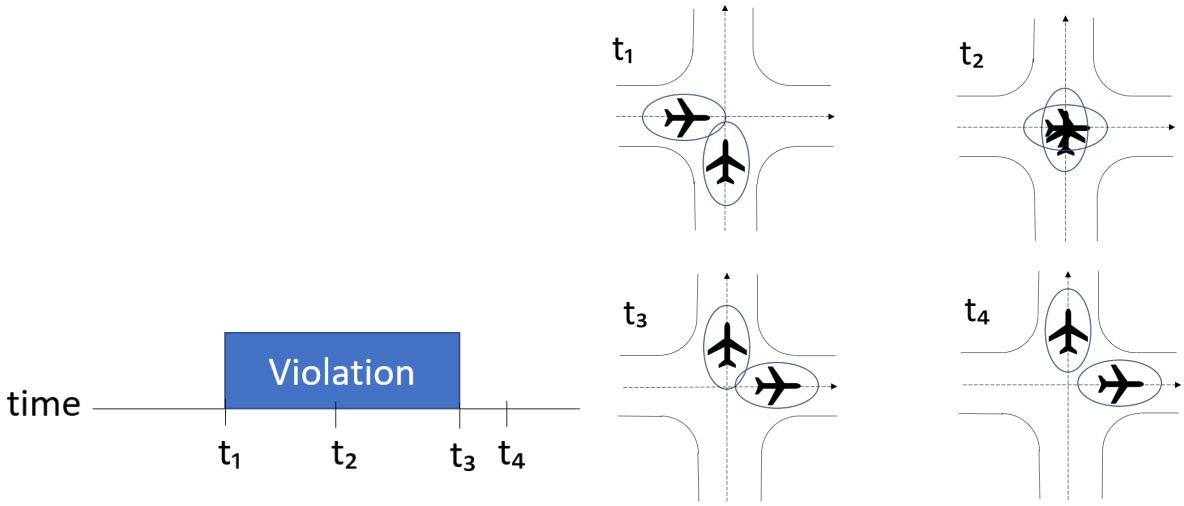

(a) Time period of a violation **(b)** Relative positions of ellipses

Figure 3: Definition of a violation. In Figure 3a, a violation is defined between times t_1 and t_3. In Figure 3b, it is shown what the relative positions are between violating aircraft for the different times given in Figure 3a based on the dynamic evolution of the violation for two aircraft travelling in a straight direction and violating at a cross section

In Figure 3, one violation is detected in a certain period of time, meaning that the task load induced by a re-planning of a ground controller is equal to one. The detection of a violation between two protected zones is determined using an algorithm for determining the relative position between two ellipses, which is discussed in subsubsection 3.4.3.

3.4.3 Determination of Violations

In this part, it is explained how violations are determined. This is done by first providing a general description of the algorithm used to detect the relative position between two protected zones. Then, using this algorithm, an example calculation is provided for determining the relative position between two ellipses. Lastly, it is specified how the outputs of this algorithm are interpreted to determine a violation.

General Description of Algorithm

To determine whether there is a violation between two protected zones, the relative position between two protected zones is determined using the algorithm created by G.B. Hughes and M. Chraibi [26] based on the approach to characterize the relative position of two ellipses defined by F. Etayo et al. [27]. This algorithm first determines the symmetric matrix of each of the two protected zones, which are symmetric matrix A and B. The inputs of each symmetric matrix are the parameters that determine the dimensions of the protected zone given in subsubsection 3.4.1, namely the length, width, speed and k_{weight} parameter. Furthermore, the coordinates of the center of the protected zone and the heading of the protected zone are used as input for the symmetric matrix of the protected zone. Using both symmetric matrices, the characteristic polynomial of the pencil $\lambda \cdot A + B$ is determined and is given in Equation 2.

$$f(\lambda) = det(\lambda \cdot A + B) = \lambda^3 + a \cdot \lambda^2 + b \cdot \lambda + c \tag{2}$$

After the polynomial given in Equation 2 is turned monic, the coefficients a, b and c are interpreted. Based on the values of these coefficients, in combination with the associated outcomes of s_1, s_2, s_3 and s_4 using these coefficients, the algorithm outputs the relative position between the two protected zones [26].
In this research, the algorithm is applied for each time step between each pair of ellipses that are present at that time step in the simulation, when the horizontal and vertical distance between the centers of the ellipses are smaller or equal to the summation of the semi-major axes "a" of both ellipses and a safety factor. This is done to make sure only aircraft that are relatively close to each other are taken into account, making the

application of the algorithm more efficient and faster. The safety factor is set to 18 meters to make sure all combinations of different aircraft that are moving close to each other are captured.

Example Calculation of Relative Position

To better understand the principle of the algorithm used, an example calculation is given using Algorithm 1 given in Appendix A. This is done based on the scenario given in Figure 4.

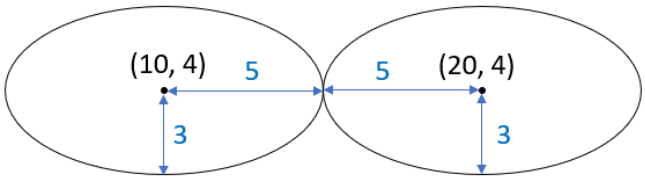

Figure 4: Scenario of two protected zones with their dimensions and locations

In Figure 4, two protected zones are given with their dimensions and locations. To determine what the relative position is of the two protected zones, the symmetric matrix for each of these zones are computed. The left protected zone is considered to be for aircraft 1, and the right protected zone is considered to be for aircraft 2. Therefore, the values of the parameters that are used for the construction of the symmetric matrices are $h_1 = 10$, $k_1 = 4$, $h_2 = 20$, $k_2 = 4$, $A_1 = A_2 = 5$, $B_1 = B_2 = 3$, and $\varphi_1 = \varphi_2 = 0$. The resulting symmetric matrices are hereby:

$$A = \begin{pmatrix} 0.04 & 0 & -0.4 \\ 0 & 0.11 & -0.44 \\ -0.4 & -0.44 & 4.78 \end{pmatrix}, \quad B = \begin{pmatrix} 0.04 & 0 & -0.8 \\ 0 & 0.11 & -0.44 \\ -0.8 & -0.44 & 16.78 \end{pmatrix}$$

Based on these symmetric matrices, the characteristic polynomial of the pencil $\lambda \cdot A + B$ with the resulting coefficients are hereby given:

$$f(\lambda) = det(\lambda \cdot A + B) = \lambda^3 - \lambda^2 - \lambda + 1 \tag{3}$$

Using these coefficients, the resulting values for s_1, s_2, s_3 and s_4 are $s_1 \approx$ -1, $s_2 \approx 4$, $s_3 \approx$ -8 and $s_4 \approx 0$. As s_4 is approximately equal to zero, s_2 bigger than zero and s_3 smaller than zero, the algorithm returns that the protected zones are externally tangent to each other. This result is in line with the scenario shown in Figure 4. From G.B. Hughes and M. Chraibi [26], nine other relative positions between the protected zones could occur. In this research, all these ten relative positions are considered because all these relative positions could occur between the protected zones. The algorithm computes all these relative positions, and are visualized in Figure 5.

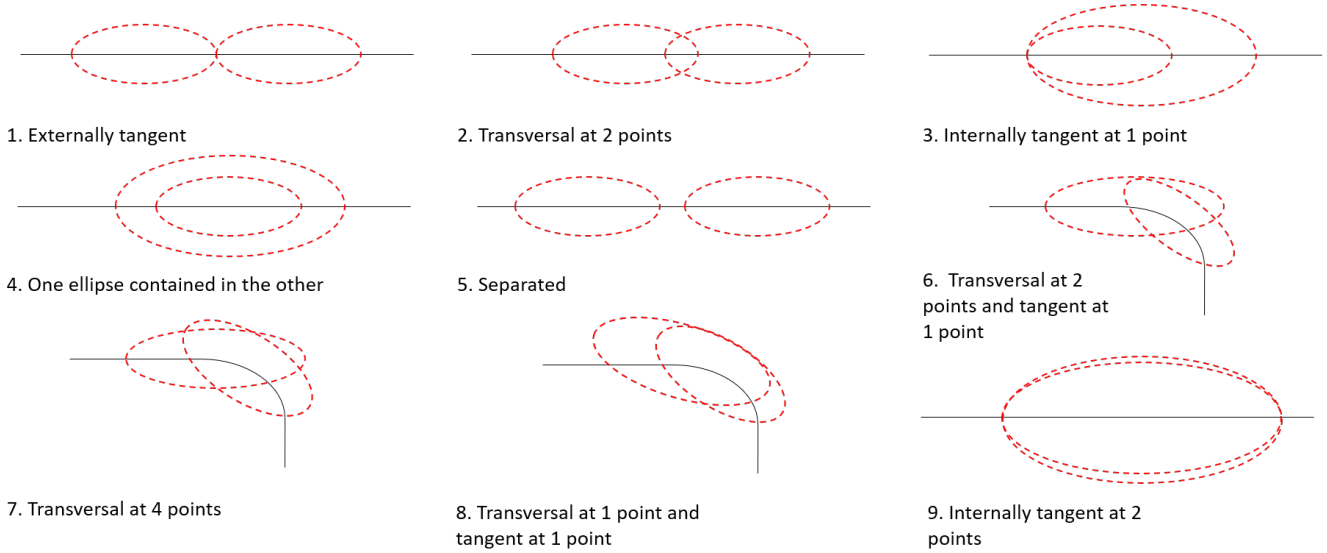

Figure 5: The different relative positions of two protected zones. A tenth possible relative position also exists, where two protected zones coincide

From Figure 5, it can be seen that the relative positions of two protected zones are determined for aircraft travelling on the same path, as the same relative positions hold for aircraft travelling on neighbouring paths. Furthermore, a possibility also exists where two protected zones coincide, which is not visualized.

Interpretation of Algorithm Results
Based on the definition of a violation, given in subsubsection 3.4.2, the interpretation of the relative positions for this research can be determined. From the relative positions given in Figure 5, it can be obtained that the only relative position that is not considered as a violation is relative position 5, where the two protected zones are separated. Therefore, when a relative position between two protected zones is found other than relative position 5, it can be concluded that at the concerning time point, there is a violation. This violation happens between the time steps when relative position 5 is detected for that specific pair of ellipses, which is conform the violation definition specified in subsubsection 3.4.2. However, when a violation is detected at the start of the simulation, then the violation time interval is between the start of the simulation until the first time relative position 5 is detected. Also, when there is a violation detected in the last time step of the simulation, the violation time interval is between the last time relative position 5 is detected for that specific ellipse pair and the final step of the simulation.
Furthermore, the task load is measured per controller sector, meaning that the location of the violations need to be defined per sector. It is hereby assumed that the coordinates of the location of a violation is defined as the average of the coordinates of the centers of two ellipses when they are in violation for the first time in a certain violation time interval. Also, besides being measured per sector, task load is measured per 10 minutes. This time period is chosen based on discussions with operational experts, and is chosen to ensure that moments containing a high number of potential re-plannings determined by the ground controller are better captured, as these moments are expected to generate high task load. Lastly, violations regarding aircraft taxiing behind each other are omitted, as no mental re-plannings of ground controllers are necessary in this case. Aircraft are considered to be taxiing behind each other when the last three passed taxiway or runway nodes of both aircraft are the same.
This working mechanism for determining the relative positions between aircraft is hereby called the Violation Tool.

4 Verification & Validation

In this section, the verification and validation steps are presented. This is done by first discussing the verification in subsection 4.1. Then, in subsection 4.2, it discussed how similar the routes of the aircraft from

the historical ASTRA data and the SIMP-based simulation are for the same flight schedule, as similarity between the routes of the different datasets is important to accurately and realistically simulate possible locations of violations between aircraft captured by the violation algorithm in the considered maintenance scenarios. At last, in subsection 4.3, the violation-based task load metric and Dynamic Density-based task load metric are compared with each other to obtain similarities. For both validation steps, a distinction is made between the northern and southern direction of runway use to better understand the relation between the metrics for the different flows representative for these different directions. The days considered for modeling are chosen based on the most frequently used runway configurations at Schiphol.

4.1 Verification

To make sure verification is applied correctly, the verification techniques described by Sargent [28] are considered. During the implementation of the Violation Tool and Dynamic Density model, continuous verification is performed. Based on the different building blocks that result in the model, independent testing of these different blocks was performed. Furthermore, errors are resolved as much as possible during the process, and an interactive display was used to verify that the routes and violations of shapes are simulated correctly. Also, small test scenarios are created to verify the model's behaviour concerning violation detection, and to analyse whether the intended performance of the model is met. Furthermore, individual agent behavior is carefully followed throughout the system to ensure correctness. Lastly, the Dynamic Density model uses the same length in time interval as the Violation Tool to provide equal comparison.

4.2 Path Validation

In the first validation step, the routes of the aircraft extracted from the historical ASTRA data are compared with the routes of the aircraft generated by the SIMP algorithm in the simulator. This comparison was done for two different scenarios. The first scenario is on the 17th of July between 08:00 and 16:00, taking into account different inbound and outbound peaks for northern runway use. The second scenario is on the 18th of July between 08:00 and 16:00, taking into account the different inbound and outbound peaks for southern runway use. In this step, the measure that is used to compare the historical and simulated trajectories, represented by time series data, is the Pearson Product-Moment Correlation method. This method is suitable for comparing the ASTRA data and route data generated by SIMP, as there is a linear relation between both datasets, with relatively few outliers. Therefore, this method is used to compare both datasets.

4.2.1 Northern Runway Use: 2019-07-17 08:00 - 16:00

The task load determined by the Dynamic Density model using the ASTRA data and SIMP route data for the period between 08:00 2019-07-17 and 16:00 2019-07-17 is given in Figure 6 for the sectors Center, North and South.
From these figures given in Figure 6, it can be concluded that the predicted task load for both datasets mainly follow the same pattern over all sectors. For sector Center, it can be seen that the dynamic density calculated using the SIMP data is on average lower than the result of the ASTRA data because the aircraft planned by the SIMP algorithm move faster over the infrastructure than the real aircraft obtained from the ASTRA data. This happens because the routes are planned for each individual aircraft without taking into account the routes of other aircraft, which always results in the shortest route possible with the highest speed possible. However, in the ASTRA data, the real routes of aircraft are affected by other traffic flows. As a result, the task load experienced by ground controllers in the SIMP-based simulations is lower than the task load experienced by ground controllers during real operations because the aircraft stay for a shorter time in the sectors, meaning that the controllers need to pay less attention to these aircraft over time, resulting in a lower task load over time.

For sectors North and South, it can be seen that also a clear pattern is visible between the outcomes for the ASTRA and SIMP datasets. However, it can also be obtained that there are cases that the task load calculated using SIMP data is higher than the task load predicted by the ASTRA data. This has two reasons, where the first reason is related to the quality of the ASTRA data. For some cases, the exact location of push-backs could not be retrieved correctly using the ASTRA data. As this variable is a task load variable for sectors North and South in the Dynamic Density model, a lower task load is predicted for these sectors

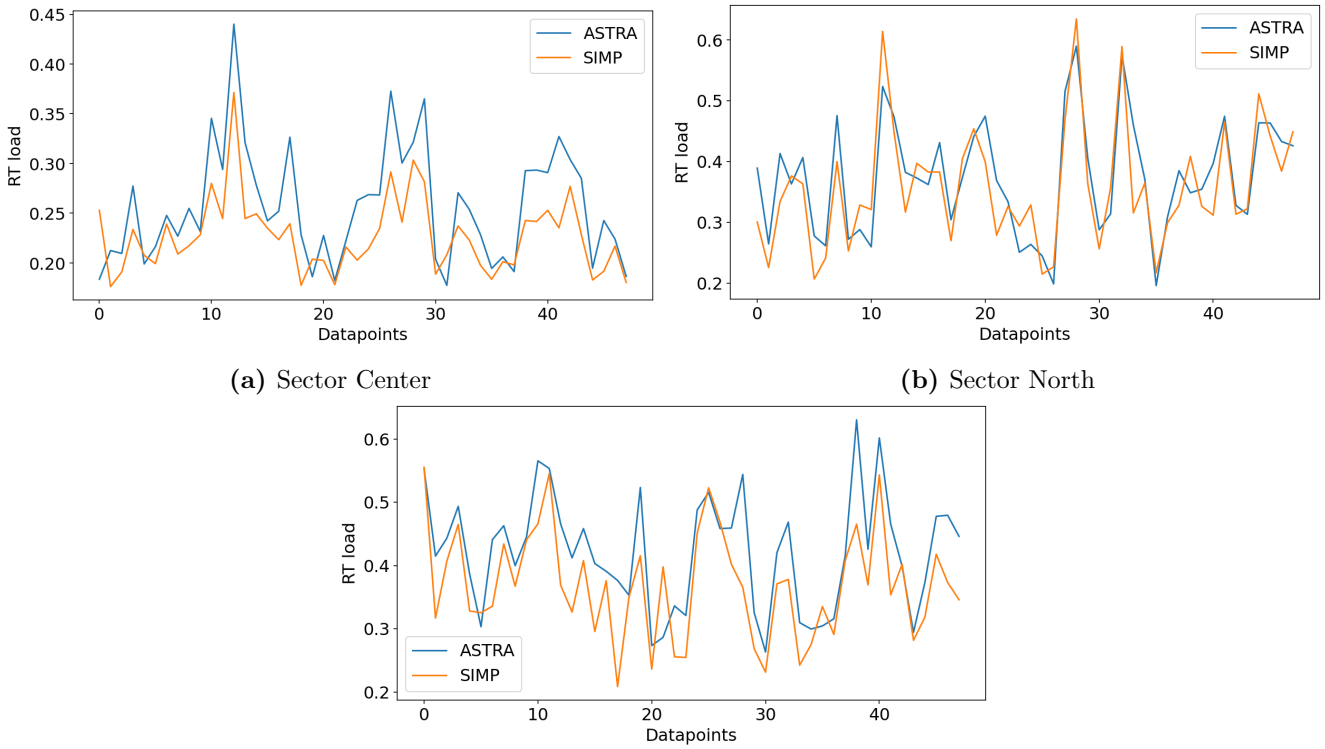

(a) Sector Center

(b) Sector North

(c) Sector South

Figure 6: The measure of Dynamic Density with SIMP versus Dynamic Density with ASTRA for sectors Center, North and South: 2019-07-17 08:00-16:00

compared to cases where push-backs are retrieved correctly. The second reason is that some aircraft are directed in a different direction by the SIMP algorithm than what is registered in the ASTRA data. For the most part, this is because of the implementation of the layout constraints to separate flows in northern and southern direction at the black dotted flow split line given in Figure 1a. As a result, some aircraft are directed via the south by the SIMP algorithm, but in the ASTRA data, these are directed via the north. In this case, a higher task load is predicted for the SIMP algorithm in the North sector, and a lower task load is predicted in the South sector. In this scenario, the other way around also happens, but most redirected aircraft now move via the north than via the south. The layout constraint has the biggest impact on aircraft departing and arriving at gates close to this layout constraint, as the shortest path is now blocked for some aircraft, and these are now redirected in the other direction.

To better indicate the insights given, Figure 7 shows the distribution of aircraft locations given in the ASTRA data and route data generated by the SIMP algorithm for timesteps 9, 10, 11 and 12 for the given day, which is from 09:30 till 10:10 on 17/07/2019. In this case, the aircraft locations are logged per time step.

From Figure 7, it can be obtained that more aircraft locations are registered in sector Center for the ASTRA data in Figure 7a than for the SIMP data given in Figure 7b. The reason is that more aircraft travel slower in real operations compared to trajectories computed by the SIMP algorithm when passing the Zwanenburg runway (18C/36C) via the south. This results in a higher task load prediction for the ASTRA data compared to the SIMP route data for the given period, which is shown in Figure 6a. Furthermore, for sector North, it can be obtained that the quantity and location of aircraft locations on the taxiways are similar for the ASTRA and SIMP route data. However, in Figure 7b, it can be obtained that there are locations on the taxiways that register more aircraft locations for the SIMP route data compared to the ASTRA data shown in Figure 7a. This is because now more aircraft travel via the north for the SIMP data compared to the ASTRA data. This results in a higher task load prediction for sector North for the SIMP data compared to the ASTRA data for the given period, and is shown in Figure 6b. At last, for sector South, more aircraft locations are registered for the ASTRA data compared to the SIMP data because the aircraft move slower over the infrastructure for the ASTRA data compared to the SIMP data. This results in a higher task load pre-

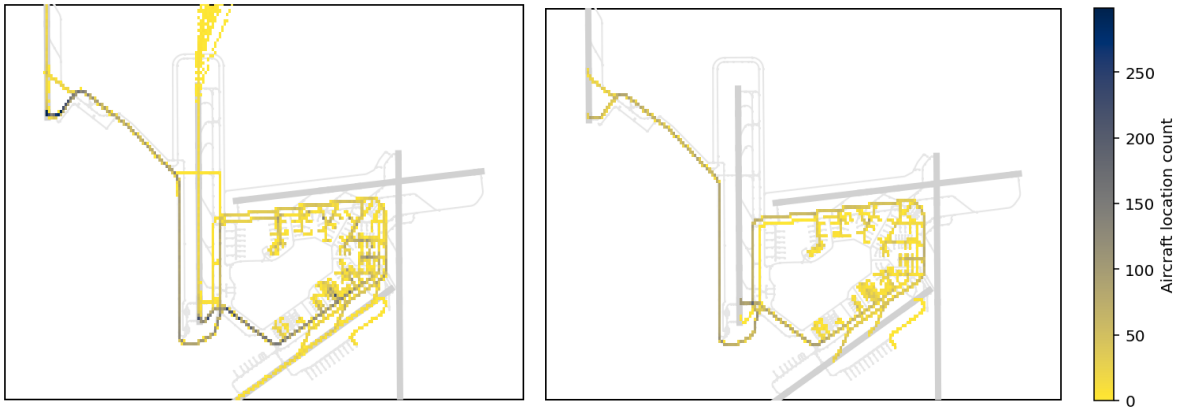

(a) ASTRA data **(b)** SIMP route data

Figure 7: Aircraft location count for aircraft given in the ASTRA and SIMP data for the period between 09:30 till 10:10 on 17/07/2019. The aircraft locations are logged per time step

diction for sector South for the ASTRA data compared to the SIMP route data, which is shown in Figure 6c.

For each of the three sectors, the Pearson Product-Moment coefficient is determined for the predicted task load between the ASTRA and SIMP route data with its p-value, and given in Table 1.

Sector	**Pearson Statistic**	**Pearson P-Value**
Center	0.858	< 0.05
North	0.867	< 0.05
South	0.810	< 0.05

Table 1: Pearson correlation coefficient and concerning p-value per sector for the path validation and northern runway use

From Table 1, it can be concluded that for all sectors in the given period, and using these specific runway configurations, the Pearson correlation coefficient gives a high correlation between the ASTRA and SIMP route data. Furthermore, for all three sectors, the p-value represents a significant relation between the datasets, meaning that the observed statistics is not drawn by coincidence. Therefore, it can be concluded that there is a relation between the ASTRA and SIMP data for northern runway use, and that the SIMP algorithm can be used for northern runway use without re-calibration of the SIMP algorithm.

4.2.2 Southern Runway Use: 18/07/2019 08:00 - 16:00

The task load calculated by the Dynamic Density model using the historic ASTRA data and SIMP route data for the period between 08:00 2019-07-18 and 16:00 2019-07-18 is given in Figure 8 for the sectors Center, North and South.
From Figure 8, the same conclusions as for the northern runway use, presented in subsubsection 4.2.1, can be drawn. Namely, there is a similar pattern for both datasets over all sectors. Furthermore, the predicted task load using the SIMP data is lower than the predicted task load using the ASTRA data for sector Center. However, this is now also the case for sector North. The reason is because the quality of the ASTRA data is better in this sector, and most push-backs are now captured. This is less the case for sector South, where still some aircraft are left out because of missing push-backs. Furthermore, re-directions still occur as in subsubsection 4.2.1, but this is now less the case as the shortest path of aircraft are now less influenced.
For each of the three sectors, the Pearson Product-Moment coefficient is determined with its p-value, and is presented in Table 2.
From Table 2, it can be concluded that for all sectors in the given period, the Pearson correlation coefficient gives a high correlation between the ASTRA and SIMP data outputs. Furthermore, for all three sectors,

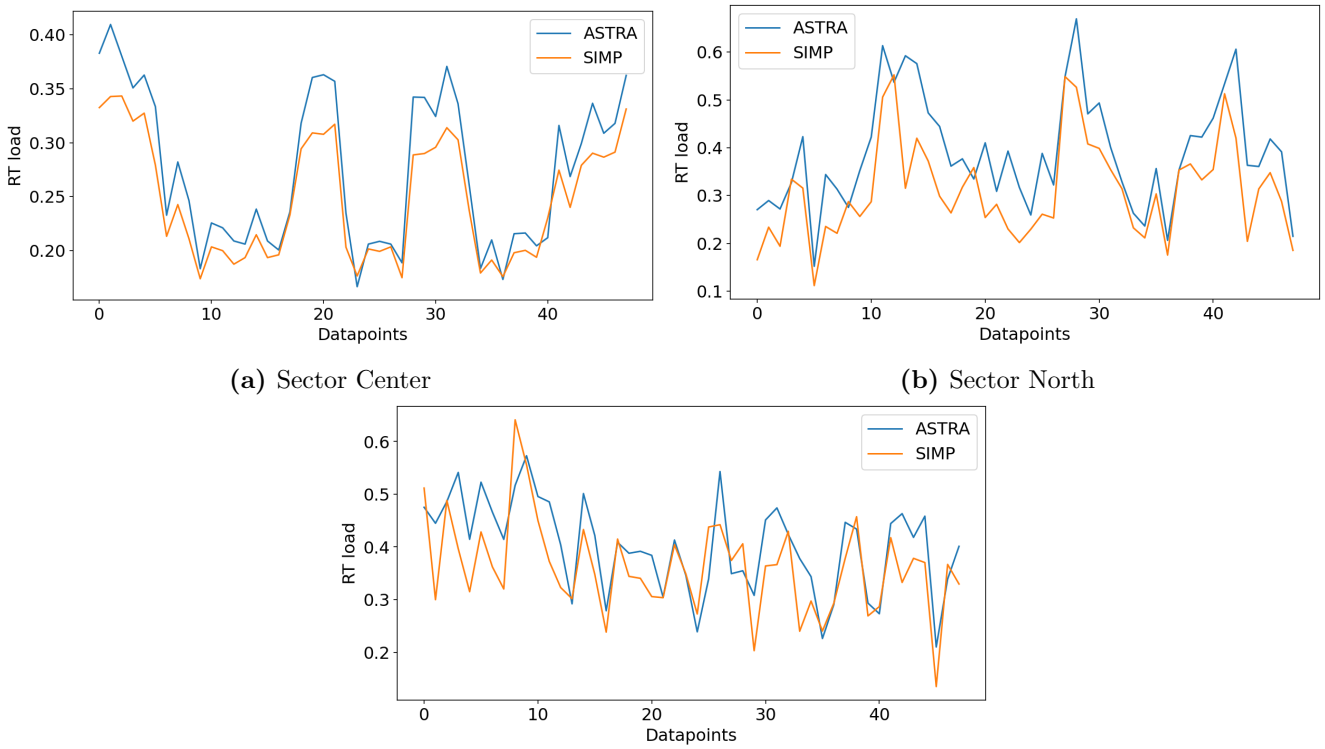

(a) Sector Center

(b) Sector North

(c) Sector South

Figure 8: The measure of Dynamic Density with SIMP versus Dynamic Density with ASTRA for sectors Center, North and South: 2019-07-18 08:00-16:00

Sector	Pearson Statistic	Pearson P-Value
Center	0.984	< 0.05
North	0.851	< 0.05
South	0.754	< 0.05

Table 2: Pearson correlation coefficient and concerning p-value per sector for path validation and southern runway use

the p-value represents a significant relation between the datasets, meaning that the observed statistics is not drawn by coincidence. Therefore, it can be concluded that there is a relation between the ASTRA and SIMP data for southern runway use, and that the SIMP algorithm can be used for southern runway use without it being re-calibrated.

4.3 Task Load Metric Validation

In this step, the predicted task load using the Dynamic Density method is compared with the predicted task load using the principle of separation violations. This is done to assess similarities between the two proposed task load measures. As for the path validation in subsection 4.2, the traffic scenario on the 17th of July between 08:00 and 16:00, and the traffic scenario on the 18th of July between 08:00 and 16:00 is considered. The measure that is used to validate the outcomes in this step is the Spearman Rank-Order Correlation method. This method is a suitable correlation method to be used for the two variables because they have a monotonic relation which each other, and can be ranked. The Pearson method is not suitable in this case because the relation between the two variables is not linear, and contains a significant number of outliers.

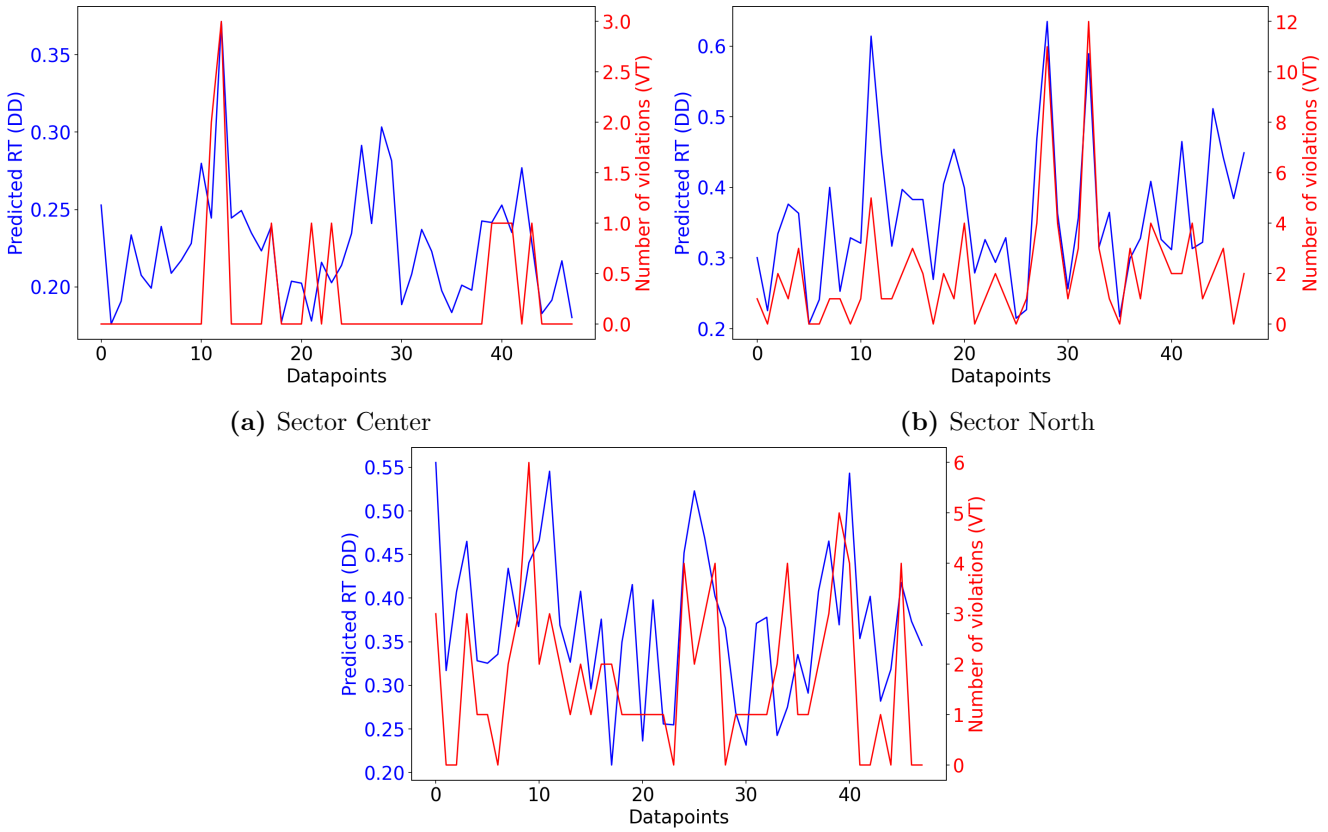

(a) Sector Center

(b) Sector North

(c) Sector South

Figure 9: The comparison of the violation-based task load measure using the Violation Tool (VT) and Dynamic Density-based task load measure using the Dynamic Density (DD) model for sectors Center, North and South: 2019-07-17 08:00-16:00

4.3.1 Northern Runway Use: 17/07/2019 08:00 - 16:00

In this part, the task load measures calculated using the Violation Tool and the Dynamic Density model are compared with each other for the period between 08:00 17/07/2019 and 16:00 17/07/2019, and are shown in Figure 9 for sectors Center, North and South.
In Figure 9a, it can be obtained that the Violation Tool does not measure violations in most intervals. However, the Dynamic Density model does measure task load in most intervals, and shows peak moments. These peak moments are a result of aircraft moving through the Center sector to depart from the Polder (36L) and Zwanenburg (36C) Runway. Ground controllers have to communicate with all these aircraft, which increases the RT load. In many of these cases, the Violation Tool does not measure violations, as there are no conflicting flows in the Center sector because aircraft are taxiing behind each other to the thresholds of their runways. In these cases, ground controllers do not have to solve any conflicts. However, there are cases where there is a peak in violations measured, which is in time intervals 11 and 12. The aircraft traversals and violations in these intervals, which is in the period between 09:50 and 10:10 on 17/07/2019, are given in Figure 10. In Figure 10a, it can be obtained that aircraft flows moving along the south of the airport conflict with aircraft moving along the north of the airport at the intersection north of taxiway Quebec. This happens when 36C is used for takeoffs, meaning that aircraft departing from 36L need to taxi via taxiway Zulu. From Figure 10b, it can be obtained that these conflicting flows are captured by the Violation Tool for the given interval by measuring the violations between the aircraft of these different flows. For the other violations measured in the other time intervals by the Violation Tool, also departing aircraft from different flows loose separation from each other at intersections. It is expected that this results in an increase in task load, but this is in some cases not captured by the Dynamic Density model. Overall, for sector Center, it can be concluded that for the given scenario there is a mismatch in capturing task load between the two measures.

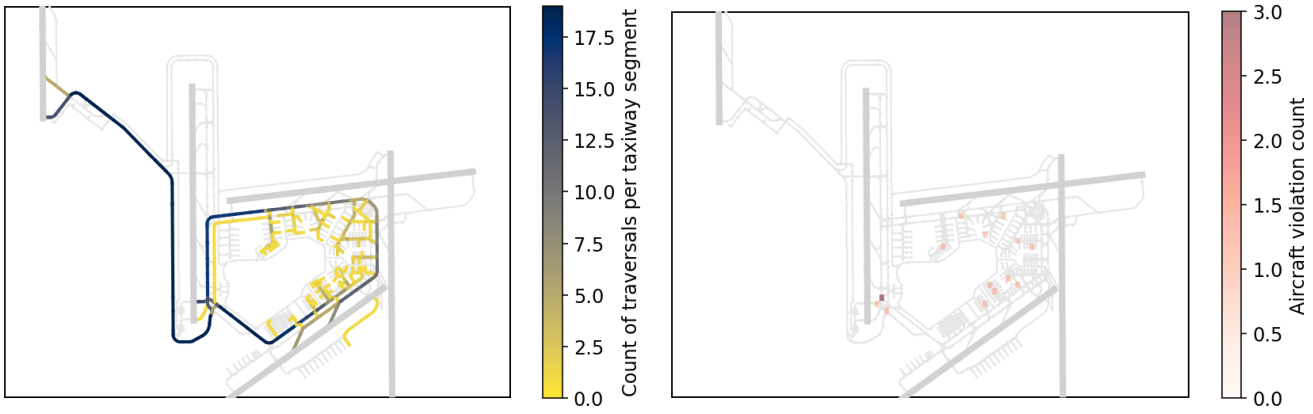

(a) Aircraft traversals **(b)** Aircraft violations

Figure 10: Aircraft traversals and violations in the period between 09:50 till 10:10 on 17/07/2019

From Figure 9b and Figure 9c for sectors North and South, it can be concluded that there is a similar pattern visible for the two task load measures, where both low and high traffic peaks are captured. In the Dynamic Density model, the number of push-backs and apron movements strongly impact the predicted task load. Therefore, for sectors North and South, the relation between the Dynamic Density-based and violation-based task load outputs are established by the number of push-backs on the aprons, and the violations that happen on the apron between departing aircraft, and between aircraft leaving the apron and aircraft taxiing along or to the apron. The number of violations and predicted RT load is low when the number of push-backs and apron movements is low, and high when there are a high number of push-backs and movements over the apron. This relation is visible for both sectors North and South in the given figures.

To conclude whether there is a relation between the violation-based and Dynamic Density-based task load metric for northern runway use, the Spearman Rank-Order Correlation method is applied for the scenarios defined in Figure 9. The outcomes of the correlation analysis including the p-values are provided in Table 3.

Sector	**Spearman Statistic**	**Spearman P-Value**
Center	0.225	0.125
North	0.589	< 0.05
South	0.489	< 0.05

Table 3: Spearman correlation coefficient and concerning p-value per sector for metric validation and northern runway use

From Table 3, it can be obtained that there is a low correlation for sector Center between the outcomes of the Dynamic Density model and the Violation Tool. However, the resulting p-value indicates that the result is non-significant, meaning that this result can not be accepted. The reason that this p-value is low is because little output is generated by the Violation Tool. However, it can be concluded that this little output happens for most cases for these runway configurations, given the low number of conflict locations. Therefore, it is hereby excepted that there is no relation between the violation-based task load metric and Dynamic Density-based task load metric for sector Center given northern runway use.
For sector North, the outcomes of the two metrics are moderately correlated with each other. This means that there are some relationships obtained between the two datasets, which can also be obtained from Figure 9b. However, as there is a moderate correlation, both metrics are not replaceable for sector North. The p-value for sector North is lower than 0.05, meaning that the obtained result is significant.
For sector South, the outcomes of the two metrics are low correlated with each other, meaning that there is little relationship between the two outcomes. These relationships are visible in Figure 9c, but not enough to be considered moderately correlated. The p-value for sector South is lower than 0.05, meaning that the

obtained result is significant. Based on the obtained results, it can be concluded that both metrics are needed for task load prediction for northern runway use.

4.3.2 Southern Runway Use: 18/07/2019 08:00 - 16:00

In this part, the task load measures calculated using the Violation Tool and the Dynamic Density model are compared with each other for the period between 08:00 18/07/2019 and 16:00 18/07/2019, and are shown in Figure 11 for sectors Center, North and South.

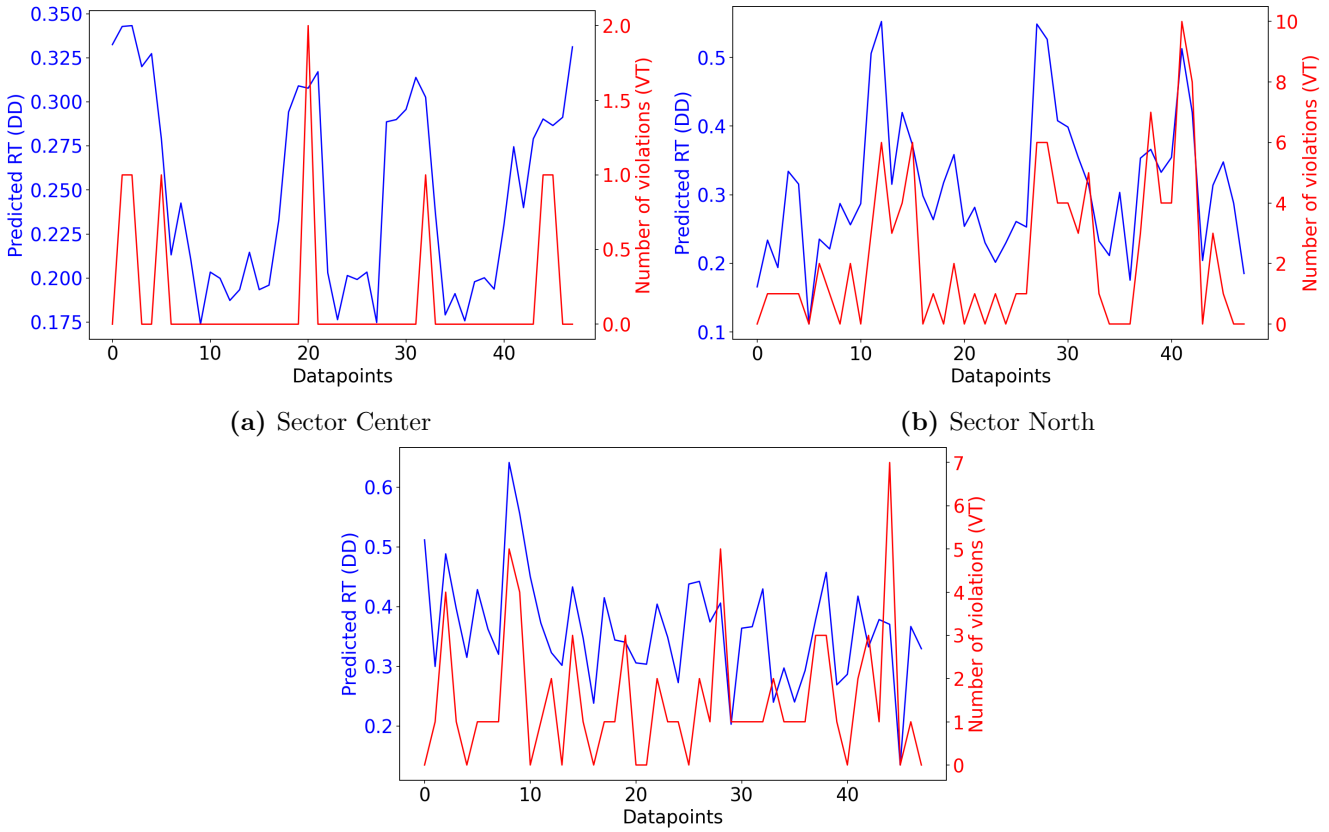

(a) Sector Center

(b) Sector North

(c) Sector South

Figure 11: The comparison of the violation-based task load measure using the Violation Tool (VT) and Dynamic Density-based task load measure using the Dynamic Density (DD) model for sectors Center, North and South: 2019-07-18 08:00-16:00

From Figure 11a, it can be obtained that violations only occur in the Center sector during inbound peaks and outbound peaks, where the Dynamic Density model predicts task load peaks. In this case, few violations occur during these peak periods because few conflicting aircraft flows occur in this scenario for the given runway configurations.
Furthermore, from Figure 11b, it can be obtained that there is a similar pattern between the outcome of the Dynamic Density model and the Violation Tool for sector North, with the same reason as specified in subsubsection 4.3.1.
Subsequently, from Figure 11c, it can be obtained that there is also a pattern visible between the Dynamic Density and Violation Tool outcome for sector South as for sector North. However, this pattern is less for sector South than for sector North, where also misalignments between the outcomes occur. The most obvious one occurs in time interval 44, where there is a significant peak in detected violations, but no significant peak in predicted task load by the Dynamic Density model. The reason for this peak is that a small number of aircraft departing from the apron in the South sector violate with aircraft arriving at this apron. This has a strong impact on the number of violations detected by the Violation Tool, but not by the Dynamic

Density model, as only the number of aircraft, average number of bay traffic and number of pushbacks are the indicators for task load for the South sector.

To determine whether there is a relation between the violation-based and Dynamic Density based task load metric for southern runway use, the Spearman Rank-Order Correlation method is applied for the scenarios defined in Figure 11. The outcomes of the correlation analysis including the p-values are provided in Table 4.

Sector	**Spearman Statistic**	**Spearman P-Value**
Center	0.407	< 0.05
North	0.774	< 0.05
South	0.404	< 0.05

Table 4: Spearman correlation coefficient and concerning p-value per sector for metric validation and southern runway use

From Table 4, it can be obtained that there is a low correlation between the outcomes of the Violation Tool and Dynamic Density model for sector Center and sector South for the given scenario. However, for sector North, the correlation between the outcomes of both models is high, meaning that a strong relation between the datasets is obtained for the given scenario for sector North. This relation is also visible in Figure 11b, where a pattern is visible between the two variables. The p-values for all sectors are lower than 0.05, meaning that the obtained statistics are significant. Based on the obtained results, it can be concluded that there are relations observed between the outcomes of both models, but to provide a better representation for task load for the maintenance scenarios, both metrics are used.

5 Experimental Set-Up

In this part, the set-up for the agent-based simulation experiments for the considered taxiway maintenance scenarios is considered. This is done by first discussing the runway configurations modeled in this research in subsection 5.1. Then, in subsection 5.2, the simulation plan to generate the results is presented.

5.1 Runway Configurations

The runway configurations considered in this research are determined based on potential conflicting flows that emerge because of the maintenance scenario, as these flows are expected to impact the task load for ground controllers. Based on discussions with operational experts, these conflicting flows only happen during real operations when runway 18R/36L (Polder Runway) and 18C/36C (Zwanenburg Runway) are operated in opposite direction. This means that one of the two runways is used for landings, and the other runway is used for takeoffs. The most used runway configuration for landing on 18R and takeoff from 18C is 18R/18C+18L, and the most used runway configuration for landing on 36C and takeoff from 36L is 36C+36R/36L. However, runway configurations for landing on 18C and takeoff from 18R, and runway configurations for landing on 36L and takeoff from 36C do not exist, as takeoff from 18R and landing on 36C is not possible given the taxiway network of Schiphol Airport. Therefore, the runway configurations that are considered in this research are 18R/18C+18L and 36C+36R/36L.
The traffic flows for which 18R is used for landings and 18C for takeoffs without any maintenance is presented in Figure 12a. In this figure, it can be noticed that conflicting flows happen between outbound flows at the intersection below taxiway Delta and on taxiway Bravo, and between the inbound flow and outbound flow at the intersection below taxiway Charlie and on taxiway Bravo. Furthermore, potential conflicts also happen at the orange arrow south of taxiway Quebec, as different flows now need to make use of one taxiway segment. The traffic flows for this runway configuration with maintenance is presented in Figure 12b. Compared to the nominal case, it can be seen from Figure 12b that taxiway Delta and a part of taxiway Alpha below the maintenance part are now used in both directions because of the maintenance scenario. As a result, it is expected that the task load increases in sector Center because, in this sector, now more flows are in conflict with each other compared to the nominal scenario. Therefore, ground controllers in sector Center now need to conduct more re-plannings to solve these conflicting flows, which increases the task load. Furthermore, it

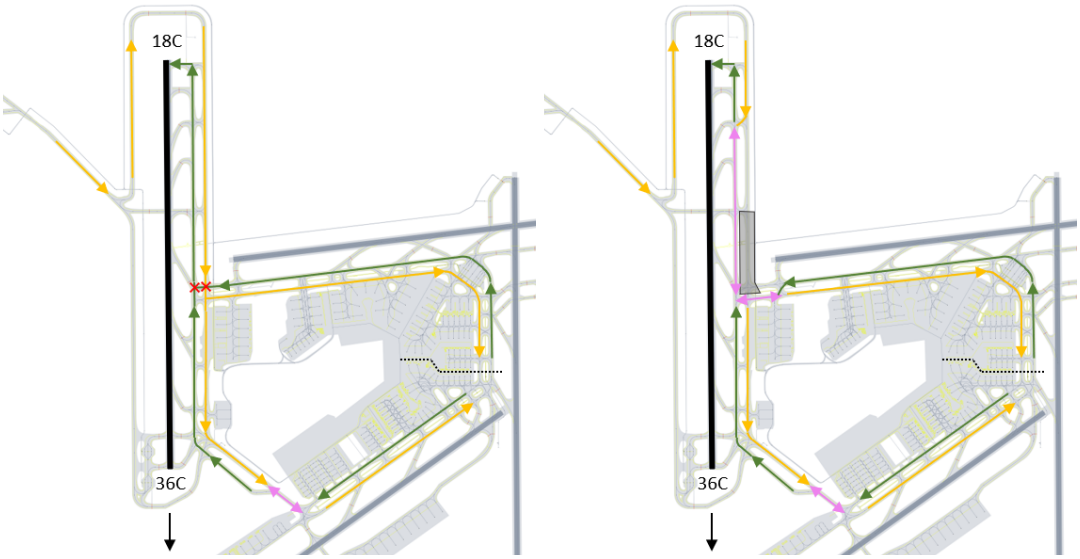

(a) Nominal case **(b)** Maintenance case

Figure 12: Traffic flows for landing on 18R and takeoff from 18C. The green arrows are outbound traffic, the orange arrows are inbound traffic, the violet arrows are flows in both direction, and the red crosses are locations of conflicting flows

is expected that the task load in the other sectors is not impacted by the maintenance scenario as the traffic flows in these sectors are not impacted.

The traffic flows for which 36C is used for landings and 36L for takeoffs without any maintenance is presented in Figure 13a. In this figure, it can be noticed that conflicting flows happen between outbound flows at the intersection below taxiway Charlie and on taxiway Bravo, and between the inbound flow and outbound flow at the intersection below taxiway Charlie and on taxiway Alpha. Furthermore, potential conflicts also happen at the orange arrow south of taxiway Quebec, as different flows now need to make use of one taxiway segment. To obtain the differences with the maintenance scenario, the traffic flows for this runway configuration with maintenance is presented in Figure 13b. Compared to the nominal case, just as for the other runway configuration given in Figure 12, it can be obtained from Figure 13b that taxiway Delta and a part of taxiway Alpha below the maintenance scenario are now used in both directions because of the maintenance scenario. As a result, it is expected that the task load increases in sector Center because, in this sector, now more flows are in conflict with each other compared to the nominal scenario. Furthermore, it is expected that the task load in the other sectors is not impacted by the maintenance scenario as the traffic flows in these sectors are not impacted.

For the given maintenance scenario, runway configurations where the Polder and Zwanenburg Runway are not used in opposite direction are not of interest because the flow of aircraft moving from and to the Polder and Zwanenburg Runway are not impacted such that extra bottlenecks or potential locations of violations occur. Therefore, it is expected that the task load of ground controllers is not impacted in all sectors for the other runway configurations. Furthermore, operations on runways other than the Polder and Zwanenburg Runway are not of interest for this maintenance case as the traffic flows for these runways do not pass the taxiway under maintenance.

5.2 Simulation Plan

The simulations were conducted using the agent-based simulator MAASMO-sim developed at TU Delft, written in Python, and done for each of the two runway configurations given in subsection 5.1. For these simulations, the metrics that were used to measure task load were the predicted task load by the Dynamic

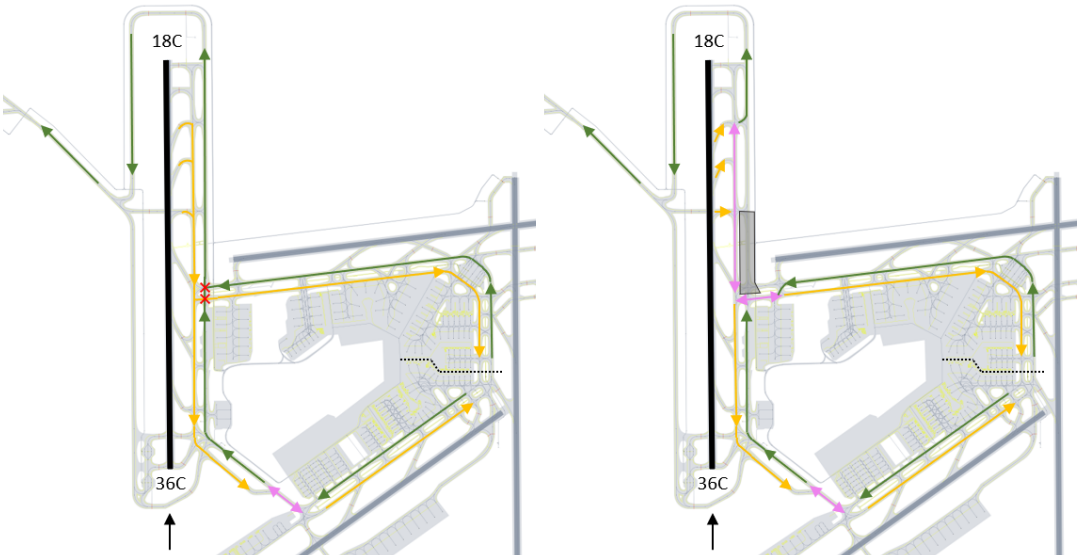

(a) Nominal case **(b)** Maintenance case

Figure 13: Traffic flows for landing on 36C and takeoff from 36L. The green arrows are outbound traffic, the orange arrows are inbound traffic, the violet arrows are flows in both direction, and the red crosses are locations of conflicting flows

Density model and the predicted violation-based task load calculated using the Violation Tool. Both were used to quantify task load for the given maintenance scenarios. The flight schedules that were used to simulate task load are all flight schedules from the year 2019, as the traffic was demanding and the two runway configurations were used relatively often in this year. For each of these runway configurations, simulations were run per flight schedule when this runway configuration was active. These flight schedules were randomly drawn from the year 2019 to include different operational dynamics as much as possible, and were used by the MAASMO-sim to predict task load for the maintenance case and the nominal case for each of these flight schedules.
To determine the necessary number of simulations, we first checked whether the simulation outputs were normally distributed using the Shapiro-Wilk test. For runway configuration 18R/18C+18L, the test proved that all simulation outcomes were non-normally distributed, except for the Dynamic Density outputs for sector South. Furthermore, for runway configuration 36C+36R/36L, the test proved that all simulation outcomes were non-normally distributed. Therefore, for all cases, the number of times simulations are run was determined by the coefficient of variation c_v defined in Equation 4.

$$c_v = \frac{\sigma}{\mu} \tag{4}$$

In Equation 4, σ is the standard deviation of the model output, and μ is the mean value of the model output [29]. The coefficient of variation was determined for all sectors, for the nominal and maintenance case and for both task load metrics. The simulations were stopped when the coefficient of variation stabilized over all sectors, cases and metrics.
For runway configuration 18R/18C+18L, all measures stabilized after 60 simulation runs. However, for the nominal case, when the Violation Tool was used to calculate the violation-based task load for sector South, stability was reached after 120 simulation runs. Furthermore, for runway configuration 36C+36R/36L, most measures stabilized after 60 simulation runs. However, for the maintenance case, where the Violation Tool was used for sector North, stability was reached after 130 simulation runs. The outcomes were analyzed for the nominal case, and the maintenance case. This was done by generating heatmaps of routes and locations of violations for the nominal case to better understand the outcomes of both metrics. Hereafter, the impact of the taxiway maintenance scenario was analyzed based on the difference in task load measured for the

maintenance case compared to the nominal case per time interval. Herefore, heatmaps were generated to show the differences in routes and violations, and this impact was tested for significance using a Vargha-Delaney A-test per controller's sector.

6 Results & Discussion

In this part, the results and discussions of these results are presented. This is done by presenting the results and discussions first for the nominal case and then for the maintenance impact for runway configuration 18R/18C+18L in subsection 6.1, and then for runway configuration 36C+36R/36L in subsection 6.2. Finally, an overall evaluation is provided in subsection 6.3.

6.1 18R/18C+18L

For runway configuration 18R/18C+18L, the results for the Dynamic Density model are provided in Table 5, and the results for the violation-based task load metric are provided in Table 6.

Sector	Nominal	Maintenance impact	A-test
Center	0.30074 ± 0.05111	0.01119 ± 0.00426	0.565
North	0.33516 ± 0.10218	0.00239 ± 0.00725	0.506
South	0.35646 ± 0.09893	0.00073 ± 0.01118	0.502

Table 5: Predicted RT load by the Dynamic Density model for runway configuration 18R/18C+18L: Mean ± standard deviation

Sector	Nominal	Maintenance impact	A-test
Center	0.68374 ± 0.89219	6.68246 ± 5.15170	0.874
North	1.70294 ± 1.97519	0.32650 ± 0.87247	0.541
South	1.64020 ± 1.60604	-0.00256 ± 0.97402	0.496

Table 6: Predicted number of re-plannings made by the ground controller by the Violation Tool for runway configuration 18R/18C+18L: Mean ± standard deviation

In Table 5 and Table 6, next to the results for both task load measures, the results of the performed Vargha-Delaney A-test between the maintenance and nominal case is given to indicate whether the obtained impact is significant [30]. The results are discussed by first discussing the nominal case in subsubsection 6.1.1, and then the maintenance impact in subsubsection 6.1.2.

6.1.1 Nominal Case

From Table 5, it can be obtained that the average predicted task load by the Dynamic Density model is moderately low. However, based on the path validation done in subsection 4.2, this predicted task load is most probably a little higher for real operations, but then still moderately low for all sectors. This is according to the expectations, because busy traffic moments where three runway are used at the same time contain build up and build down times with relatively low task load for ground controllers, and contain peak moments where the task load is relatively high. In this case, the average load is taken, which results in the outcome being located between the outcomes of these moments.
Furthermore, from Table 6, it can be seen that on average, two re-plannings by a ground controller per three time intervals is necessary for sector Center. Furthermore, for sectors North and South, on average, five re-plannings per three time intervals is necessary. To better understand the locations and quantity of these violations, the resulting flows produced by the SIMP algorithm for the nominal case are presented in Figure 14a, and the resulting heatmap of the detected violations are given in Figure 14b. In Figure 14a, the color dark blue relates to relatively many taxiway traversals, and the yellow color relates to relatively few taxiway traversals. Furthermore, in Figure 14b, the dark red colors relate to relatively many violations

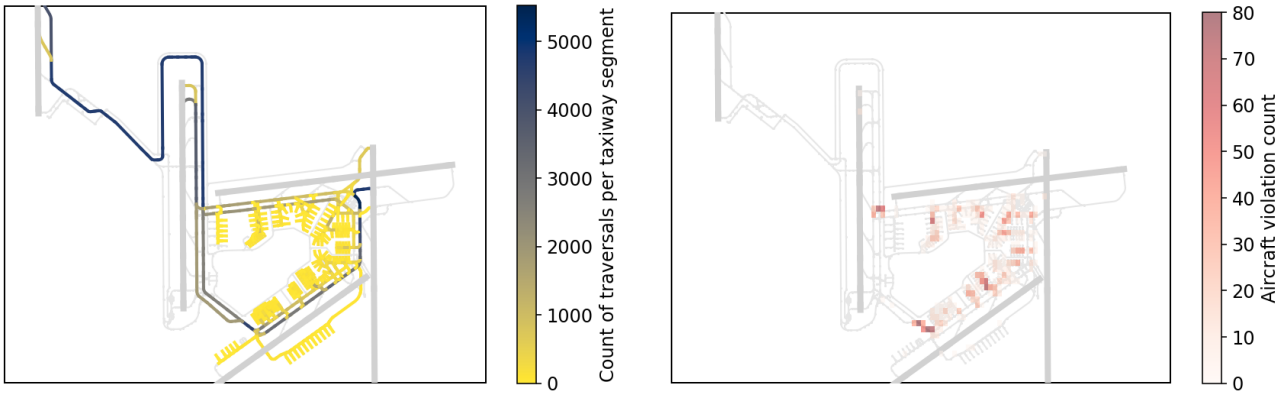

(a) Traversals of taxiway segments

(b) Location of violations

Figure 14: Traversals and violations for the nominal case and for 18R/18L+18C. In Figure 14a, the color dark blue relates to relatively many taxiway traversals, and the yellow color relates to relatively few taxiway traversals. Furthermore, in Figure 14b, the dark red colors relate to relatively many violations measured at that location, and the more light red colors relate to relatively few violations measured at that location

measured at that location, and the more light red colors relate to relatively few violations measured at that location. It may be noticed from Figure 14a that the resulting flows are similar to the expected flows shown in Figure 12a. Furthermore, from Figure 14b, it may be noticed that the locations of the violations on the taxiways are in line with the expected locations of violations shown in Figure 12a and with locations of conflicting flows shown in Figure 12a. Namely, most violations occur at the intersection between the Charlie taxiway and Bravo taxiway, and below taxiway Quebec. However, from Figure 14b, it can be seen that most of the violations occur at the aprons. This happens as ground controllers need to solve a lot of violations at the apron because aircraft normally need to wait for one another for departure. However, the intensities of violations differ per apron, where the most violations happen at aprons that are used most often by aircraft in the used flight schedules, and on aircraft stand taxilanes that serve relatively more gates than other taxilanes. Furthermore, it may be noticed from Figure 14b that also violations occur at the intersection between taxiway and apron. This is in line with the expectations, as these violations happen between aircraft that taxi along this apron and with aircraft departing and arriving on the apron, and between aircraft departing and arriving on this apron.

6.1.2 Maintenance Impact

In Table 5, it can be seen from the 'Maintenance impact' column that the predicted impact in RT load by the Dynamic Density model increases slightly in sectors Center, and negligible in sectors North and South. Furthermore, the Vargha-Delaney A-test confirms this impact for sector Center by returning a 56.5% chance that a randomly selected average RT load for the maintenance case is higher than a randomly selected average RT load for the nominal case. Therefore, it can be concluded for sector Center that there is a small difference between the nominal and maintenance case. However, for sectors North and South, the A-test returned close to 0.5, meaning that almost no differences are obtained between the nominal and maintenance case.

In Table 6, it can be seen from the 'Maintenance Impact' column that the predicted impact in re-plannings by ground controllers in sector Center increases severely. Namely, on average, twenty-one extra re-plannings per three intervals are expected to be done by the ground controller for the maintenance case compared to the nominal case. Furthermore, the impact for sector North is that the controller makes one extra re-planning per three intervals, and the impact for sector South is very small and negative, but the standard deviation is relatively high, meaning that the outcome for sector Center is spread around zero. These outcomes are confirmed by the Vargha-Delaney A-test, with a very high chance for sector Center that a randomly drawn task load output is higher for the maintenance case than for the nominal case. Therefore, it can be concluded that the violation outcomes for the maintenance case are very different than the outcomes for the nominal

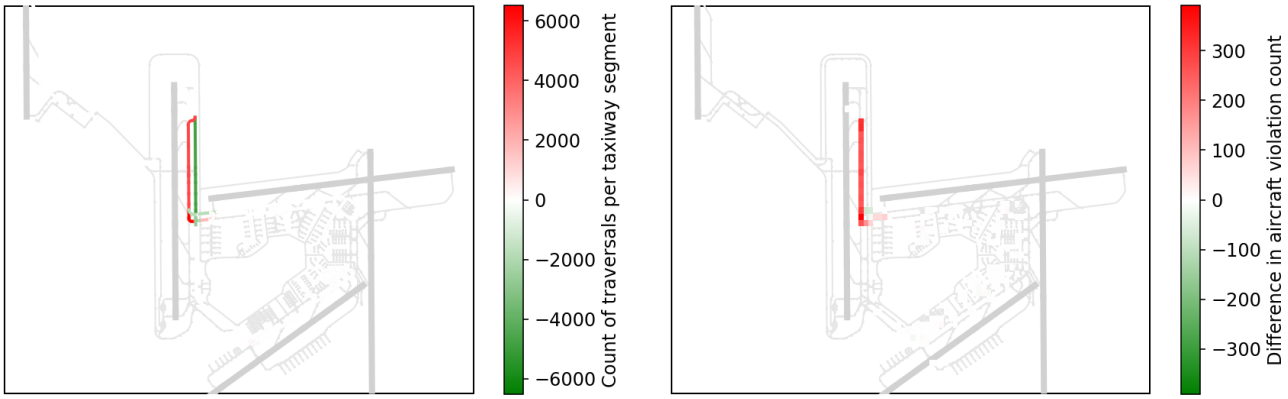

(a) Difference in taxiway traversals

(b) Difference in violation count

Figure 15: Difference in traversals and violations for 18R/18L+18C. In Figure 15a, the red color relates to more taxiway traversals and the green color relates to less taxiway traversals. Furthermore, in Figure 15b, the red color relates to more violations, and the green color relates to less violations

case. Furthermore, it can be concluded for the resulting A-test for sector North that the differences are very small, and that there is almost no difference obtained for sector South.
When comparing the outcomes of the Dynamic Density model and Violation Tool with each other, the A-tests suggests relatively similar results for sectors North and South. However, large differences are obtained for sector Center. To better understand these differences, the difference in taxiway traversals is given in Figure 15a, and the difference in violation count is given in Figure 15b. In Figure 15a, the red color relates to more taxiway traversals and the green color relates to less taxiway traversals. Furthermore, in Figure 15b, the red color relates to more violations, and the green color relates to less violations.
In Figure 15, it can be obtained that arriving aircraft now have to make use of the Delta taxiway instead of the Charlie taxiway for the maintenance case compared to the nominal case. For departing aircraft moving via the north, the difference is now that aircraft divert to taxiway Alpha to move below the taxiway part under maintenance to then continue moving onto taxiway Delta. Furthermore, for aircraft departing via the south, the flows do not change compared to the nominal case. All these differences in flows are conform expectations discussed in section 5.
The results in impact for the Dynamic Density model given in Table 5 are in line with the change in resulting flows presented in Figure 15a. For sector Center, the chance that the RT load increases is low because routes of aircraft passing through these sectors do not change that much, meaning that aircraft stay approximately the same time in the sector and communication time between pilot and controller is not impacted that much. Furthermore, for sectors North and South, almost no differences in predicted task load are obtained as no route differences in these sectors occur.
Furthermore, the results in impact for the violation-based task load metric given in Table 6 are in line with the change in location and quantity of violations shown in Figure 15b. For sector Center, it can be obtained that the number of violations increases severely as the departing and arriving flights all need to make use of the Delta taxiway and the Alpha taxiway below the part of the taxiway under maintenance. Therefore, the ground controller needs to re-plan one aircraft in each pair of conflicting aircraft for these parts of the taxiways. It is expected that this has a severely high impact on the task load for ground controllers, which is captured by the Violation Tool. Furthermore, for sector North, the impact detected by the Violation Tool is low as only extra violations are expected to occur between the departing aircraft that now need to divert to taxiway Alpha in front of the maintenance closure, and the arriving aircraft that taxi via taxiway Alpha via the north. A part of these extra violations are in sector North, and therefore it is expected that the task load in sector North increases slightly, which is detected by the Violation Tool. Then, for sector South, it is expected that no differences in re-plannings by controllers happen, as the routes in this sector do not change.
The reason that there are differences in outcomes between the Dynamic Density model and the Violation

Tool for sector Center and North is that the Violation Tool captures task load induced by violations between aircraft on the taxiways, and the Dynamic Density model not when using SIMP. In subsection 4.2, it was obtained that there is a relation between push-back operations and violations. However, as these routes on the aprons do not change, this relation cannot be obtained for this maintenance scenario and this runway configuration.

6.2 36C+36R/36L

For runway configuration 36C+36R/36L, the results for the Dynamic Density model are provided in Table 7, and the results for the violation-based task load metric are provided in Table 8.

Sector	Nominal	Maintenance impact	A-test
Center	0.31932 ± 0.05838	0.01158 ± 0.00571	0.555
North	0.30379 ± 0.07599	0.00380 ± 0.00486	0.513
South	0.26446 ± 0.07909	-0.00003 ± 0.00122	0.5

Table 7: Predicted RT load by the Dynamic Density model for runway configuration 36C+36R/36L: Mean ± standard deviation

Sector	Nominal	Maintenance impact	A-test
Center	0.54973 ± 0.81459	3.98797 ± 3.12624	0.856
North	1.00437 ± 1.38686	0.22295 ± 0.55400	0.540
South	1.16393 ± 1.40311	0.0 ± 0.04678	0.5

Table 8: Predicted number of re-plannings made by ground controller by the Violation Tool for runway configuration 36C+36R/36L: Mean ± standard deviation

In Table 7 and Table 8, next to the results for both task load measures, the results of the performed Vargha-Delaney A-test between the maintenance and nominal case is given to indicate whether the obtained impact is significant [30]. The results are discussed by first discussing the nominal case in subsubsection 6.2.1, and then the maintenance impact in subsubsection 6.2.2.

6.2.1 Nominal Case

From Table 7, it can be seen that the average predicted task load by the Dynamic Density model is moderately low. However, based on the explanation from subsection 4.2, it is expected that these outcomes are slightly higher for real operations than the SIMP-based simulation model is used. Nevertheless, the given outcomes are expected based on traffic patterns for inbound peaks.
From Table 7, it can be obtained that on average, two re-plannings per four intervals are required by ground controllers in sector Center. Furthermore, for sectors North and South, one re-planning per interval is expected to be done by ground controllers. To better understand these outcomes, the routes generated by the SIMP algorithm for this runway configuration are given in Figure 16a. In Figure 16a, the color dark blue relates to relatively many taxiway traversals, and the yellow color relates to relatively few taxiway traversals. The flows generated in this figure are mainly the same as the flows given in Figure 13a. Based on these flows, the locations of violations are given in Figure 16b. In Figure 16b, the dark red colors relate to relatively many violations measured at that location, and the more light red colors relate to relatively few violations measured at that location. In this figure, the locations of the violations on the taxiways is in line with the expected locations of violations shown in Figure 13a, meaning that potential violations that need to be solved by controllers are captured. It may be noticed from Figure 16b that the most taxiway violations occur below taxiway Quebec. The reason that this happens is because that part of the infrastructure is used in both ways by departing and arriving traffic, meaning that both flows intersect with each other at that location. This relation is also visible in Figure 16a, where that part of the infrastructure is used approximately twice as much as the other taxiway parts adjacent to this part. The number and locations

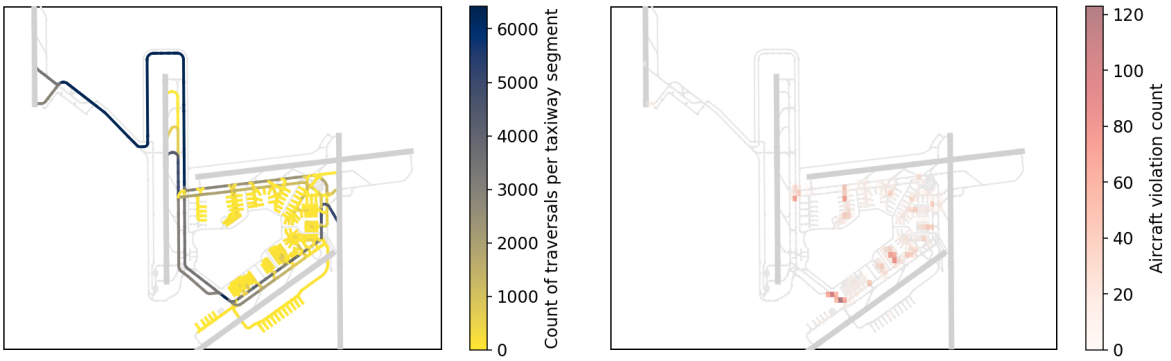

(a) Traversals of taxiway segments

(b) Location of violations

Figure 16: Traversals and violations for nominal case and for 36C+36R/36L. In Figure 16a, the color dark blue relates to relatively many taxiway traversals, and the yellow color relates to relatively few taxiway traversals. Furthermore, in Figure 16b, the dark red colors relate to relatively many violations measured at that location, and the more light red colors relate to relatively few violations measured at that location

of violations on and adjacent to the apron differs per apron, which has the same reason as for the nominal case for runway configuration 18R/18L+18C, explained in subsubsection 6.1.1.

6.2.2 Maintenance Impact

From the 'Maintenance impact' column in Table 7, it can be seen that the impact determined by the Dynamic Density model is very low for sector Center, and negligible for sectors North and South. The Vargha-Delaney A-test returns a similar result, where the chance is 55% that a randomly drawn task load outcome from the Dynamic Density model is higher for the maintenance case than for the nominal case. Therefore, it can be concluded that there is a small difference between the task load outcome for the maintenance case and the nominal case for sector Center. Furthermore, the A-test returns 0.513 for sector North and 0.5 for sector South for the Dynamic Density model, meaning that there are no differences obtained between both cases for these sectors.
From the 'Maintenance impact' column in Table 8, it can be obtained that the number of detected violations in the Center sector increases severely for the maintenance case compared to the nominal case. The Vargha-Delaney A-test confirms that there is a big difference between both cases for this sector, as this test returns an 85.6% chance that a randomly drawn task load outcome from the Violation Tool is higher for the maintenance case then for the nominal case. Furthermore, for sector North, the average number of violations detected is one extra per five intervals, which is relatively low. Therefore, the A-test returns 0.54, which indicates that the differences between the two cases for sector North is small. Then, for sector South, the average impact is zero, and is confirmed by the A-test for returning 0.5, meaning that there are no differences obtained between both cases for this sector.
To better understand these results, the differences in number of traversals of taxiway segments is given in Figure 17a and the difference in violation count is given in Figure 17b. In Figure 17a, the red color relates to more taxiway traversals and the green color relates to less taxiway traversals. Furthermore, in Figure 17b, the red color relates to more violations, and the green color relates to less violations. From Figure 17a, it can be obtained that aircraft departing from 36L and move along the north now need to divert from the Bravo taxiway to the Alpha taxiway to go around the taxiway maintenance part and further taxi via taxiway Delta instead of taxiway Charlie. Furthermore, it can be obtained that aircraft departing from 36L and move along the south now need to divert via taxiway Alpha onto taxiway Delta for the maintenance case. The routes for aircraft landing on 36C do not change for the given maintenance case. All these routes correspond to the routes presented in Figure 13b. Based on these generated routes by the SIMP algorithm, it can be obtained that these changes in routes result in a small increase in RT load compared to the nominal case because aircraft now stay longer in sector Center because of the de-tours, which results in more communication events between the controller and pilot. However, for sectors North and South, no clear route changes occur,

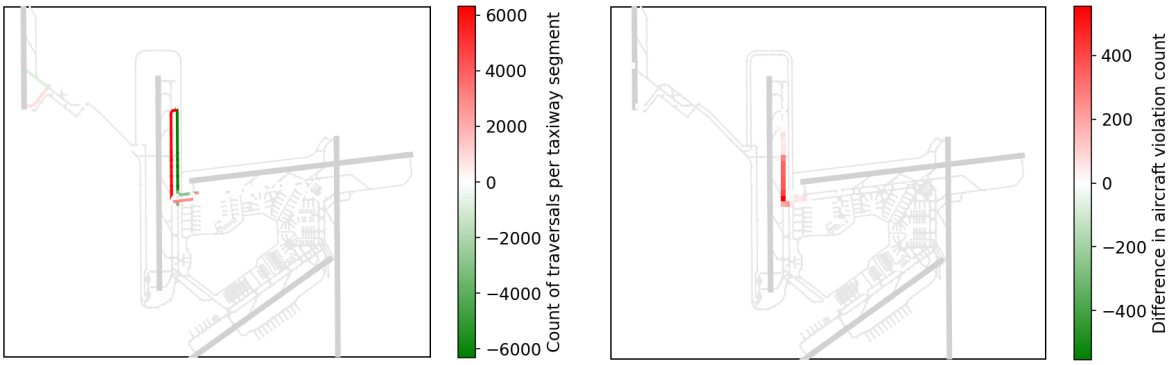

(a) Difference in taxiway traversals

(b) Difference in violation count

Figure 17: Difference in traversals and violations for 36C+36R/36L. In Figure 17a, the red color relates to more taxiway traversals and the green color relates to less taxiway traversals. Furthermore, in Figure 17b, the red color relates to more violations, and the green color relates to less violations

meaning that this results in negligible RT impact.
From Figure 17b, it can be observed that the number of detected violations increases around the maintenance site, of which most in sector Center, and some in sector North. In sector Center, these violations happen between departing aircraft and arriving aircraft on the Alpha and Delta taxiway. This increases the task load for the controller for sector Center severely, as this controller now needs to re-plan each aircraft in the conflict pair of aircraft for these two taxiways. Furthermore, the task load for sector North increases slightly, as departing aircraft moving via the North now violate the protected zones of arriving aircraft moving via taxiway Alpha because these departing aircraft now need to divert from the Bravo to the Alpha taxiway because of the maintenance scenario. No changes in violations are detected for sector South, as the routes do not change in that sector because of the considered maintenance scenario.
The reason for the differences obtained between the Dynamic Density-based and violation-based task load metrics are the same as discussed in the last part in subsubsection 6.1.2.

6.3 Overall Evaluation

For the nominal case, both the Dynamic Density model and Violation Tool have proven that they can estimate representative task load related outcomes for both runway configurations. The Dynamic Density model returns task load expected for the given runway configurations. Furthermore, the Violation Tool has proven to return locations and number of instances that are related to task load, which was not captured by the Dynamic Density model.
However, for the maintenance case, the Violation Tool showed that it could return outcomes that are better related to task load than the Dynamic Density model when using the SIMP algorithm as path planner. Namely, for both runway configurations, the paths did not change significantly for the maintenance case compared to the nominal case in all sectors, which was verified by ground controllers. However, the Violation Tool returned an output for sector Center that translates in a high task load increase for that sector because of more flows being in violation with each other. However, the Dynamic Density model did not capture this as this metric is more related to the individual routes than to the conflicts between these routes. Therefore, operational experts argued that the outcomes from the Violation Tool are better related to task load for the maintenance case compared to the Dynamic Density model, given that only shortest paths are generated.
Based on these observations, it can be concluded that small changes in the flows of aircraft because of taxiway maintenance could potentially have a big impact on the task load experienced by the ground controller of that sector. The flows of aircraft were not impacted much by taxiway maintenance. However, the emergence of an additional conflicting flow because of the maintenance scenario could locally impact the traffic flows such that the ground controller would need to put a lot of effort to solve these conflicting flows, leading to a high task load for this ground controller. These local conflict locations only impact the controller responsible for the sector in which the conflict is located. Therefore, other sectors do not experience this impact because

the controllers responsible for these sectors did not have extra work to do.

7 General Discussion

In this part, different discussion points regarding this research are presented.

7.1 Minimum Separations

The minimum separations detected by the Violation Tool are only depended on the speed, width and length of the aircraft. However, in real operations, these separations are also depended on more dynamic operational properties, such as weather, airline and location on the manoeuvring area. Therefore, the result of the violation-based task load calculation are expected to be different when including these extra properties.

7.2 Definition of Protected Zones

In this research, the definition of the protected zones are based on the minimum separations that aircraft should keep between each other. Although the violations of these protected zones gives an indication of which aircraft should've been re-planned, not all aircraft are taken into account with this definition. For example, aircraft that are approaching the same intersection from different taxiways, but are not conflicting with each other, could already be re-planned by the controller to ensure safety. These re-plannings are not taken into account, inducing a limitation on the given methodology and results. Therefore, it could be more representative to change the definition of the protected zones to the area of regard of the controller, that changes dynamically based on perceptions of controllers whether a new re-planning is necessary. However, this approach is very controller depended, meaning that close collaboration with ground controllers is necessary, which was not possible for this research.

7.3 Conflict Resolution

In reality, conflicts between aircraft are solved by the controller. However, the dynamics that follow from these resolutions are not taken into account by the proposed methodology. Therefore, violations that are measured might not happen in real operations, or certain violations that might occur in real operations are not taken into account. This places a limitation on the trustworthiness of the obtained results.

7.4 Definition of Conflicts

In this research, the assumption is made that a conflict induces a unity task load on the controller based on discussions with operational experts. However, the experienced task load by the controller could be different depending on the type of violation. For example, task load experienced by solving apron violations could be lower than task load experienced by solving violations between aircraft leaving the runway and taxiing aircraft, as there is more uncertainty involved.

7.5 Runway Configurations for Validation

The runway configurations used for the validation are different than the runway configurations used for the analysis. Although some similarities are expected to be the same for the different runway configurations, including the relation between push-backs and violations, it might be more accurate and representative to use the same runway configurations for validation as for analysis.

7.6 Operational Applicability of Runway Configuration 36C+36R/36L

In this research, one of the two runway configurations that are studied is runway configuration 36C+36R/36L. Although this runway configuration is used during nominal operations, this configuration is most probably never used during the studied maintenance scenario. Namely, in the maintenance scenario, departing aircraft from 36L and landing aircraft on 36C make use of the Delta taxiway, where the landing aircraft have priority over the departing aircraft for safety reasons. However, it is uncertain when aircraft land, meaning that it is difficult for the controller to provide clearance to the departing aircraft to make use of the Delta taxiway.

Therefore, the flows shown in Figure 13a will never be obtained for runway configuration 36C+36R/36L for the given maintenance scenario.

7.7 Deterministic

Outcomes generated by the Dynamic Density model and Violation Tool are deterministic, meaning that the same outcome is generated per scenario. In reality, more stochastic processes are present, which include weather, delays of aircraft, towing traffic and the aircraft movements themselves. Therefore, this makes the outcomes rather simplistic compared to the real operations.

7.8 Task Load Indicators

This research introduced a new additional metric next to the already used Dynamic Density model to describe task load. However, more task load indicators may exist that impact the controllers for the given taxiway maintenance scenario. Based on discussions with ground controllers, these indicators might include aircraft delays and towing movements. For this taxiway maintenance scenario, it is expected that towing movements have a large impact on the task load of ground controllers. This is because to the right of the Charlie runway and above the taxiway maintenance scenario a platform for aircraft is located. For the given maintenance scenario, towing movements from and to this platform now need to move over the Delta runway, meaning that it is expected that these taxiway movements have a large impact on the task load of ground controllers in sector Center.

7.9 Aircraft Kinematics

In this research, aircraft travel from start to goal node following their shortest path, and with their highest speed possible because the paths of other aircraft are not taken into account. However, in real operations, aircraft move slower over the surface because conflict resolution is taken into account. Although the results have shown that locations of potential violations were captured well by the provided methodology, changing the aircraft kinematics to relate them more to real operations could potentially result in more accurate results regarding conflict location and quantification because the moments of and quantity of re-planning of ground controllers is now better captured.

7.10 Impact on Aircraft Flows

In this research, the impact on the traffic flows as a result of the taxiway maintenance scenario for the two runway configurations were small. However, this impact could be larger for different maintenance scenarios. For example, closing down a taxiway for maintenance such that the entrance and exit of an apron is blocked could result in aircraft moving via a different apron entry or exit, which has a big influence on the aircraft flows, and potentially also on the task load experienced by ground controllers.

8 Conclusion & Future Work

This research aimed to evaluate the impact of taxiway maintenance on the task load of ground controllers for different runway configurations. The given goal has partially been achieved by making use of the single-agent path planning algorithm SIMP in the context of the existing agent-based simulator for airport surface movement operations, where its calculated paths are used for a Dynamic Density model for Ground Control, and for a newly introduced metric that aimed to calculate the re-plannings of ground controllers. The paths generated by SIMP were validated using real operational route data, and both metrics were compared to each other for northern and southern runway use. Then, both metrics were used to evaluate the task load experienced by ground controllers for a taxiway maintenance scenario and two runway configurations. Different flight schedules were considered for each of these runway configurations, where the difference in aircraft flows and locations of potential violations were compared between the nominal and maintenance scenario.
As an outcome, it can be concluded that the emerging of additional conflicting flows because of taxiway maintenance has a high impact on the task load of ground controllers. Although the flows of aircraft were

not impacted that much for taxiway maintenance scenarios, an additional conflict between different flows could potentially have a large impact on the task load of ground controllers. These conflicts are runway configuration dependant. Furthermore, this increase in task load happens locally, meaning that only the controller responsible for the sector where these additional flow conflicts happen experience extra task load.

In this study, only differences in aircraft flows are considered. For future studies, it is recommended to also include different operational indicators that could be impacted by taxiway maintenance. These indicators include the delay of aircraft and towing traffic. Furthermore, it is recommended to further work on this principle of violation detection by implementing an algorithm that solves these violations based on controller decision-making to optimize violation quantification, and to value different types of violations differently. Also, it is recommended to simulate more taxiway maintenance scenarios for different locations on the airport infrastructure to better understand the impact of taxiway maintenance on the task load of ground controllers.

References

[1] K. Fines, "Agent-based distributed planning and coordination for resilient airport surface movement operations (master of science thesis)," *TU Delft*, 2019.

[2] M. Brouwer, E. van Calck, J. Knoester, T. Joustra, N. Schmidt, and S. Heblij, "Baan beschikbaarheid strategie 2015," 2016. Internal document.

[3] Air Traffic Control The Netherlands, "Werkboek ut spl gnd," 2023. Internal document.

[4] Air Traffic Control The Netherlands, "Conops schiphol ground control," 2022. Internal document.

[5] MovingDot, "Functional analysis of schiphol twr-c," *Knowledge and Development Centre Mainport Schiphol*, 2017.

[6] K. Brookhuis, C. van Driel, T. Hof, B. van Arem, and M. Hoedemaeker, "Driving with a congestion assistant; mental workload and acceptance," *Applied Ergonomics*, vol. 40, no. 6, pp. 1019–1025, 2008. DOI: 10.1016/j.apergo.2008.06.010.

[7] W. Rouse, J. Hammer, and S. Edwards, "Modeling the dynamics of mental workload and human performance in complex systems," *IEEE Transactions on Systems Man and Cybernetics*, pp. 1–27, 1993. DOI: 10.1109/21.257761.

[8] S. Hart and L. Staveland, "Development of nasa-tlx (task load index): Results of empirical and theoretical research," *Advances in Psychology*, vol. 52, pp. 139–183, 1988. DOI: https://doi.org/10.1016/S0166-4115(08)62386-9.

[9] E. Wilschut, "The impact of in-vehicle information systems on simulated driving performance: Effects of age, timing and display characteristics," 2009. Thesis, University of Groningen.

[10] R. Mogford, J. Guttman, S. Morrow, and P. Kopardekar, "The complexity construct in air traffic control: A review and synthesis of the literature," *CTA INCORPORATE*, 1995. Report no.: DOT/FAA/CT-TN9S/22.

[11] S. Brunia, "Task load estimation for atc ground control: A dynamic density-based analysis (master of science thesis)," *TU Delft*, 2023.

[12] J. The, "Optimizing ground movements considering taxiway renovation," 2020.

[13] Z. Chua, M. Cousy, M. Causse, and F. Lancelot, "Initial assessment of the impact of modern taxiing techniques on airport ground control," *SESAR*, p. 8, 2016. DOI: 10.1145/2950112.2964589.

[14] M. von der Burg, J. Kamphof, J. Soomers, and A. Sharpanskykh, "Towards autonomous airport surface movement operations using hierarchical multi-agent planning," 2024. Available at SSRN: https://ssrn.com/abstract=4916874.

[15] L. Cohen, T. Uras, T. Kumar, and S. Koenig, "Optimal and bounded-suboptimal multi-agent motion planning," *Proceedings of the Twelfth International Symposium on Combinatorial Search (SoCS 2019)*, pp. 44–51, 2019. DOI: https://doi.org/10.1609/socs.v10i1.18501.

[16] J. Kamphof, "Design and analysis of tug-enabled engine-off taxiing operation using hierarchical multi-agent planning (master of science thesis)," *TU Delft*, 2022.

[17] Air Traffic Control The Netherlands (LVNL), "Amsterdam/schiphol aerodrome ground movement chart - ad 2.eham-gmc.1," 2024.

[18] Royal Schiphol Group, "Traffic review 2023," 2023.

[19] Royal Schiphol Group, "Cobra complan mjop goh rijbaan a a13-a15 fase 5: Ova 35753," 2021. Internal document.

[20] LVNL, "Ass2 conops schiphol ground control," 2022. Internal document.

[21] M. Phillips and M. Likhachev, "Sipp: Safe interval path planning for dynamic environments," *Proceedings - IEEE International Conference on Robotics and Automation*, p. 5628–5635, 2011. DOI: 10.1109/ICRA.2011.5980306.

[22] M. von der Burg and A. Sharpanskykh, "Modelling and analysis of autonomous airport surface movement operations based on multi-agent planning: Explorative case study at amsterdam airport schiphol," *European Journal of Transport and Infrastructure Research*, vol. 25, no. 1, pp. 1–23, 2025. DOI: https://doi.org/10.59490/ejtir.2025.25.1.7459.

[23] M. von der Burg and A. Sharpanskykh, "Exploring human-automation interactions in next-generation airport surface movement operations: an agent-based modelling approach," *SESAR*, pp. 1–9, 2024.

[24] D. Yuan, X. Zhu, Y. Zou, and Q. Zhao, "Integrated optimization of scheduling for unmanned follow-me cars on airport surface," *Scientific Reports*, pp. 1–23, 2024. DOI: https://doi.org/10.1038/s41598-024-58918-7.

[25] S. van Oosterom, M. Mitici, and J. Hoekstra, "Dispatching a fleet of electric towing vehicles for aircraft taxiing with conflict avoidance and efficient battery charging," *Transportation Research Part C*, vol. 147, pp. 1–21, 2023. DOI: https://doi.org/10.1016/j.trc.2022.103995.

[26] G. Hughes and M. Chraibi, "Calculating ellipse overlap areas," *Computing and Visualization in Science*, vol. 15, no. 5, pp. 291–301, 2012. DOI: 10.1007/s00791-013-0214-3.

[27] F. Etayo, L. Gonzalez-Vega, and N. del Rio, "A new approach to characterizing the relative position of two ellipses depending on one parameter," *Computer Aided Geometric Design*, vol. 23, no. 4, pp. 324–350, 2006. DOI: 10.1016/j.cagd.2006.01.002.

[28] R. Sargent, "Verification and validation of simulation models," *Proceedings of the 2010 Winter Simulation Conference*, pp. 166–183, 2010. DOI: 10.1109/WSC.2010.5679166.

[29] A. Sharpanskykh, "Lecture 5: Analysis of simulation results; slide 3," 2022.

[30] A. Sharpanskykh, "Lecture 5: Analysis of simulation results; slide 8," 2022.

A Appendix

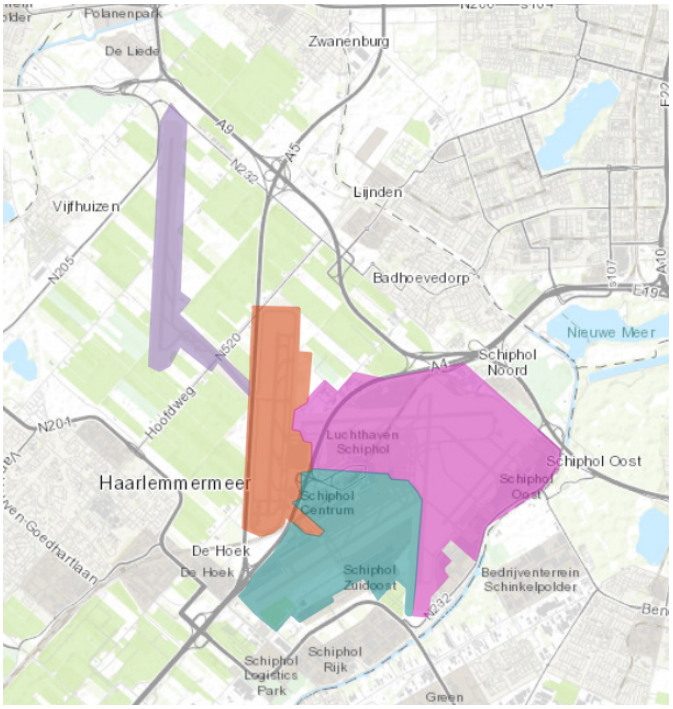

Figure A.1: All sectors at Schiphol Airport: Sector West (Purple), Sector Center (Orange), Sector South (Blue) and Sector North (Pink)

Algorithm 1 Relative position of two protected zones. In this algorithm, h_1 and k_1 are the translation coordinates of the center of the ellipse of aircraft 1 with respect to the origin of the given coordinate system. The same holds for h_2 and k_2, which are the coordinates of the center of the ellipse of aircraft 2. Furthermore, l_{ac1} and l_{ac2} are the lengths of aircraft 1 and aircraft 2, w_{ac1} and w_{ac2} are the widths of aircraft 1 and aircraft 2, $k_{weightac1}$ and $k_{weightac2}$ are the weight factors of aircraft 1 and aircraft 2, v_{ac1} and v_{ac2} are the speeds of aircraft 1 and aircraft 2, and φ_1 and φ_2 are the headings of aircraft 1 and aircraft 2 [26].

Input: h_1, h_2, k_1, k_2, l_{ac1}, l_{ac2}, w_{ac1}, w_{ac2}, $k_{weightac1}$, $k_{weightac2}$, v_{ac1}, v_{ac2}, φ_1, φ_2

$A_1 \leftarrow l_{ac1} \cdot k_{weightac1} + v_{ac1}$
$A_2 \leftarrow l_{ac2} \cdot k_{weightac2} + v_{ac2}$
$B_1 \leftarrow \frac{w_{ac1}}{2} \cdot k_{weightac1} + v_{ac1}$
$B_2 \leftarrow \frac{w_{ac2}}{2} \cdot k_{weightac2} + v_{ac2}$

Determine coefficients of symmetric matrix A for the protected zone of aircraft 1

$a_{1,1} \leftarrow \frac{cos^2(\varphi_1)}{A_1^2} + \frac{sin^2(\varphi_1)}{B_1^2}$
$a_{1,2} \leftarrow \frac{sin(\varphi_1)\cdot cos(\varphi_1)}{A_1^2} - \frac{sin(\varphi_1)\cdot cos(\varphi_1)}{B_1^2}$
$a_{2,2} \leftarrow \frac{sin^2(\varphi_1)}{A_1^2} + \frac{cos^2(\varphi_1)}{B_1^2}$
$a_{1,3} \leftarrow \frac{-cos(\varphi_1)\cdot(h_1\cdot cos(\varphi_1)+k_1\cdot sin(\varphi_1))}{A_1^2} + \frac{sin(\varphi_1)\cdot(k_1\cdot cos(\varphi_1)-h_1\cdot sin(\varphi_1))}{B_1^2}$
$a_{2,3} \leftarrow \frac{-sin(\varphi_1)\cdot(h_1\cdot cos(\varphi_1)+k_1\cdot sin(\varphi_1))}{A_1^2} + \frac{cos(\varphi_1)\cdot(h_1\cdot sin(\varphi_1)-k_1\cdot cos(\varphi_1))}{B_1^2}$
$a_{3,3} \leftarrow \frac{(h_1\cdot cos(\varphi_1)+k_1\cdot sin(\varphi_1))^2}{A_1^2} + \frac{(h_1\cdot sin(\varphi_1)-k_1\cdot cos(\varphi_1))^2}{B_1^2} - 1$

Determine coefficients of symmetric matrix B of the protected zone of aircraft 2

$b_{1,1} \leftarrow \frac{cos^2(\varphi_2)}{A_2^2} + \frac{sin^2(\varphi_2)}{B_2^2}$
$b_{1,2} \leftarrow \frac{sin(\varphi_2)\cdot cos(\varphi_2)}{A_2^2} - \frac{sin(\varphi_2)\cdot cos(\varphi_2)}{B_2^2}$
$b_{2,2} \leftarrow \frac{sin^2(\varphi_2)}{A_2^2} + \frac{cos^2(\varphi_2)}{B_2^2}$
$b_{1,3} \leftarrow \frac{-cos(\varphi_2)\cdot(h_2\cdot cos(\varphi_2)+k_2\cdot sin(\varphi_2))}{A_2^2} + \frac{sin(\varphi_2)\cdot(k_2\cdot cos(\varphi_2)-h_2\cdot sin(\varphi_2))}{B_2^2}$
$b_{2,3} \leftarrow \frac{-sin(\varphi_2)\cdot(h_2\cdot cos(\varphi_2)+k_2\cdot sin(\varphi_2))}{A_2^2} + \frac{cos(\varphi_2)\cdot(h_2\cdot sin(\varphi_2)-k_2\cdot cos(\varphi_2))}{B_2^2}$
$b_{3,3} \leftarrow \frac{(h\cdot cos(\varphi_2)+k\cdot sin(\varphi_2))^2}{A_2^2} + \frac{(h\cdot sin(\varphi_2)-k\cdot cos(\varphi_2))^2}{B_2^2} - 1$

Calculate coefficients of det($\lambda \cdot$ [A] + [B]) = $\lambda^3 + \mathbf{a} \cdot \lambda^2 + \mathbf{b} \cdot \lambda + \mathbf{c}$
Interpret coefficients of $\lambda^3 + \mathbf{a} \cdot \lambda^2 + \mathbf{b} \cdot \lambda + \mathbf{c}$ (once turned monic)

$s_4 \leftarrow -27 \cdot c^2 + 18 \cdot c \cdot a \cdot b + a^2 \cdot b^2 - 4 \cdot a^3 \cdot c - 4 \cdot b^3$
$s_1 = a, s_2 = a^2 - 3 \cdot b, s_3 = 3 \cdot a \cdot c + b \cdot a^2 - 4 \cdot b^2$
if $s_4 < 0$ **then**
    Return: Protected zones transverse each other at two points
else if $s_4 > 0$ **then**
    if $s_1 > 0$ & $s_2 > 0$ & $s_3 \geq 0$ **then**
        $u = \frac{-a-\sqrt{s_2}}{3}$, $v = \frac{-a+\sqrt{s_2}}{3}$
        $[M] = u \cdot [A] + [B], [N] = v \cdot [A] + [B]$
        if $(m_{2,2} \cdot det(M) > 0$ & $det(M_{1,1}) > 0)$ OR $(n_{2,2} \cdot det(N) > 0$ & $det(N_{1,1}) > 0)$ **then**
            Return: One protected zone is contained in the other
        else
            Return: Protected zones transverse each other at four points
        end if
    else
        Return: Protected zones are separated
    end if
else
    "See next page"

if $s_2 > 0$ & $s_3 < 0$ **then**
  Return: Protected zones are externally tangent to each other
else if $s_1 > 0$ & $s_2 > 0$ & $s_3 > 0$ **then**
  $\beta = \frac{9 \cdot c - a \cdot b}{2 \cdot s_2}, \alpha = \frac{4 \cdot a \cdot b - a^3 - 9 \cdot c}{s_2}$
  $[M] = \beta \cdot [A] + [B], [N] = \alpha \cdot [A] + [B]$
  if $det(M_{3,3}) > 0$ **then**
    if $det(N_{3,3}) > 0$ **then**
      Return: Protected zones transverse each other at two points and are tangent at one point
    else
      Return: Protected zones are internally tangent at one point to each other
    end if
  else if $det(M_{1,1}) + det(M_{2,2}) > 0$ **then**
    Return: One protected zone is contained in the other
  else
    Return: Protected zones are internally tangent at two points to each other
  end if
else
  $\alpha = \frac{-a}{3}$
  $[M] = \alpha \cdot [A] + [B]$
  if $(det(M) = 0$ & $det(M_{3,3}) \leq 0) OR (det(M) \neq 0$ & $det(M_{3,3}) \leq 0$ & $(\frac{det(M)}{(m_{1,1} + m_{2,2})} < 0))$ **then**
    Return: Protected zones coincide
  else if $det(M) \neq 0$ & $det(M_{3,3}) > 0$ **then**
    Return: Protected zones transverse each other at one point and are tangent at one point
  else
    Return: Protected zones are internally tangent at one point to each other
  end if
end if=0

II

Literature Study

1

Introduction

Royal Schiphol Group (RSG) wants to carry out its runway maintenance as efficiently and optimally as possible. To make this possible, Schiphol and its partners have drawn up the Runway Maintenance Strategy (In Dutch; Baanonderhoudsstrategie (BOS)). This strategy states that runway work will be saved up over a certain period, and then clustered and carried out integrally at a single point in time without causing the performance of individual assets to fall below the desired level [13]. Following the BOS, maintenance plans have been drawn up for the runways, but not yet for the taxiways. When making maintenance plans for the taxiways, it is important to take into account the traffic handling of aircraft at the airport to ensure that this handling can continue to take place safely and as planned.
The problem is now that taxiway maintenance timing is determined based on technical necessity, and often not based on the impact on ground operations. Including the impact on operations is then done at a later stage, resulting in maintenance projects being pushed through because it is not operationally feasible. This pass-through can be prevented by quantifying effects on operations at an early stage. This allows these effects to be taken into account when planning maintenance. An important operational effect that depends on maintenance planning is the impact on the workload of ground controllers. This workload should not become too high due to runway and taxiway maintenance, otherwise safety and ground capacity at the airport will deteriorate. It is therefore essential to study the relationship between the closure of (parts of) taxiways due to maintenance and the workload of ground controllers in order to test the feasibility of maintenance plans. However, there are no maintenance models that take into account workload as an indicator.

The goal of this report is to provide a literature study that results in a research plan that supports in providing insight in the impact of taxiway maintenance on the workload of ground controllers. This is done by reading literature about taxiway maintenance and the workload of ground controllers, and its related areas. These related areas emerge from the observations done in the taxiway maintenance and workload parts of the literature study.

This report is structured as follows. First, in chapter 2, the maintenance planning process for both the runways as for the taxiways are discussed. Then, in chapter 3, the airside airport operations at Amsterdam Airport Schiphol (AAS) are described. Hereafter, in chapter 4, the Ground Control unit at Schiphol Airport is discussed. Consequently, in chapter 5, the workload of ground controllers is discussed. Then, in chapter 6, the violations of minimum separations between aircraft is discussed. Hereafter, in chapter 7, the principle of multi-agent path finding and single-agent path planning algorithms are discussed. Finally, in chapter 8, the proposal for this research is given, including the research methodologies to be used and its related work packages.

2

AAS Maintenance Planning

In this chapter, the different aspects of runway and taxiway maintenance are described. In section 2.1, the runway maintenance planning process is described. Then, in section 2.2, the taxiway maintenance planning process is described. Hereafter, in section 2.3, the requirements for the model made in this project are given. Lastly, in section 2.4, the taxiway maintenance scenario for this research is described.

2.1. Runway Maintenance

To make sure runway maintenance is planned efficiently, Royal Schiphol Group has set up a runway maintenance strategy (in Dutch; Baanonderhoudsstrategie (BOS)), which is subdivided into three phases over time [43].
In the first phase of the runway maintenance strategy, the runway availability strategy is set up. This strategy, delivered in 2016, is made to give insight into important aspects of runway availability and the influence of maintenance on this. The outcome of this phase is an advice from AAS on a new long-term strategy [43].
In the second phase of the runway maintenance strategy, a quantitative analysis was set up. Using this analysis, research has been done for the optimal future runway maintenance strategy, including possible differentiation by runway. The outcome of this phase, delivered in 2018, is a runway maintenance strategy from sector and environmental perspective. Furthermore, this strategy consists of medium and heavy maintenance variants, and includes the preferred maintenance period [43].
In the third phase of the runway maintenance strategy, the runway implementation strategy and long-term plan are set up. This strategy and plan, made in 2019, are made per runway for the chosen runway maintenance strategy. The outcome of this phase is a long-term maintenance plan for each runway with type, nature and extent of work per maintenance moment [43].
Each of these phases are described more in-depth in the following subsections. In subsection 2.1.1, phase 1 is described. Hereafter, in subsection 2.1.2, phase 2 is described. Then, in subsection 2.1.3, phase 3 is described.

2.1.1. Phase 1: Runway Availability Strategy

From 2010 onwards, it has been noticed that the traffic volume increases, but the availability of runways decreases. The consequence of this could be that the on-time performance of air traffic will deteriorate, the peak-hour capacity will be obstructed, more pressure will be applied to get planned maintenance feasible, nuisance for local residents will increase as fewer preferential runways are used and that there will be risk of interference in the operational management process from the competent authority because necessary exemptions are not granted automatically. Furthermore, an intensification of maintenance activities on airside infrastructure is anticipated in the coming years. Therefore, the runway availability strategy is reassessed. The reassessed strategy should balance the operational excellence, environmental capacity and technical feasibility. The outcomes of this reassessment are in this subsection discussed [13]. For the purpose of this study, only the parts of the strategy that deal with the effects of runway maintenance are discussed.

Sustainability & Declared Capacity

For Schiphol airport, it is very important that the declared hourly capacity, on the basis of which slots are allocated and schedules are set, can be realised in practice under (almost) all circumstances. In this case, the hourly capacity is the maximum number of take-offs and landings that are able to take place in an hour. Sustainability is an indicator of the reliability of the declared hourly capacity and indicates the percentage of time in which the declared hourly capacity can be achieved [13].
The relation between the declared capacity (DC) and sustainability is given in Equation 2.1.

$$S = \frac{min(DC, C_i)p_i}{DC} \tag{2.1}$$

In Equation 2.1, S is the sustainability, i is the indicator for the runway configuration, C_i is the hourly capacity for runway capacity i, p_i is the usage rate for runway configuration i and DC is the chosen Declared Capacity. In this case, the chosen Declared Capacity is the number of movements per hour the slot coordinator is allowed to schedule [13].
If there is limited availability of the runway system during a certain period of the year, the use of runway configurations will change, simply because some runways are not available. Usually, this results in temporarily lower sustainability. Using Equation 2.1, it may be noticed that a good measure could be to lower the Declared Capacity by reducing the number of slots. In practice however, this reduction in the number of slots issued is not easily possible because slots are almost always linked to historic rights. Therefore, it cannot be prevented that the sustainability will decrease [13].
However, when increasing the Declared Capacity in a future situation by, for instance, developments of the ATM system, it is possible to take into account an anticipated reduction of the sustainability. If it is anticipated that runway availability will be severely restricted in the future as a result of a chosen maintenance strategy, this may give cause to abandon the desired growth in Declared Capacity. This could limit the airport's growth potential, resulting in reduced revenue generation. Furthermore, choosing a lower sustainability is not an option because this could limit the profits generated by the airport and its stakeholders. Therefore, the runway maintenance strategy needs to ensure that the increase in Declared Capacity over time is taken into account, and that the sustainability is not greatly affected [13].

Taxi Times & Fuel Use

The taxi times and fuel use my be impacted due to runway maintenance. When the taxi time of an aircraft increases, the fuel use of an aircraft increases, and therefore also the climate impact and costs of airlines increases. Therefore, limiting the taxi times is one of the aspects that are taken into account when planning maintenance [13].
From the analysis that has been made by Schiphol, it is concluded that the effect of runway maintenance on fuel consumption is stronger in the summer season than in the winter season. The reason is not only due to having more flights in the summer, but also because parallel take-offs/landings are more frequent in the summer months due to the more favourable weather.
When looking at the effects of maintenance on fuel consumption per runway, it can be obtained that the fuel consumption decreases when the Polder Runway is under maintenance. When the Kaag Runway is in maintenance, the fuel consumption increases severely because most of the flights now have to make use of the relatively far-way laying Polder Runway. The impact on fuel consumption when there is maintenance on the Aalsmeer Runway or Buitenveldert Runway is not that significant compared to the closure of other runways. However, a positive effect on fuel consumption is obtained when the Zwanenburg Runway is closed due to maintenance because then a shorter route via W5 to the Polder Runway is created [13].

Delays

When only using data for the first inbound peak, it can be concluded that the impact on the delays of aircraft due to maintenance over the whole year is approximately the same. To minimise the delay during the first inbound peak, maintenance is best carried out in the summer months, if only optimising on the first inbound peak [13].
Despite the fact that there is more traffic in the summer months and thus it might be thought that there would be more chance of delays in summer, the opposite turns out to be true. This is because in winter, due to the poorer weather, there is more chance of having to apply 1+1 runway use during

the first inbound peak due to runway maintenance. In summer, due to the predominant possibility of using 1+2 in the first inbound peak, this problem occurs to a lesser extent [13].

Effect on Ground Control Workload

No specific analyses are done to give insight into the effect of runway maintenance on the ground control workload. However, Air Traffic Control the Netherlands (LVNL) has specified that Ground Control is currently a limiting factor for airport capacity. The workload of a ground controller is determined, among other indicators, by the RT load. This RT load relates to how many aircraft are taxiing to and from the runway. Now, the rough assumption can be made that this number of aircraft in the taxi phase is proportional to the duration of the taxi phase. Indeed, the longer the taxi phase, the higher the number of aircraft in the taxi phase at a given hourly capacity. Since the additional fuel costs determined earlier are highly dependent on the overall duration of the taxi phase, it can be argued that aiming to minimise fuel costs for the taxi phase of all flights simultaneously is a minimisation of the ground controller's workload. However, it should be noted that this relationship is all explanatory. The unavailability of a major taxiway (e.g. Bravo) may result in opposing taxi flows, increasing (much) the ground controller's workload [13].
From this, it could be argued that closing down the Kaag Runway results in a higher workload compared to closing down other runways because the total fuel costs for the airlines are higher when closing down the Kaag Runway.

Snowballing

It has been obtained that snowballing has a negative effect on the workload of ground controllers and long-term delays. Snowballing is the knock-on effect of delays over a longer period of time, due to the traffic volume exceeding handling capacity for a longer period of time. This effect occurs mainly when the daily volume is relatively high. Therefore, a recovery after a disruption is difficult because throughout the day, traffic volume is close to handling capacity. Furthermore, it is difficult to implement a recovery because use of runway configuration 2+2 is constrained. So, the runway maintenance strategy should take into account snowballing to limit the effects on the workload of ground controllers and delays. To limit snowballing, it is recommended to undertake maintenance in the preseason due to lower traffic demand compared to the summer season [13].

Nuisance Perception of Local Residents

Runway maintenance could have a negative effect on the nuisance perception of local residents because less preferential runways may be used more during maintenance, which increases the perception of nuisance experienced by local residents. However, the local residents do have preferences concerning runway maintenance. One of these preferences is that runway maintenance is undertaken in the winter period instead of in the summer period. Furthermore, their preference is that maintenance is undertaken by day, and not by night. Also, they don't want that maintenance takes place during the weekends, and that maintenance works are combined as much as possible. Furthermore, the maintenance works needs to be announced well in advance and widely, it needs to take place as little as possible and as short as possible. When quantifying the effects of maintenance works on the nuisance of local residents, it is obtained that the outcomes of this quantification confirms the preferences of the local residents [13].

General Outcome

Based on the findings of phase 1, it is recommended that major maintenance works for all the runways needs to take place in the preseason, and all the normal maintenance works for all the runways need to take place in the main season (summer period). Further refinement of this strategy is made in the following phases [13].

2.1.2. Phase 2: Quantitative Analysis

In this case, long-term runway maintenance works leads to closure of the runway for approximately 16 weeks. Furthermore, there needs to be a maintenance interval of at least 7 till 8 years. Also, maintenance works during day and night need to be taken into account. Based on these findings, further refinement of this strategy has been done by performing a benchmark, and by defining which period is best to perform maintenance based on the outcome of the benchmark. The benchmark is discussed in the first sub-subsection, and the definition of the periods is discussed in the second sub-subsection [44].

Maintenance Type	Maintenance Goal	U/S	Maintenance Perspective
Heavy Maintenance	Integral heavy maintenance, clustering of assets, until next heavy maintenance in 15 years	10-16 weeks, 24/7	15, 30, 45 years
Medium Maintenance	Replace coating to ensure the performance of the coating, especially skid resistance and water retention capacity, for the next 7-8 years	3-4 weeks 24/7, during the night (14-20 week lead time of a full runway)	7-8 years
Light Maintenance	Ensuring operational quality and preventing unnecessarily accelerated degradation of assets. Maintenance of assets that cannot wait until the next medium or heavy maintenance moment.	1 week 24/7	Yearly (maximum 1 runway simultaneously under maintenance)
Normal/ regular Maintenance	Ensuring operational availability/ EASA compliancy	Night	High frequency (monthly/ 6 weeks)

Table 2.1: Characteristics per maintenance type [44]

Benchmark

In the first sub-phase, a benchmark with other airports was performed. This benchmark was performed to give insight into how maintenance can be best carried out. Differentiation is made between airports containing one runway and airports containing multiple runways. Based on this benchmark, it has been decided to cluster maintenance in heavy, medium and light maintenance. Furthermore, it is concluded that a fixed maintenance cycle is applied to limit the number of maintenance moments. Also, the preference is to apply maintenance during the day instead of during the night, due to costs and quality. It has further been obtained that heavy maintenance can not only be done during the night [44]. The characteristics per maintenance type are defined, and are presented in Table 2.1.

Maintenance Period

Based on the benchmark presented in the last sub-subsection, the optimal period to undertake runway maintenance is studied. This period should result in the least expected additional cost due to delays due to runway maintenance. To obtain this, three different implementation periods are defined. The first period is the summer full closure, which is from week 16 until week 36. Then, the second period is the winter full closure, which is from week 37 until week 15, not including week 48 until week 4. The third execution period is during the night, with only maintenance windows from 20:00 till 06:00 considered realistic. In this case, heavy maintenance can only be undertaken for a full-day regime (24/7), so this maintenance type only applies for summer or winter full closure. However, medium maintenance could also be undertaken during summer nights [44].
Then, for each runway in maintenance and for each implementation period, three different aspects are determined. The first aspect is the implementation costs for medium and heavy maintenance. Then, the second aspect is the expected delay costs for the runway system for medium and heavy maintenance. At last, the third aspect is the number of severely annoyed and sleep disturbances for medium and heavy maintenance. However, for the quantitative analysis, only the implementation costs and expected delay costs are taken into account. The reason is, is that for the third aspect, the outcomes of the calculations are not representative for the real nuisance experienced by local residents [44].
The result of the quantitative analysis are preferred periods for medium and heavy maintenance, and are presented in Table 2.2.

The runway maintenance strategy includes integrality, predictability and planability of maintenance works [44]. Using the outcomes of this second phase, the third phase structures an implementation strategy per runway, which is discussed in subsection 2.1.3.

Runway	Heavy maintenance	Medium maintenance
18R-36L	Summer full closure	Summer full closure or night
18C-36C	Summer full closure	Summer full closure
18L-36R	Summer full closure	Summer full closure
06-24	Summer full closure	Summer full closure or night
09-27	Summer full closure	Winter full closure

Table 2.2: Preferred maintenance periods based on quantitative analysis [44]

Runway	Upcoming maintenance moment	Maintenance type	Subsequent maintenance moment	Maintenance type
18C-36C	2019	transition	2023	heavy
18L-36R	2022	tbd	2029	tbd
18R-36L	2021	heavy	2028	medium
06-24	2024	medium	2031	heavy
09-27	2025	tbd	2032	tbd
04-22	2020	transition	2027	tbd

Table 2.3: Maintenance moments per runway

2.1.3. Phase 3: Implementation Strategy

In this research, the maintenance strategy per runway, including the exits till 150 meters from the centre line of the runway, has been given concrete form. This means that per runway, the maintenance cycle over time is determined. Here, a first subsequent year of maintenance is planned and then, based on the interval of 7/8 years, all subsequent maintenance perspectives are shown over time. Furthermore, the work to be carried out per maintenance perspective based on currently available information has been determined, and thus the type of maintenance has been determined, which is medium or heavy. Also, a cost estimate of the work per maintenance perspective was determined, including tail items, indexation and engineering costs. Moreover, an overview of activities and studies required in time to verify the planned work and determine whether the scope of work needs to be adjusted for next maintenance perspective has been determined [46].
Other inputs that are taken into account to determine the maintenance moments are any capacity requirements from the operation; pre-existing agreements made under EASA compliancy; compliance with safety requirements or other established laws, regulations or standards; compliance with internal policies and the ability to implement (necessary) innovations [46].
To determine the activities for each maintenance moment, the condition and behaviour of key assets based on specific characteristics were investigated. Due to lack of data, the determination of the maintenance cycle and related scope of work during this study was mainly done based on age of some defining assets [46].
This results in the maintenance planning per runway, given in Table 2.3.

In Table 2.3, the 'transition' is defined as a transition maintenance moment performed to meet the next defined maintenance moment. Furthermore, 'tbd' ('To be decided') means that it is for now not clear if it concerns heavy or medium maintenance. In this case, more data needs to be made available to shed more light on this Table 2.3.
The defined maintenance schedule is a principle schedule that complies with the defined maintenance strategy. It gives a high degree of predictability and thus provides "peace of mind" for all stakeholders. Furthermore, the planning provides structure for the future, allowing for the timely implementation and preparation of desired innovations. It is no longer possible to schedule maintenance of any magnitude every year or every 2 years, but maintenance must fit within the established structure and principles.

2.2. Taxiway Maintenance

Taxiway maintenance is a complex procedure that has impact on aircraft, the airport, the ATM system, the environment, local residents and other related stakeholders. Therefore, it is important that taxiway maintenance is planned such that all the norms and values of these stakeholders are taken into account.

However, compared to the runway maintenance strategy specified in section 2.1, there is currently no taxiway maintenance strategy. To create such a strategy, several analyses are made to properly identify the impact of taxiway maintenance, which is a similar approach as in the first phase of the runway maintenance strategy. In this section, the different indicators that are effected by taxiway maintenance are described in subsection 2.2.1. Then, in subsection 2.2.2, a study of MovingDot is discussed, where the impact on taxi times due to taxiway maintenance is researched.

2.2.1. Affected Indicators

In this subsection, the most important indicators that are affected by taxiway maintenance are described. It may be noticed that not all indicators are critical for certain maintenance works.

Runway Configuration

For Schiphol, it is of high priority that the accessibility and capacity of the runways are maintained [34]. However, it is sometimes unavoidable that certain runways are less, or not, accessible due to taxiway maintenance. Therefore, another runway configuration could be used to deliver a certain runway capacity, and to make sure other runways are made more accessible [47]. The chosen runway configuration has impact on the taxi times, but also on the nuisance experienced by the local residents because less preferential runways may be used in this case.

Taxi Distance, Taxi Time & Fuel Burn

The taxi time and/or taxi distance may be higher due to taxiway maintenance because aircraft are re-routed when the normal route is blocked, is not preferential anymore or another runway configuration is used. This older route may not be preferential anymore because this route contains now more interactions with other traffic than the newly defined route [38]. This increase in taxi time and/or increase in taxi distance increases the fuel burn, and therefore the emissions [16]. Although it is true that an increase in taxi distance means an increase in taxi time, the other way around is not true. It could be that on a certain route more start and stops of aircraft occur, which results in higher taxi times for the same taxi distance. By taking this difference into account, bottlenecks can be obtained [57].

Gate Planning

Certain gates cannot be used anymore because the taxiways from and to these gates are closed due to maintenance. This closure means that aircraft are coupled to other gates, affecting the taxi times of aircraft and apron capacity [47].

Push-Back Way Variation

Push-back procedures may be different due to taxiway maintenance. This difference in push-back direction is applied to limit the effects on alternating traffic routes and because of limiting space constraints [47]. This variation in push-back may result in a higher taxi time for aircraft because the push-back procedure takes longer.

Ground Control Workload

Due to change in traffic flows as a result of taxiway maintenance, Ground Control workload may increase. This is because aircraft are now longer under control of Ground Control and/or more potential interactions between aircraft occur due to fewer and more busy flows. Also, it may occur that opposing traffic is of use on a taxiway, or that only a single taxiway can be used to enter or exit a certain bay. This significantly influences the ground control workload [47]. Furthermore, change in gate planning may also result in a higher workload for Ground Control because more aircraft are being handled from a single gate, but controlled by the same number of ground controllers that are in control of that gate.

2.2.2. Taxiway Maintenance Tool by MovingDot

MovingDot has created a prototype for a taxiway maintenance tool based on fast-time simulation, which is made to gain operational insight for strategic advisors and works and asset planners when developing strategic and tactical maintenance plans. This taxiway maintenance tool facilitates the modelling of various taxiway maintenance scenarios. In this case, a scenario is specified as a specific configuration of the airport surface layout, with certain alternations due to maintenance works. The output of this analysis tool are operational indicators, which are linked with the decision-making aspects [57].

Decision-Making Aspects

Because the taxiway maintenance tool supports the creation of a workable maintenance strategy, various decision-making aspects need to be taken into account. The aspects that are discussed are the On-Time Performance (OTP), the capacity, the runway preference, controller workload, tow movements, taxiway lighting, safety and financial maintenance costs [57].

Operational Indicators

The operational indicators that are measured within the maintenance tool are taxi time (and delay), taxi distances and flight throughput because these indicators are quantifiable and are well related to the different decision-making aspects. Next to these indicators, five different heatmaps can be generated, which show traffic flows, average taxi speeds, stop and start locations, nodes and segments, and differences between two selected scenarios. The defined indicators can be linked to these heatmaps [57].

User Protocol

The four steps of using the tool is to implement a maintenance plan, define a model configuration, run the simulation and analyse the results, and give conclusions and iterate if necessary [57].
The model configuration is defined by a condition and scenario. The conditions are dependent on the flight schedule and runway configuration, and the scenarios are based on the Airport Surface Layout. Conditions are assigned with alphabetical designators and scenarios are assigned with numerical designators. Simulation runs (SR) are then combinations of scenarios and conditions. These runs are assigned with alphanumerical designators, for example SR-A1 (Condition A, Scenario 1) [57].
The results of the simulation are presented in two types of dashboards, which are the Report Analysis and Replay Analysis. The Report Analysis is generated for each condition and summarises the main results for the chosen scenarios for the given condition, and the Replay Analysis is a browser-based playback dashboard which replays an animation of the simulation, as well as an emergence of the previously mentioned operational indicators of the Report Analysis [57].
The first step of analysing the result is to study the Report Analysis by comparing the different scenarios. Then, the second step is to generate the taxi time graph that superimposes taxi time evolution for all scenarios, for a single condition. Hereafter, the third step is to generate the delta-speed heatmap to locate bottlenecks. After that, a Replay Analysis for the scenario that requires further investigation is undertaken. At last, iterations may be applied based on refinement of the maintenance plan, flight schedule and/or runway configuration [57].

2.3. Model Requirements

To ensure that the model best represents the context of the problem from a maintenance perspective, it is important that the model satisfies certain requirements. These requirements are set-up in collaboration with Royal Schiphol Group, and are hereby listed:

1. The model needs to be a fast-time model because the model advises Schiphol on a strategic level.
2. The model needs to be reliable, so the number of unknown crashes needs to be limited as possible.
3. The model needs to be able to analyze route changes.
4. The model only takes into account current operations, so no taxibots for example.
5. The model does not need to take into account kinematics if it limits the model performance.
6. The model needs to comprehend bottleneck situations.
7. The runtime of the model is not a limiting factor in obtaining the right solution.
8. In the model, aircraft follow the preferred routing as much as possible.

2.4. Taxiway Maintenance Scenario

In this research, a specific taxiway maintenance scenario is considered to be simulated, and is chosen based on planned taxiway maintenance interventions for relevance. In this case, different parts of the infrastructure are planned to go into maintenance. However, based on discussions with maintenance experts, a demanding part of the infrastructure that is most valuable to be used in this research is taxiway C3 till cross-section A21B. The reason that this is a demanding taxiway part is because this part is each time pushed to later time periods to undergo maintenance due to operational infeasibility. This part is shown in Figure 2.1.

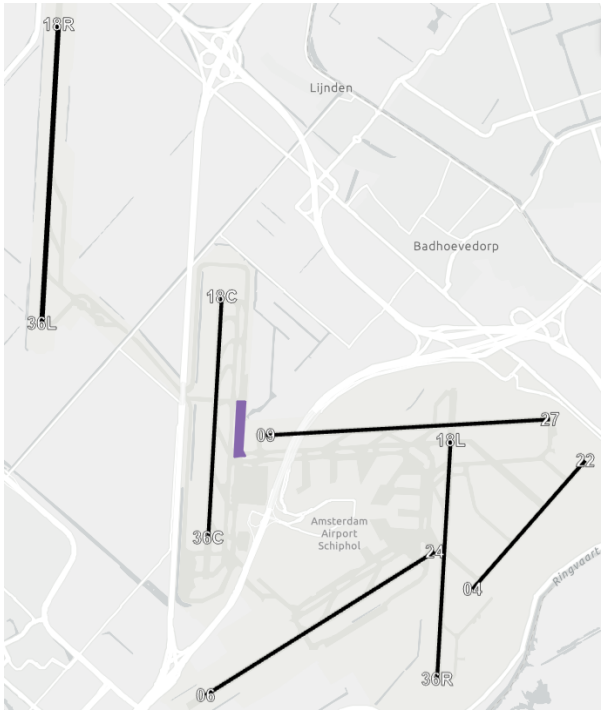

Figure 2.1: Taxiway maintenance work considered in this research: Taxiway C3 till cross-section A21B

In Figure 2.1, it can be obtained that mainly traffic flows moving from and to the Polder Runway and Zwanenburg Runway are influenced by this maintenance work. To better understand these flows and other operational indicators discussed in this chapter, a literature study is conducted on surface movement operations. The results of this study are presented in chapter 3.

3

AAS Airside Airport Operations

In this chapter, the airside airport operations at Amsterdam Airport Schiphol (AAS) are described using different sections. In section 3.1, the general principles of surface movement operations are described. Then, in section 3.2, the different airside infrastructure components are described. Hereafter, in section 3.3, the runway capacity factors are described. Then, in section 3.4, the different properties and factors of runway configurations at Schiphol Airport are explained.

3.1. Surface Movement Operations

In this section, the different components of the concept of surface movement operations are described. In subsection 3.1.1, the airport system is described. Then, in subsection 3.1.2, the different priority rules during aircraft operations are described. At last, in subsection 3.1.3, the Airport Collaborative Decision Making (A-CDM) and its Milestone Approach are explained.

3.1.1. Airport System

The airport system consists of different components that are related to each other. These components are specified in Figure 3.1. All aircraft at the airport follow the same procedure along these components. Furthermore, all aircraft that land on the runway are taxied via the taxiway system by the Air Traffic Control to the apron, and are assigned to a specific aircraft stand [29]. In total, Schiphol contains 222 aircraft stands. Of these aircraft stands, 91 stands are connected aircraft stands and 131 stands are disconnected aircraft stands [48]. When an aircraft departs, the aircraft is pushed back from the stand onto the apron, and is taxied by Air Traffic Control via the taxiway system to the runway [29]. This study concerns Ground Control (GC). Therefore, only the aircraft operations between the runway and apron are of interest. To study these components in more detail, in section 3.2, specifications are given for the runway system, taxiway system and aircraft stands at Schiphol. Aircraft stands are covered in this case because the usage of the aircraft stands have a direct impact on the aprons itself [29].

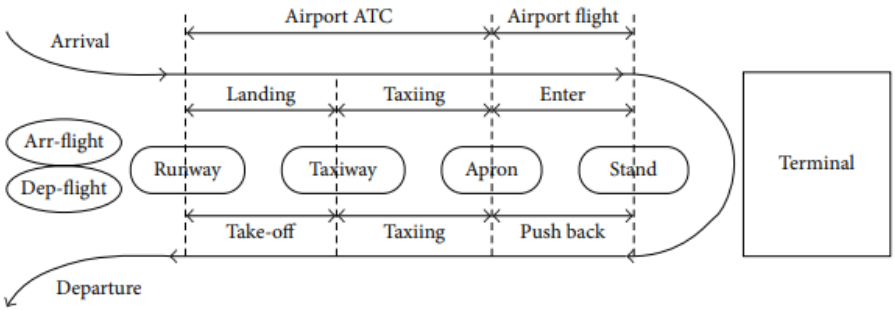

Figure 3.1: General operation flow in an airport [29]

3.1.2. Priority Rules

At Schiphol Airport, certain priority rules are set up for standard traffic scenarios. There are three priority rules. The first priority rule is that taxiing traffic from the right has priority, unless the taxiing traffic has received other instructions from the GC. The second priority rule is that taxiing traffic has priority over towing traffic, unless the taxiing aircraft and tow tractor driver have been given different instructions. For the last priority rule, it is stated that fire vehicles with blue flashing lights have priority over all traffic except take-off and landing air traffic [3].

3.1.3. A-CDM

Schiphol has implemented the Airport Collaborative Decision Making (A-CDM) as the method of joint capacity management between all operational partners contributing to airport operations [51]. The goal of A-CDM is to improve operational efficiency, predictability and punctuality to the Air Traffic Management (ATM) network and the airport stakeholders. For the turn-around processes, Eurocontrol has set-up the A-CDM Milestone Approach [20]. This approach is given in Figure 3.2.

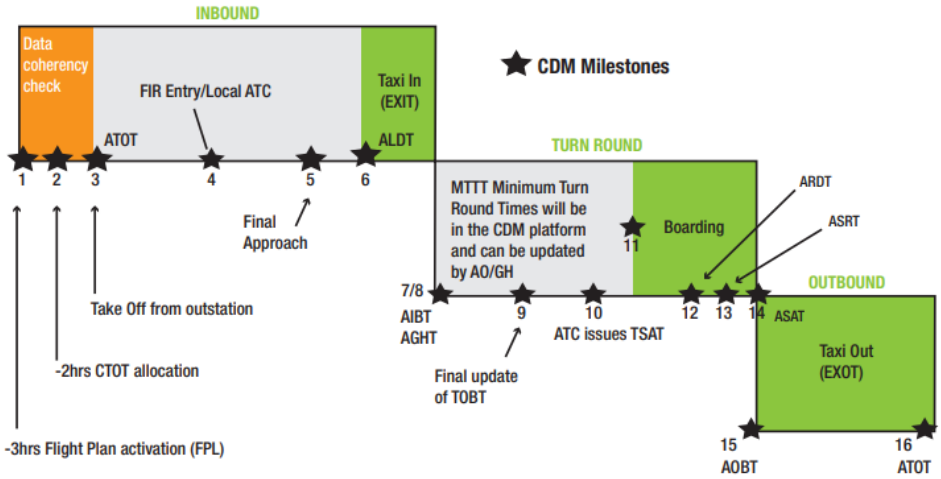

Figure 3.2: The A-CDM Milestone Approach [20]

For this approach, the first 6 Milestones are part of the inbound process. At Milestone 1, the International Civil Aviation Organisation (ICAO) flight plan is submitted to the Air Traffic Control (ATC). Furthermore, the A-CDM platform is initiated for this specific flight and all the information is processed. Normally, this takes place 3 hours before Estimated Off-Block Time (EOBT). Hereafter, at Milestone 2, most flights will be known in the A-CDM platform, taking into account whether the flights are regulated or not. All flights that are regulated receive a Calculated Take Off Time (CTOT), and are issued at EOBT-2h. Next, at Milestone 3, the Actual Take Off Time (ATOT) from the outstation Aerodrome Of Departure (ADEP) is provided, which is directly available after the occurrence of the milestone. Hereafter, at Milestone 4, the aircraft enters the Flight Information Region (FIR) or the local airspace of the destination airport. Then, at Milestone 5, the flight enters the Final Approach phase at the destination airport. Hereafter, at Milestone 6, the aircraft touches down on the runway of the destination airport, which is defined as the Actual Landing Time (ALDT). Then, Milestone 7 till 14 are part of the turn around process. At Milestone 7, the Actual In-Block Time (AIBT) is defined, which is the time that an aircraft arrives in-blocks. Consequently, at Milestone 8, the ground handling is started, which is defined to be executed on the Actual Commence of Ground Handling Time (ACGT). The ACGT can in this case be equal to the AIBT. The ACGT is currently not defined at Schiphol Airport. Hereafter, at Milestone 9, the Target Off-Block Time (TOBT) is provided by the Aircraft Operator or Ground Handler, which is a continuous process. Then, at Milestone 10, the ATC issues the Target Start Up Approval Time (TSAT). Hereafter, at Milestone 11, the boarding process starts. During boarding, at Milestone 12, the time is defined at which the aircraft is ready to taxi. This is called the Actual Ready for Departure Time (ARDT). However, this information is currently not available at Schiphol Airport. At Milestone 13, the time that the start up is requested is defined,

which is the Actual Start Up Request Time (ASRT). The start-up approval is defined at Milestone 14, which is defined as the Actual Start Up Approval Time. This information is not defined yet at Schiphol Airport. For Milestone 15 and Milestone 16, these fall under the outbound process. At Milestone 15, the Actual Off-Block Time (AOBT) is defined, which is the time an aircraft is pushed back. Finally, at Milestone 16, the Actual Take Off Time (ATOT) is defined, which is the time that an aircraft takes off from the runway [51].

3.2. Airside Infrastructure

In this section, the different components of the airside infrastructure are described. In subsection 3.2.1, the runway system is described. Then, in subsection 3.2.2, the taxiway system is described. At last, in subsection 3.2.3, the different aircraft stands are described.

3.2.1. Runways

In total, Schiphol contains six operational active runways [7]. Three of these runways run parallel to each other and are oriented in the north-south direction. From west to east, these runways are the Polder Runway (18R/36L), Zwanenburg Runway (18C/36C) and the Aalsmeer Runway (18L/36R). Two runways lay approximately from the south/west to the north/east, which are the Kaag Runway (06/24) and Schiphol East Runway (04/22). At last, one runway lays in the east-west direction, which is the Buitenveldert Runway (09/27). The Polder Runway is both the longest and widest runway of Schiphol, with a length of 3800 meter and a width of 60 metres [48]. However, this runway is also located the furthest from the terminal area compared to the other runways. Therefore, this part of the Schiphol airside is controlled by a separate air traffic control tower, which is Schiphol Tower West (TWR-W). This control tower is located on the south-east side of the Polder Runway, next to taxiway Victor. The other runways are controlled by Schiphol Tower Centre (TWR-C), which is located on the south side of the terminal [7]. Furthermore, it may be noticed that the Schiphol East Runway is considerably shorter in length compared to the other runways [48]. Therefore, this runway is mainly used by General Aviation (GA). The runways that are used most by air traffic are the Kaag Runway and the Polder Runway [50]. The runway system of Amsterdam Airport Schiphol (AAS) is visualized in Figure 3.3. The runways are connected with the taxiways via entries and exits [7]. The taxiway system of AAS is discussed in subsection 3.2.2.

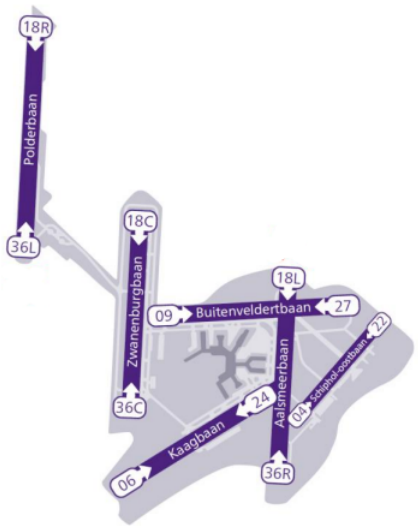

Figure 3.3: Schiphol runway system [54]

3.2.2. Taxiways

Amsterdam Airport Schiphol connects the runways with the aprons using multiple taxiways. The two main taxiways of AAS are taxiway Alpha and taxiway Bravo. Both taxiways form a double circle around the terminal, where the inner circle is taxiway Alpha and the outer circle is taxiway Bravo.

The directions of the traffic flows on both taxiways are fixed, which is clockwise on taxiway Alpha and counter-clockwise on taxiway Bravo. The double circle has an opening in the southwestern part of the airport, which is closed by Taxiway Quebec. On taxiway Quebec however, no fixed direction of traffic flow is incorporated. In this case, the direction of flow depends on the runway configuration, which will be explained in section 3.4. Other two taxiways that have a fixed direction for the traffic flows are Taxiway Charlie and Taxiway Delta, both laying parallel to and on the north-east side of the Zwanenburg Runway. The traffic flows on taxiway Charlie are in the northern direction, and the traffic flows on taxiway Delta are in the southern direction. These two taxiways are connected with taxiways Alpha and Bravo on the western side of the terminal. All runways are connected with entries and exits with the Alpha and Bravo taxiways, except the relatively far away laying Polder Runway. Three different taxiways are in use to connect the Polder Runway with the Alpha and Bravo taxiways. The first taxiway is taxiway Yankee, that is used to move around the Zwanenburg Taxiway via the northern direction. The second taxiway is taxiway Zulu, that is used to move around the Zwanenburg Runway via the southern direction. The third taxiway is taxiway Whiskey 5, that crosses the Zwanenburg Runway directly. All these three taxiways converge on the west side of the Zwanenburg Runway and continue as taxiway Victor. Taxiway Victor is directly connected to the Polder Runway [7]. The main taxiway system at Schiphol airport is visualized in Figure 3.4.

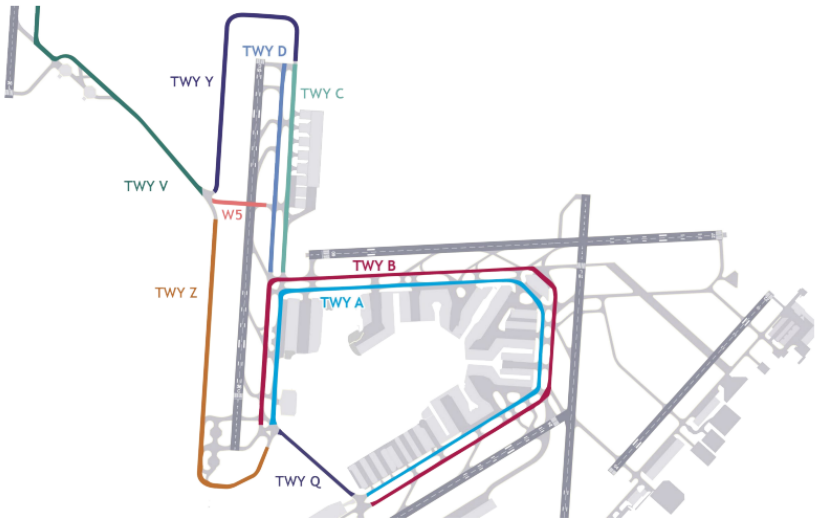

Figure 3.4: Schiphol main taxiway system [57]

3.2.3. Aircraft Stands

Schiphol contains a variety of aircraft stands that are connected to the runways via the taxiway systems. In total, there are 13 platforms and 7 piers [49]. The allocation of each aircraft to each stand depends on the category that each aircraft is assigned to. The aircraft are categorized based on the greater value of their length or wingspan. Aircraft are assigned to their smallest possible category [45]. The different categories are given in Table 3.1. At the A-platform and B-pier, only aircraft with maximum categories 3 and 4 can park there. However, at the C-pier, H/M-pier and D-pier, only aircraft with maximum category 4 can park there. Furthermore, at the D-pier, F-pier, E-platform, G-platform, M-platform and U-platform, aircraft with maximum category 8 can be allocated to these aircraft stands. At the E-pier, G-pier, J-pier, P-platform, R-platform and S-platform, aircraft with maximum category 9 can be located there. At last, at platform K, aircraft with maximum category 5 have the possibility to park there [49]. Platform K is a platform specifically designed for General Aviation [52].

3.3. Runway Capacity

Runway capacity is depended on multiple factors. These factors are number and geometric layout of runways, separation requirements imposed by ATM system, visibility, wind direction and strength, mix of aircraft, mix of movements per runway, type and location of taxiways, state and performance of ATM system and noise- and environmentally-related considerations [11]. The factors that are discussed

Category	Max. length [meter]	Max. wingspan [meter]
1	< 22,00	< 24,00
2	< 28,00	< 29,00
3	< 37,00	< 29,00
4	< 45,00	< 36,00
5	< 49,00	< 44,00
6	< 55,50	< 52,00
7	< 72,00	< 61,00
8	< 76,00	< 65,00
9	< 77,00	< 80,00
10	< 84,00	< 88,40

Table 3.1: Aircraft stand category overview [45]

in this section are separation requirements imposed by ATM and mix of aircraft in subsection 3.3.1, visibility in subsection 3.3.2, wind direction and strength in subsection 3.3.3, mix of movements per runway in subsection 3.3.4, and noise- and environmentally-related considerations in subsection 3.3.5. The other factors are not discussed, because these are not seen as relatable variables for this research.

3.3.1. Separation Requirements & Mix of Aircraft

To ensure safety on the runway, sufficient spacing between consecutive aircraft needs to be ensured. This spacing can be expressed in time or in distance. The spacing between consecutive aircraft can be determined based on 4 different pairs of movements, which are A-A (arrival followed by arrival), D-D (departure followed by departure), A-D (arrival followed by departure) and D-A (departure followed by arrival). For A-A and D-D, the minimum distance between the different pairs of movements are determined based on the classes the trailing and leading aircraft are assigned to. Aircraft are assigned to a class based on their Maximum Take Off Weight (MTOW). This differentiation is done to limit the effects of wake turbulence of the leading aircraft on the trailing aircraft [11]. This wake turbulence is created when there is an increase in pressure below the wing of an aircraft and an decrease in pressure on top of the aerofoil. This difference in pressure creates vertices behind the wing, which may influence the trailing aircraft [8]. In general, the heavier the leading aircraft compared to the trailing aircraft, the larger the separation distance between the two aircraft to take into account wake turbulence. Therefore, when a mix of aircraft for A-A and/or D-D is defined that limits the separation distances between the aircraft, the higher the throughput of aircraft, and the higher the capacity of the runway [11].
For an arriving aircraft followed by a departing aircraft (A-D), the requirement is that an arriving aircraft must be safely out of the runway first before the take-off run of the departing aircraft can start. This is regardless of the classes of aircraft that are involved in this case [11].
For a departing aircraft followed by an arriving aircraft (D-A), the arriving aircraft must be at least 2 nautical miles away from the runway when departure run begins. Furthermore, this arriving aircraft cannot touch down before the preceding departing aircraft has lifted-off [11].

3.3.2. Visibility

Visibility is a factor that determines runway capacity because the lower the visibility, the larger the separation between arriving aircraft, and the lower the runway capacity. Also, when there is low visibility, depended runway use cannot be applied, which may limit the runway capacity [6]. Regarding visibility, there are two types of visual conditions, which are Visual Meteorological Conditions (VMC) and Instrument Meteorological Conditions (IMC). VMC is the state where the visibility for pilots is sufficient to maintain visual separation between other aircraft and the ground. When this is not the case, IMC applies, where pilots are required to primarily use their flight instruments. IMC applies by a visibility less than approximately 4,8 kilometres and a cloud ceiling less than approximately 300 meter [9].

3.3.3. Wind Direction & Strength

When the wind direction and/or wind strength is such that certain runways can not be used, this may impact the runway capacity of the airport. According to ICAO and the Federal Aviation Administration

(FAA) standards, it is determined that planes land and take-off in the direction of the wind [53]. Furthermore, in general, the crosswind limits at airports are between 15 and 25 knots, and the tailwinds are normally limited to 10 knots [28]. However, at Schiphol airport, the maximum allowable crosswind is 20 knots and the maximum allowable tailwind is 7 knots [4].
The most dominant wind direction at Schiphol is the direction southwest south [32].

3.3.4. Mix of Movements per Runway

The mix of movements per runway is the distribution of arrivals and departures on a runway. In a certain period of time, a runway can be used only for arrivals, only for departures or mixed. In general, the capacity of a runway is higher when this runway is only used for departures then only for arrivals, given the same mix of aircraft [18].

3.3.5. Noise- and Environmentally-Related Considerations

The capacity of the runway system is also depended on noise and environmental regulations because this factor has impact on the use of certain runways and runway configuration. In this case, there is a difference between daytime and night-time. Daytime is between 06:00 and 23:00 and night-time is between 23:00 and 06:00. During the daytime inbound peak, 2+1 (2 landings and 1 departure) runways are used. Furthermore, during the daytime outbound peak, 1+2 (1 landing and 2 departures) runways are used. However, during night-time, 1+1 is used. If the weather allows it, during the night-time, runways 18R-36L and 06-24 are preferred to use due to the lowest noise impact. If it is not possible to use these runways, then runway 18C-36C or 09-27 are used. In either way, runway 18L-36R is not used during night-time and runway 04-22 is closed during the night [21]. In general, during northern wind conditions, runway 36L is used for departures and runway 06 is used for landings to limit the noise impact on the surrounding area as much as possible. During peak take-off periods, runway 36C can be brought into service, and during peak landing periods, runway 36R can be brought into service. The same construction holds during a southern wind, but the runway use changes from departure to arrival or the other way around. In that case, runway 18R is used for arrivals and runway 24 for departures. Runway 18C is then used during peak landing periods and runway 18L is then used during the peak departure periods [23].

3.4. Runway Configuration

At Schiphol Airport, a large number of runway configurations are possible. A runway configuration is the set of active runways that are used for either landing or taking off traffic [21]. On average, Schiphol changes the runway configuration 14 times per day. The most important factors that influence the runway configurations are noise regulations, traffic demand, weather conditions and disruptions [6]. The effect of noise and weather conditions on runway operations are already discussed in section 3.3. Therefore, in this section, only traffic demand and disruptions are discussed in subsection 3.4.1 and subsection 3.4.2. Furthermore, the occurrence of different runway configurations are discussed in subsection 3.4.3

3.4.1. Traffic Demand

One of the factors that determines the number of runways used at Schiphol Airport is the traffic volume of the inbound and outbound flows. Two runways are in use during the off-peak; one for landing and one for take-offs. The number of runways in use during the inbound and outbound peak is 3 runways. Like was mentioned in subsection 3.3.5, during the inbound peak, 2 runways are used for landings and 1 for take-offs. However, during the outbound peak, 2 runways are in use for take-offs and 1 for landings. Between these two peaks, four runways may be used simultaneously for a short period of time, which is called the transition period. In that case, two runways are used for landings and two runways are used for take-offs [17].

3.4.2. Disruptions

There is always the possibility that disruptions occur that influence the choice of runway configuration. Examples of disruptions are bird strikes, technical failures of runway systems and snow removal on the runway [39]. Another reason that a change in runway configuration is used is because a certain part of the infrastructure is closed due to maintenance [6].

3.4.3. Configuration Frequency

To determine how many times the different runway configurations are used, an analysis is applied on a dataset containing the duration of each used runway configuration in the period between the first of May 2023 and the first of October 2023.
In Figure 3.5, the ranked number of occurrences of the thirty most occurring runway configurations are presented, and in Figure 3.6, the ranked durations that runway configurations were in use in the given time period as a fraction of the total available time are presented for the thirty longest occurring runway configurations. From these graphs, only the runway configuration containing more than two runways in use are analyzed because these runway configurations are mainly in use during peak periods, meaning that the workload of ground controllers is relatively high compared to off-peak periods when often runway configurations containing 2 runways is used. Based on this, it can be noticed that the runway configurations in the top four most occurring runway configurations containing three runways are the same runway configurations in the top four longest occurring runway configurations, which are 18R/24+18L, 18R+18C/24, 06/36L+36C, 06+36R/36L. It may further be noticed that two runway configurations with four runways occur relatively often compared to all other runway configurations, which are 18R+18C/24+18L and 06+36R/36L+36C. These two runway configurations are configurations that are in use between a departure peak and landing peak. In this case, the 18R+18C/24+18L configuration is a transition configuration between 18R/24+18L and 18R+18C/24, and the 06+36R/36L+36C configuration is a transition configuration between 06/36L+36C and 06+36R/36L, which is in line with the number of times these runway configurations are in use. The runway configuration that occurs the most is 18R/24+18L, and the runway configuration that occurs the longest is 18R/24. Using the total number of occurrences over all runway configurations in the period between 01/05/2023 and 01/10/2023, it can be obtained that the average change in runway configuration is 18,9 changes per day, which is higher than the 14 changes per day over the whole year given in the introduction of this section.

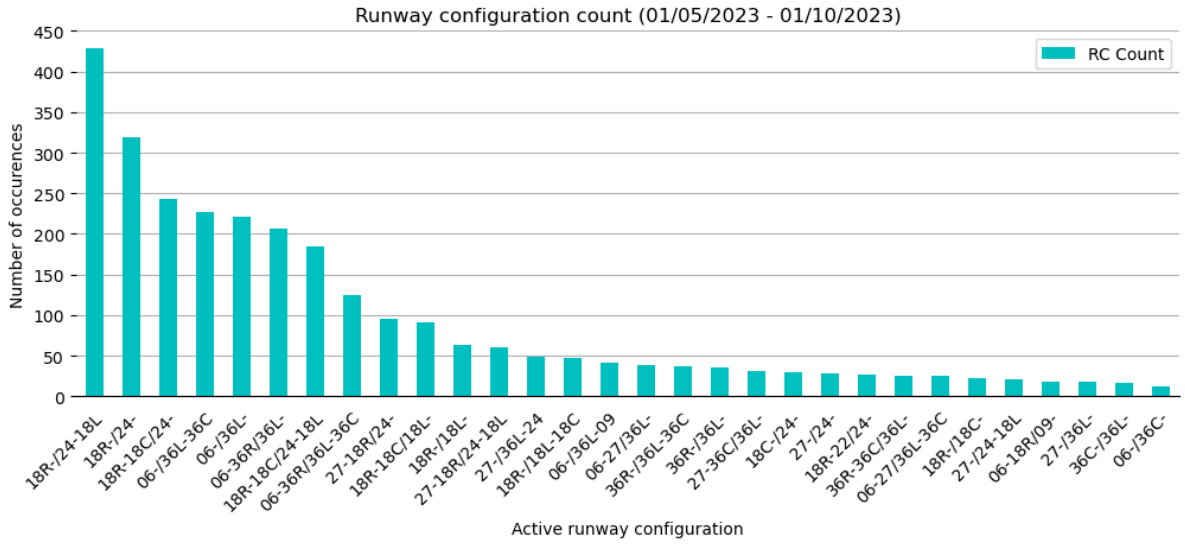

Figure 3.5: Runway configuration count from 01/05/2023 till 01/10/2023

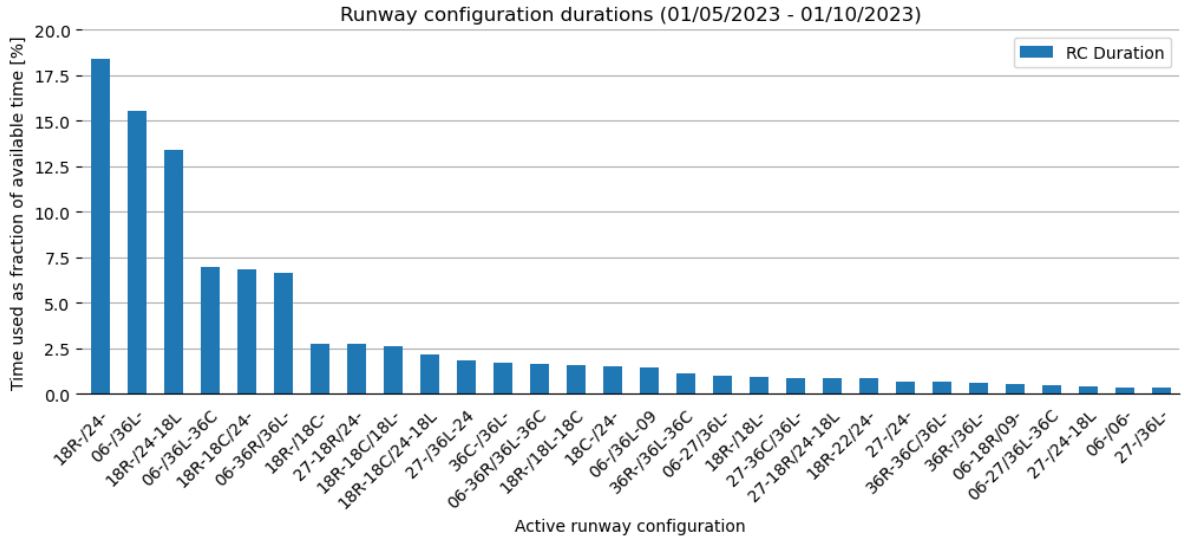

Figure 3.6: Runway configuration durations from 01/05/2023 till 01/10/2023

3.4.4. Runway Configurations for this Research

In section 2.4, it was discussed that mainly traffic flows from and to the Polder Runway and Zwanenburg Runway are influenced by the given maintenance work. From this chapter about airport operations, it can be concluded that aircraft routes are mostly determined by the runway configurations. Therefore, to better understand which runway configurations are interesting for this research, discussions with operational experts were carried out. From these discussions, it was obtained that only runway configurations in which the Polder Runway and Zwanenburg Runway are used in opposite direction were interested to consider for this workload research because then conflicting flows emerge. The only runway configurations that comply with this requirement and are operational feasible are runway configurations 18R/18C+18L and 36C+36R/36L. For runway configuration 18R/18C+18L, the flows for the nominal and maintenance case are given in Figure 3.7. Furthermore, for runway configuration 36C+36R/36L, the flows for the nominal and maintenance case are given in Figure 3.8. In both these figures, the green arrows are outbound traffic, the orange arrows are inbound traffic, the violet arrows are flows in both direction, and the red crosses are locations of conflicting flows.

Based on the changes in flows between the maintenance case and nominal case in Figure 3.7 and Figure 3.8, it can be obtained that more conflicting flows emerge. These conflicting flows are expected to induce an increase in workload for ground controllers as ground controllers have to manage these flows from conflicting. To better understand the work of the ground controller, a literature study is conducted on this, and is presented in chapter 4. Then, in chapter 5, the workload of the ground controller is discussed.

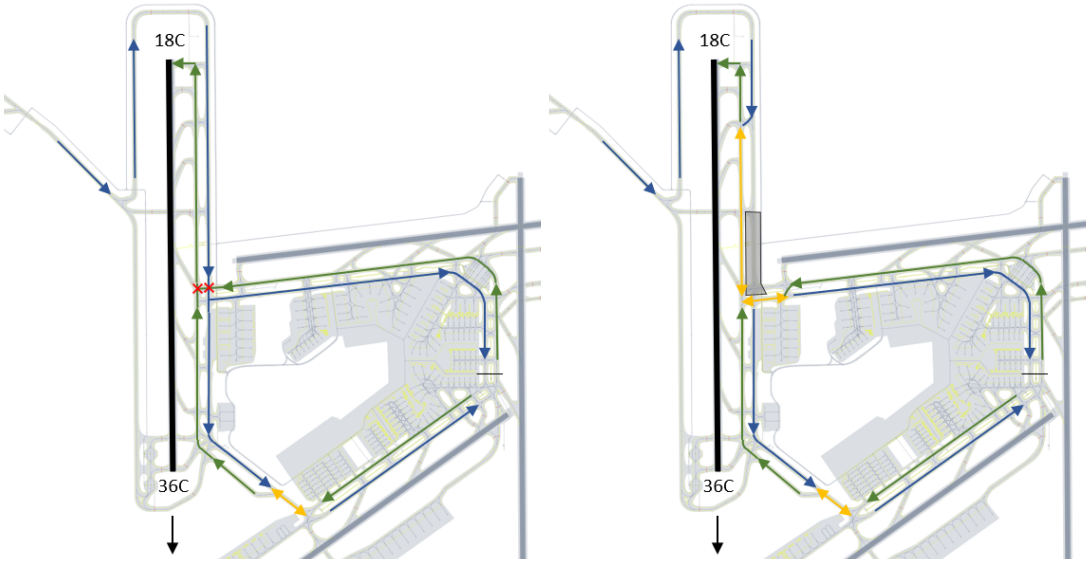

(a) Nominal case (b) Maintenance case

Figure 3.7: Traffic flows for landing on 18R and takeoff from 18C. The green arrows are outbound traffic, the orange arrows are inbound traffic, the violet arrows are flows in both direction, and the red crosses are locations of conflicting flows

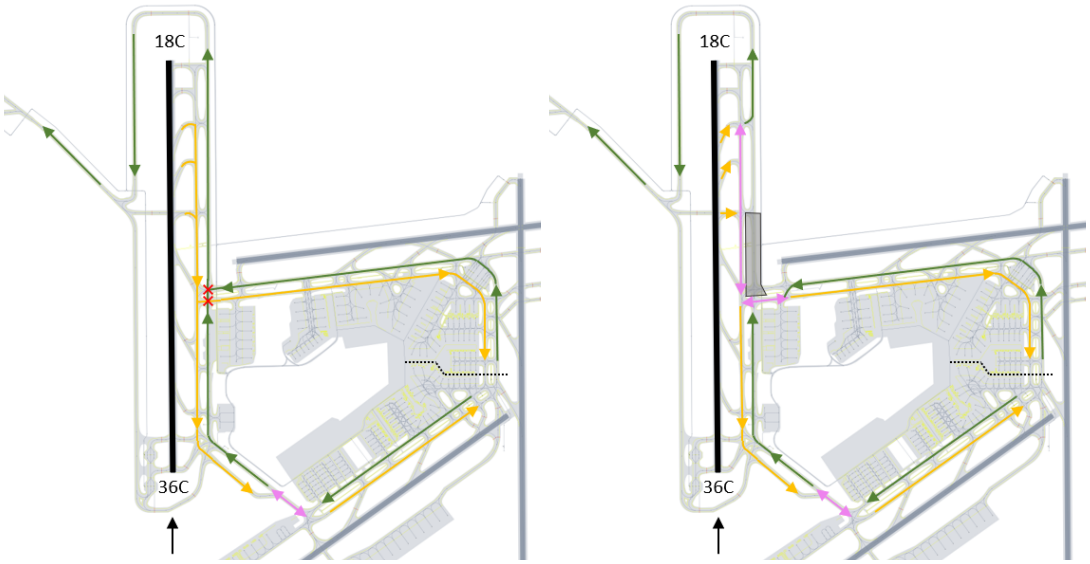

(a) Nominal case (b) Maintenance case

Figure 3.8: Traffic flows for landing on 36C and takeoff from 36L. The green arrows are outbound traffic, the orange arrows are inbound traffic, the violet arrows are flows in both direction, and the red crosses are locations of conflicting flows

4

AAS Ground Control

In this chapter, the Ground Control unit at Schiphol Airport is discussed. In section 4.1, the responsibilities of the ground controllers are explained. Then, in section 4.2, the different tasks of the ground controllers are explained. Hereafter, in section 4.3, the Ground Control procedures for inbound and outbound flights are explained. Subsequently, in section 4.4, the different goals of the ground controllers are explained. Then, in section 4.5, the different Ground Control sectors are explained. Hereafter, in section 4.6, the direct colleagues of ground controllers in TWR-C are described. Then, in section 4.7, the console the ground controllers work behind is explained. Lastly, in section 4.8, the most relevant screens that are located on the console of the ground controllers are explained.

4.1. Responsibilities

A ground controller is an air traffic controller who is responsible for all movements on the maneuvering area, excluding available and inoperable runways and exits [3]. The maneuvering area is in this case part of the airport area where aircraft take-off, land and taxi, excluding the platforms [1]. This means that for outbound flights, aircraft communicate with Ground Control between push-back and entering the runway, and for inbound flights, aircraft communicate with Ground Control between exiting the runway and parking at the aircraft stand. Furthermore, the ground controller has the responsibility to provide Aerodrome control service, Flight information service and alerting service for aircraft, towing traffic and vehicle movements. The Apron Planning & Control (APC) department handles the towing traffic, but the responsibility of the towing traffic is of Ground Control. The tow controller, who is part of the APC department, asks permission to the ground controller for entering the manoeuvring area by towing traffic. Remaining tow movements in the field are handled on own initiative by the tow controller [2].

4.2. Tasks

One of the most important tasks of the ground controller is to prevent collisions involving aircraft on the airside surface, excluding the runways. Furthermore, this controller has the task to maintain communication with aircraft under his responsibility. This includes giving instructions to prevent collisions involving aircraft, giving push-back and taxi instructions, giving instructions to prevent uncontrolled or unauthorised entry of runways, giving information to pilots about changes in weather circumstances and the status of navigation equipment and re-clearance of aircraft. Other tasks that could be executed by the ground controller are checking the label of the taxiing aircraft on the radar screen, giving instructions to pilots about correct transponder use and fill in the label manually on the TWR-system. These tasks could be executed in the scenario of low and reduced visibility or when the runway controller or another ground controllers asks to due to the handover of a taxiing aircraft to their sector. Furthermore, important tasks that ground controllers require to do are handing over departing aircraft and aircraft that are about to cross an available runway to the runway controller, assigning remote holding positions to aircraft, operating the taxiway lightning and alerting in case of emergencies [37].

4.3. Procedure

At Schiphol airport, the Ground Control procedure for an outbound flight is hereby explained. The Ground Control is involved for an outbound flight the moment start-up is cleared by the Outbound Planner (OPL). In that case, the flight strip of that flight appears on the flight strip screen of the ground controller. Before further information can be given by the pilot, all checks need to be done to make the aircraft ready for push-back. When the aircraft is ready for push-back, the pilot informs this to the ground controller of the concerning sector via the concerning frequency. Then, the controller clears the aircraft for push-back or holds the aircraft. When the push-back permission is perceived by the pilot from the ground controller, the pilot contacts the push-back driver for push-back. However, if the push-back did not start within one minute after receiving permission, the pilot needs to contact the ground controller again to ask permission. When the aircraft is cleared for push-back, the pilot receives further instructions. These instructions could be to hold after push-back, to hold to let another aircraft pass, or to start taxiing. In the case the aircraft starts taxiing, the pilot receives the route to the runway from the controller. In many cases, these routes are part of the standard taxi routes that are used at Schiphol. However, in some cases, other routes are used. During taxiing, the communication between the pilot and controller is kept to a minimum as much as possible. Still, more communication is often needed. This could be the case when an aircraft has priority over another aircraft in an unusual matter, or when there is a special case in the manoeuvring area. If there are no disruptions on the way, the aircraft reaches the intended runway entry. At this moment, the ground controller calls the pilot to switch to the tower frequency, therefore ending the communication between these two [14].
For inbound flights, the procedure is similar to the outbound flights concerning Ground Control. In that case, the first moment of contact is when the aircraft exits the runway, and the last moment of contact is when the aircraft parks the aircraft at the aircraft stands [14].

4.4. Goals

According to ground control experts, the three main goals of a ground controller are ensuring safety, sequencing and streaming [14]. These three goals are hereby discussed in the following subsections.

4.4.1. Safety

The main aspect of ensuring safety is to make sure aircraft keep sufficient separation from one another and other vehicles or obstacles. This separation needs to be ensured over the whole area that the ground controller is responsible of. Furthermore, the ground controller needs to anticipate on the movements of vehicles that are moving or approaching the service area of this controller. This is done to make sure that potential conflicts are resolved far before happening, such that other entities, like other controllers or aircraft, are not hindered [14].

4.4.2. Sequencing

For this aspect, the main goal is to deliver an optimal sequence of outbound flow to the runway controller. The sequence the ground controller establishes has impact on the time the aircraft has to wait for take-off, so one of the goals is to limit this waiting time. The main aspects that influence sequencing are the used Standard Instrument Departures (SIDs), wake turbulence separation requirements, runway configuration, and the use of intersections. The ground controller has the responsibility to deliver an optimal prepared sequence. However, the runway controller has the responsibility to deliver an optimal starting sequence for take-off [3].

SIDs

The Standard Instrument Departures (SID) are fixed departure routes that need to be used by Instrument Flight Rule (IFR) traffic departing from Schiphol Airport, where each departing runway contains multiple SIDs. These SIDs are implemented to make sure the available airspace is optimally used. Furthermore, these SIDs avoid major residential areas around the airport as much as possible to limit the generated noise impact. SIDs are related to sequencing because the waiting time of each aircraft in the sequence depend on the individual assigned SIDs of all the aircraft in the sequence. It is desired that consecutive aircraft in the sequence have different SIDs to limit the waiting time of each aircraft, to eventually limit the Runway Occupancy Time (ROT). The reason is, is that the separation time

between two aircraft taking off is lower when two aircraft have different SIDs, which is illustrated in Figure 4.1 [3]. These differences in separation between aircraft are related to the minimum distance that needs be preserved due to wake turbulence, which is explained in the following part.

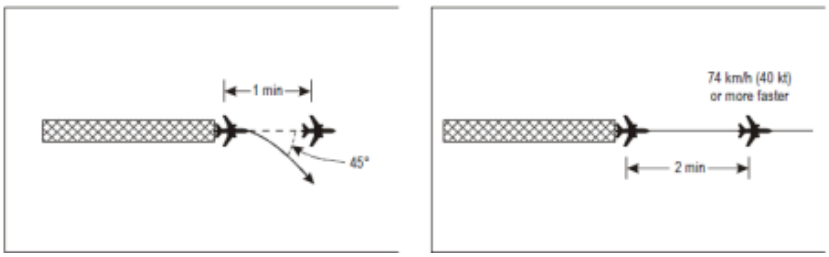

Figure 4.1: SID related separation between two aircraft [3]

Wake Turbulence Separation

The take-off time between two aircraft on a specific runway is not only depended on the choice of the SID, but also on the wake turbulence separation requirements. In subsection 3.3.1, it is explained how these differences in wake turbulence separations are defined. These separations have impact on the sequence determined by the ground controller because the different wake turbulence classes of the different aircraft in the sequence determine the separation between the aircraft in the sequence, and therefore, the throughput and capacity on the runway. For that reason, it is desired that the aircraft are sequenced by taking into account the optimal order of wake turbulence classes to limit the separation between the aircraft, and therefore increasing the runway capacity and throughput [11].

Use of Intersections

When creating the sequence, the possibility exists to not only start or insert aircraft at the start of the runway, but also to let them start or insert at an intersection, so further away from the runway threshold. The intersections are in this case used to influence the composition of the sequence for optimal streaming using the different SIDs and wake turbulence categories of the different aircraft. This is done by fitting in aircraft in the sequence that positively impact the throughput and capacity of the runway [14].

4.4.3. Streaming

For the ground controller, the goal for the aspect streaming is to make sure that the different aircraft move through the manoeuvring area as such that the resulting delay is as low as possible. An important factor of this is to make sure that the aircraft move as much as possible. This is done because moving aircraft can more easily be diverted than stationary aircraft because a moving aircraft is more flexible than a stationary aircraft. If the situation occurs that certain aircraft need to stop, then the preference is to let the more smaller aircraft stop, and to make sure the bigger aircraft keep on moving. This is because larger aircraft take longer to start moving after being stationary compared to smaller aircraft [14].

4.5. Sectors

To handle the ground traffic at Schiphol Airport, the total manoeuvring area is subdivided into geographical regions, also called sectors. These sectors are Ground Control North, Ground Control South, Ground Control West and Ground Control Centre. The different Ground Control sectors are shown in Figure 4.2. The Ground Control sectors North, South and Centre fall under the responsibility of the ground controllers in Schiphol Tower Centre (TWR-C), and Ground Control West falls under the responsibility of one ground controller located in Schiphol Tower West (TWR-W). If TWR-W is not active, then Ground Control West falls under the responsibility of a ground controller in TWR-C. The sector Ground Control North is the biggest sector, as it contains runways 09/27, 04/22 and 18L/36R. Ground Control Centre contains runway 18C/36C and Ground Control South contains runway 06/24. The final sector, Ground Control West contains runway 18R/36L. At maximum occupancy, each sector is controlled by one ground controller [3].

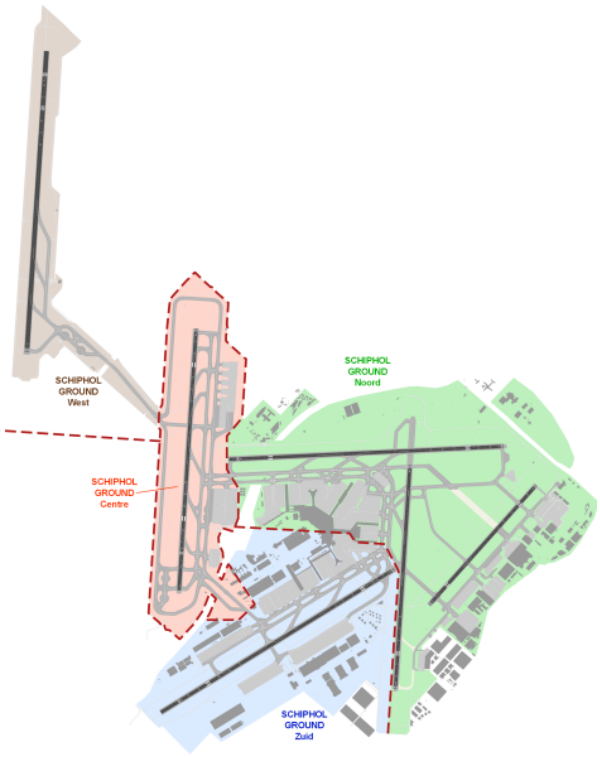

Figure 4.2: Ground Control sectors [3]

These four sectors are not always active at the same time. Like was obtained in subsection 3.4.3, runway 18R/36L is one of the most used runways. Therefore, Ground Control West is often active. However, when the traffic demand is low, the other three sectors can be handled by one ground controller. When the traffic demand increases or starts to increase, in many cases, the sectors Ground Control North and Ground Control South are activated. Sector Ground Control Centre can in this case be divided over these two sectors. When the traffic volume is very large while runway 18C/36C is active, then Ground Control Centre becomes active. These sector configurations not only change depending on traffic demand in the sectors Centre and North, but these also change depending on the number of controllers active at that moment [14].
Furthermore, the structure of the sectors may change in some cases. One common change is the change in involving taxiway Quebec from sector Centre to sector North, depending on which sector has a higher traffic demand. Another common change is the change of involving the D-pier, which is the tuning-fork-shaped pier on the border between the North and South sector, from sector North to sector South, depending on which sector has a higher traffic demand. These small changes are temporary, and can be made by the ground controllers or their supervisor. Therefore, these changes are not logged [14].

4.6. Direct Colleagues TWR-C

In this section, the colleagues that work in TWR-C, and are in direct contact with the ground controller are described, and it is described how these people impact the work of the ground controller. In subsection 4.6.1, the tower supervisor is described. Then, in subsection 4.6.2, the runway controller is described. Consequently, in subsection 4.6.3, the outbound planner is described. Hereafter, in subsection 4.6.4, the tower assistant 2 is described. Then, in subsection 4.6.5, Apron Planning & Control is described. Hereafter, in subsection 4.6.6, it is explained what the changes are concerning Ground Control communication. At last, in subsection 4.6.7, it is explained how the shift of a ground controller is transferred to another controller.

4.6.1. Tower Supervisor (SUP)

The Tower Supervisor (SUP) is the responsible person for the whole tower process. Therefore, this person is responsible for the provision and quality of all air traffic control services in the manoeuvring area and in the airborne part of the TWR's area of responsibility. One of the most important tasks of the SUP is monitoring all colleagues working within the tower. Other important tasks are making sure that the tower officials are functioning efficiently and coordinating the whole tower process. This coordination is done with all tower officials, the Approach (APP) Supervisor, the Area Control Center (ACC) supervisor, the Flow Manager Aircraft (FMA) and the Meteorological Advisor Schiphol, who is a meteorologist of the Royal Netherlands Meteorological Institute (KNMI). The Approach Supervisor has a similar task as the Tower Supervisor, but then for Approach Control, and the FMA has a big responsibility of the airside aircraft operational flows. Together with the FMA and APP SUP, the TWR SUP determines the runway configurations during the day. Furthermore, the SUP coordinates all the activities happening in the manoeuvring area. Also, this person follows the weather predictions and proactively create a handling plan. Moreover, the SUP takes all final decisions regarding the tower processes. Additionally, this person has the final responsibility in case of emergencies, in particular with regard to handling strategy. The SUP works mainly during the day, but during the night a SUP is set on standby in case availability is needed [37].
The communication between the ground controller and the SUP is mainly face-to-face. This is because both the ground controller and SUP work on the 12th floor of the TWR-C. There is frequent communication between the two, but this communication can not be seen as intensive compared to the other communication lines [14].

4.6.2. Runway Controller (RC)

At Schiphol Airport, the runway controller has the responsibility to deliver Air Traffic Control services around the landing area, which is in this case on the runways and exits. An aircraft will be handed over by the ground controller to the runway controller when this aircraft is sequenced for take-off. The runway controller hands over an aircraft to the ground controller when this aircraft exits the runway, and hands over an aircraft to the approach controller when this aircraft exits the Controlled Traffic Region (CTR) [14].
The most important tasks of the runway controller is to prevent collisions between aircraft, to handle starting and landing aircraft safely and efficiently, to provide flight information service and alerting service, to handle traffic in the Schiphol CTR's and to maintain communication with the aircraft that the runway controller is responsible of. Furthermore, the runway controller gives permission to ground controllers to cross available runways by aircraft, and gives permission for driving off or crossing available runways. Also, the runway controller coordinates with APP about the handling of approaching aircraft and departing aircraft and coordinates with TWR-W about aircraft which may be of interest to each other. Moreover, the runway controller controls the runway lights and alerts in the case of emergencies [37].
The communication between the ground controller and runway controller happens face-to-face and is mainly about giving permission to cross a certain runway. However, other special situations, like an inconvenience on the taxiway and that certain runway exits are not preferred anymore, require more communication between the two controllers [14].

4.6.3. Outbound Planner (OPL)

The Outbound Planner (OPL) creates the optimal start-up planning for all departing flights using Collaborative Decision Making (CDM). As part of this, the planner determines the times the aircraft need to be ready for start-up, so that the planner can hand over the aircraft to the ground controller at these specific times. Therefore, the outbound planner determines the distribution of start-up requests over time, such that these requests can be processed efficiently. So, it can be obtained that the outbound planner has a big influence on the ground controller because the outbound planner has a big influence on the outbound traffic flow [37].
The communication between the ground controller and outbound planner is face-to-face, and it should hereby be mentioned that the outbound planner only communicates with ground controllers controlling the North or South sector because these are the sectors where outbound planning is made for [14].

4.6.4. Tower Assistant 2 (TWR ASS-2)

Tower Assistant 2 (TWR ASS-2) supports the runway controllers. Also, the TWR ASS-2 maintains communication under responsibility of the runway controllers and ground controllers with TWR-W, drivers of vehicles and towing traffic in the manoeuvring area and along runways, airport services, external emergency services or other stakeholders. Furthermore, this assistant guides vehicles in the manoeuvring area under responsibility of the ground control. To further support the runway controllers, the TWR ASS-2 gives permission to vehicles to cross certain lanes and exits under responsibility of the runway controller, and coordinates on requesting and returning of runways with the runway controller [37].
The communication between the ground controller and tower assistant 2 is face-to-face, and mainly consists of what the assistant is doing, or should do [14].

4.6.5. Apron Planning & Control (APC)

The Apron Planning & Control (APC) department is not part of LVNL, but is part of Royal Schiphol Group. This department has two responsibilities, which are Apron and Inbound. For Ground Control communication, only the Apron responsibility is of interest, and is therefore only discussed in this case. One of the Apron responsibilities is to handle the towing traffic safely and efficiently. The towing traffic is the traffic of small vehicles that tow aircraft from one side of the airport to the other side, where no taxiing is considered. Although the towing traffic is handled by the APC department, the responsibility of these movements lies with Ground Control. The other Apron responsibility is to escort the aircraft stand crews across the taxiways when clearing snow [37].
The communication line between the ground controller and the apron planner is regularly used, and is mainly initiated by APC. Communication between APC and the ground controller could be to ask for permission from the ground controller by the apron controller to cross certain parts of the manoeuvring area [14].

4.6.6. Upgraded Communication with Ground Control

All the mentioned colleagues of ground controllers specified in the previous subsections have a direct communication link with Ground Control. It is hereby mentioned that the most intensively communication links are not used very often, and that most of these communication links are transferred to automatic links. Furthermore, face-to-face communication due to the transfer of paper flight strips is not needed anymore due to the implementation of electronic flight strips. This new technique reduces the communication needed between the ground controllers, with the runway controllers and with the outbound planner. Therefore, no communication link is intensively used anymore. In this case, the most communication is between the ground controllers. The reason is, is because problems that occur and influence the traffic flow in the other sectors, or the rearrangement of active sectors, need to be handled by communication between the two ground controllers [14].

4.6.7. Transferring of Shifts

The transferring of Ground Control shifts is not part of the operations side of the communication link, but is part of the work flow of ground controllers, and is therefore discussed.
The transfer of controller is split into two parts, where the first part is self-debrief. During this self-debrief, the acquiring controller is getting familiarized with the general conditions. Part of these conditions are the used frequency, runway lights, runway conditions and agreements with other departments. The second part of the transfer is the actual transfer [14]. During this actual transfer, details in the manoeuvring area are discussed. These details include closures and other points of interest in the field, different SIDs, emergencies (if any) and future runway changes. Finally, the previous controller indicates what still needs to be arranged and what has already been arranged in terms of conflicts. The structure of the conversation is from coarse to fine. Also, the previous controller continues to work until it's all perfectly clear to the acquiring controller. The handover only takes place when both ground controllers are convinced that the information has been fully discussed, and that they both agree that the handover can take place [3].

4.7. Console

At TWR-C, the ground controller works on the (relatively lower) outer ring behind a console. This console is visualized in Figure 4.3 [5].

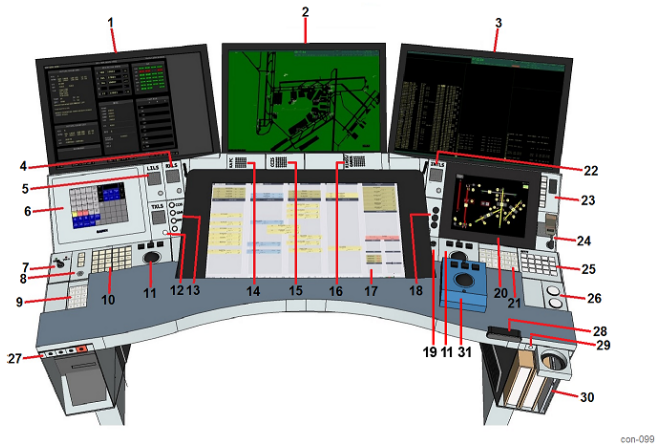

Figure 4.3: GC console [5]

The concerning parts that are represented by the different numbers in Figure 4.3 are in Table 4.1.

Number	Component	Number	Component
1	Screen CCIC/Office pc	17	EFSS-screen
2,3	TWR-screen	18	Screen switches (L, M, R) for rollball use
4	Speaker for RX (receiver) monitoring	19	Brightness control knob EFSS-screen
5	Speaker for line communication	20	ALCMS-controller screen
6	VCS	21	Mini-keyboard TWR-system (left screen)
7	VCS 1/ VCS 2-switch	22	Speaker intercom
8	Console panel VCS	23	Listening panel
9	CCIS keyboard	24	Speaker and hand microphone emergency radio system
10	Intercom panels	25	Frequency selection panel emergency radio
11	Roll ball	26	Workplace lighting controls
12	Speaker RX/TX	27	Communication aid connection points
13	Selection buttons	28	Console height adjustment controls
14	Speaker office-pc	29	Connection points communication aids (instructor)
15	CCIS-speaker	30	Keyboard TWR-system
16	Speaker GARDS/RIASS	31	Loose rollball (as an alternative to the built-in rollball)

Table 4.1: Ground control console components [5]

4.8. Screens

During its work, the ground controller uses several screens, which are visualized in Figure 4.3. This section explains the most relevant screens and how these screens are used by the ground controller. In subsection 4.8.1, the TWR-screen is explained. Then, in subsection 4.8.2, the EFSS-screen is explained. At last, in subsection 4.8.3, other relevant screens used by the ground controllers are explained.

4.8.1. TWR-Screen

The TWR-screen provides Schiphol TWR with up-to-date surveillance and flight plan data to monitor the air traffic situation in the Schiphol CTR's and Schiphol TMA's and the ground traffic situation at Schiphol Airport. This screen is made up of four modes, each with its own function. These four modes are ASDE, TAR, CAT and EDD, and are in the following parts described [5].

ASDE-Mode

In Airport Surface Detection Equipment (ASDE) mode, the TWR-screen displays the ground traffic situation. In Figure 4.3, this mode is shown and labeled under number 2. On this screen, a top view

of Schiphol Airport is displayed, where the current aircraft and vehicles are indicated with dots. Next to these dots, labels are added to provide relevant information about the aircraft and vehicles. This screen is used to create more situational awareness about what is happening in the manoeuvring area. Furthermore, it gives a clear overview of where aircraft are and where they are heading, which becomes essential during low visibility conditions. Therefore, this screen helps ground controllers to anticipate on coming scenarios. In this mode, also the Runway Visual Range (RVR), the wind speed and the wind direction can be obtained [5]

TAR-Mode

In the Terminal Area Surveillance Radar (TAR) mode, the TWR-screen displays the air traffic situation. Aircraft positions and movements are shown relative to underlying graphic maps, and are represented with dots containing labels. Furthermore, this mode shows the precipitation areas with different intensities. In comparison with the ASDE-mode, this mode is on its own not used very often by ground controllers. However, in combination with the ASDE-mode, the TAR mode can become more useful, which is explained in the CAT-mode part of this subsection [5].

CAT-Mode

In the Category (CAT) mode, the ASDE- and TAR-mode information are combined on one screen. For this, the screen is divided into two parts using a divider, with one part displaying the ASDE information, and the other the TAR information. This dividing line can be placed both horizontally and vertically on the screen. When using both the ASDE- and TAR-mode information, ground controllers become more aware of the number of aircraft landing in their sector in a certain time period [5].

EDD-Mode

In the Electronic Data Display (EDD) mode, the TWR-screen displays the flight information. In Figure 4.3, this mode is shown and labeled under number 3. The EDD gives an overview of all the inbound and outbound flights per runway. Flight strips are used, which contains information that could be relevant for the ground controller, like the starting/departing runways, aircraft stands and SID's of the different aircraft. Using this mode, the flight information can be checked and adjusted. However, this mode is used as minimal as possible [5].

4.8.2. EFSS-Screen

The Electronic Flight Strip System (EFSS) supports the ground controller with the handling of aircraft and vehicles using digital flights strips. In Figure 4.3, this screen is shown and labeled under number 17. The flight strips are presented on a interactive screen, and represent aircraft and vehicles. Relevant information about these aircraft and vehicles are placed on these strips. For an aircraft, this information could include the flight number, the inbound or outbound runway, aircraft type and slot time for departure (if outbound flight). The inbound strips are yellow, and the outbound strips are blue [5].
The EFSS is divided into multiple working bays. These different bays display what the statuses are of the different aircraft in the mavoeuvring area. The most important working bays for a TWR-C ground controller from left to right are the Passive, (Pending) Push-Back, (Pending) Taxi A and (Pending) Taxi B working bays. In the Passive bay, the flight strips of outbound aircraft are placed that are not yet cleared for push-back, but are handed over to the ground controller. When the aircraft are cleared for push-back, the flight strips of these aircraft are placed in the push-back pending or push-back bay, depending on the status of the aircraft. The Taxi A and Taxi B working bays contain the flight strips of aircraft that move over these taxiways. This division in taxiway is made to distinguish between the different flow directions of traffic. Next to these, there are also other working bays specified on the EFSS-screen, like the Settings-bay. In this bay, the boundaries of the responsibility areas of the different ground controllers can be temporarily adjusted, given the approval from the other ground controllers. There is also the bay Other, where controllers can place strips that don't fit in the other bays. Furthermore, there is also a bay where the flight strips are transferred to another controller, as well as a bay where flight strips appear when an inbound aircraft has landed. Also, there is bay where flight strips are placed that are ready to be moved to TWR. The possibility exists to write on the flight strips, to place them halfway between bays, or to let them stick out a little for extra attention. These features are all implemented to ensure that the controllers can work in a way that is most comfortable for them. In the scenario that an aircraft has parked, the strip can be removed from the screen [5].

4.8.3. Other Screens

Next to the screens that are presented in subsection 4.8.1 and subsection 4.8.2, there are other relevant screens that are mentioned in this section. There is for example the Airfield Lighting Control & Monitoring System (ALCMS) controller screen, labeled in Figure 4.3 under the number 20, that the controller can use to control the airfield lights [5]. Other screens that the controller can make use of is a screen that shows which runways are currently active, a screen that shows the incoming and outgoing flights for the next period in time and a screen that is a touchscreen that can be used to switch the communication line to another controller. This last mentioned screen becomes useful during peak traffic situations, to make sure the controllers can call each other when verbal contact is undesirable. There are more screens that can be used by the ground controller, but the ones mentioned in this section are most relevant [14].

5

Workload

In this chapter, it is explained how workload is defined and modeled in this research. In section 5.1, it is explained how workload is interpreted in this study, and how this interpretation is obtained. Then, in section 5.2, a proven task load model named Dynamic Density is discussed. Lastly, in section 5.3, the different task load metrics considered for this research are discussed.

5.1. Definition

In this section, it is specified in subsection 5.1.1 how different researchers define workload, and then it is specified in subsection 5.1.2 how workload is defined in this research.

5.1.1. Other Researchers

Throughout the literature, researchers define workload differently. Hart & Staveland (1988) [25] expresses workload as the interaction between the requirements of the task, the circumstances under which this is performed, and the behaviors, skills and perceptions of the individual. Furthermore, Rouse et al. (1993) [42] made a distinction between two types of workload, which are objective and subjective workload. In that case, objective workload is the load imposed or the load experienced, and the subjective workload is the perception of the imposed workload by a certain person. This perception leads to adaptive behaviour, which depends on the individual. Also, De Waard (1996) [19] defined workload as the result of reaction to demand. In that case, it is the proportion of the capacity that is allocated for task performance. Moreover, Brookhuis et al. (2008) [12] expresses workload as a reflection of task specifications and person characteristics. These person characteristics may include motivation, fatigue, effort, emotion, drowsiness, time-of-day, stress, individual capabilities and the strategy applied to solve the task [41] [61].

5.1.2. This Research

From subsection 5.1.1, it can be concluded that workload is a combination of task load and performer-based characteristics. Performer-based characteristics can be considered subjective, and include the effort and strategies applied to solve tasks [61]. On the other hand, task load can be considered objective [42], and is expressed as the number of tasks that someone needs to complete [33]. In the context of taxiway maintenance, task load is mainly of interest. The reason is that the changes in aircraft flows, because of taxiway maintenance, directly impact the tasks of the ground controller, but not directly the characteristics of the controller, which was obtained based on discussions with operational experts. Furthermore, nominal and maintenance scenarios can be compared objectively without performer interference. Also, this measure is more manageable than performer-based characteristics, and provides therefore a better measure to be used for maintenance plannings.

5.1.3. ATC Task Load Definition

In the literature, task load is mainly related to complexity, which is a combination of air traffic complexity and sector complexity [33] [35]. In more general terms, task load is expressed as the number of same tasks, or the number of different tasks that is associated with controlling the sectors by ground

controllers [33]. For ground controllers, one of these tasks is re-planning aircraft to make sure aircraft do not conflict with each other. Based on discussions with operational experts, is was obtained that this task is seen as one of the most demanding tasks for a ground controller. No research has been conducted on this part of the task load yet. Therefore, it is interesting to consider this indicator for this study. Another indicator that is interesting to consider for this research is Radio Telephony (R/T) data. The R/T is used by ground controllers to communicate with vehicles and aircraft within the manoeuvring area of Schiphol Airport, in which aircraft are considered most important. Therefore, R/T is a very important communication line [14]. In a previous master thesis, a model was created based on R/T data, and is discussed in section 5.2.

5.2. Dynamic Density

The Dynamic Density model for Ground Control is introduced by Stijn Brunia for his master thesis [14]. This model is a Linear Regression model consisting of multiple independent variables that are related to Dynamic Density, which is a metric related to complexity. The expression for the Linear Regression model is given in Equation 5.1.

$$Y = \sum_{i=1}^{n} W_i \cdot x_i \tag{5.1}$$

In Equation 5.1, Y is the dependent variable and W_i is the weight of the independent variable x_i. The dependent variable is in this case the percentage of time that the Radio Telephony (R/T) is used by a controller in a certain interval, also called the R/T load. The different independent variables are given in Table 5.1, and are defined for the sectors North, Center and South.

Independent variable	**Explanation**
AC Count	Average number of aircraft obtained in the given interval
Handovers	Total number of handovers obtained in the given interval
Push-backs	Total number of push-backs obtained in the given interval
Landings	Total number of landings obtained in the given interval
Bay Traffic	Number of bays that contain at least two aircraft in the given interval
RC Switch	Equal to 1 when there is a runway configuration switch in the given interval, else equal to 0

Table 5.1: Independent variables of Dynamic Density model

In the research of Stijn Brunia, the model was trained for each sector, where the resulting weights of the Linear Regression model are presented in Table 5.2

Feature	**N**	**S**	**C**
Intercept	0.063	0.030	0.131
AC Count	0.065	0.091	0.039
Handovers	0.011	0	0
Pushbacks	0.018	0.021	0
Landings	0	0	0.007
Bay traffic	0.013	0.023	0
RC Switch	0.036	0	0

Table 5.2: Weights of Dynamic Density model

The input of this model is runway configuration and Airport Surveillance Tracker (ASTRA) data. This makes the model in its current state not flexible to be used in this research, as no ASTRA data is available for the given maintenance scenario [14].

5.3. Task Load Metrics

The task load metrics used in this research are the number of re-plannings made by the ground controller in a certain time interval, and the Dynamic Density metric measured using the Dynamic Density model described in section 5.2. The re-planning metric is considered to measure qualitative aspects of task load, as the complexity of problem solving is considered. Furthermore, this metric aims to quantify cognitive task load, as this metric captures mental decision-making. On the other hand, Dynamic Density includes mainly quantitative aspects of task load, as this indicator better captures the management of multiple aircraft and situational monitoring [14]. Therefore, both metrics are used to aim to get a better idea of task load.

Based on discussions with operational experts, a representative approach for taking into account these re-plannings is by letting aircraft travel from A to B using their shortest path, and count the number of times aircraft conflict with each other. As these aircraft conflict with each other, controllers should've solved these conflicts, meaning that re-plannings were necessary. Ground controllers are responsible for maintaining minimum separation between aircraft in their controlled sector. Therefore, a representative approach is to define a re-planning when two aircraft are too close to each other. This is called a violation, and its implementation and detection is discussed in chapter 6. Furthermore, the Dynamic Density metric is considered by changing the input of the Dynamic Density model from ASTRA data to shortest route data to make sure this measure can be used together with the other re-planning metric. The principle that is used to plan shortest paths is Multi-Agent Path Finding, and is discussed in chapter 7.

6

Violations

In this chapter, it is described how violations are defined based on the approach given in section 5.3. This is done by first discussing the minimum separations required for modeling in section 6.1, and then how violations are detected in section 6.2.

6.1. Minimum Separation

Ground controllers are responsible to ensure sufficient separation between aircraft in their controlled sector. These separations are influenced by a significant number of factors, like speed, weight and dimensions of the aircraft, weather conditions, but also the geometric properties of the airport. However, no specific requirements have been set up for minimal separations in the area controlled by ground controllers. At Schiphol airport, separation between aircraft is determined based on agreements between aircraft and controllers, but no specific values are determined that represent minimum separations. Therefore, in subsection 6.1.1, different approaches to aircraft separations by different researches are specified. Based on these researches and discussions with operational experts, in subsection 6.1.2, the separation requirements used in this research are explained.

6.1.1. Previous Research

In the literature, different approaches for minimum separation between aircraft in the area controlled by ground controllers are specified. These different approaches are explained in this subsection.

Separation Based on Weight Class

In the research conducted by Van Oosterom et al. (2023) [58] on the use of electric towing vehicles, different separations are defined depending on the weight class of the aircraft, and are specified as a distance from the centre of the aircraft shown in Figure 6.1. In that research, the assumption is made that the minimum separation distance that an aircraft needs to keep from its centre to other aircraft is for narrow-body aircraft 40 meters, for wide-body aircraft 50 meters and for heavy-wide-body aircraft 60 meters.

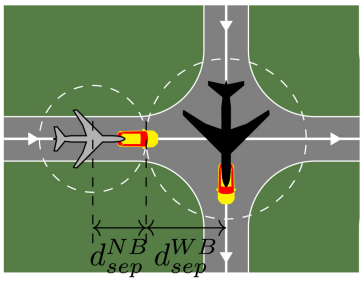

Figure 6.1: The minimum required separation distance between a narrow-body and a wide-body aircraft when making use of electric towing vehicles [58]

Separation Based on Edge-Relations

In a multi-agent planning model for autonomous airport surface movement operations at Amsterdam Airport Schiphol, created by Von der Burg & Sharpanskykh [59], separation between aircraft in the area controlled by ground controllers is ensured by the radius from the agent's dimensions and a safety distance. This radius is equal to the maximum value between the wingspan and the length of the aircraft, divided by two. The safety distance depends on two different edge-relations between two agents. The first relation is defined as the scenario when two agents travel along the same path. In this first relation, the safety distance is defined as three times the radius of the agent in front, which is incorporated such that the trailing agent stays cleared of the engine blast of the leading agent. In the second relation, both agents are travelling on neighbouring edges, but not along the same path. In this relation, the safety distance is equal to the average radius of the two agents radii. Currently, the safety distance is not enforced in the model.

Separation Based on Speed

D. Yuan et al. (2024) [62] has specified a conflict detection model for their research on integrated optimization of scheduling for unmanned follow-me cars (UFMC) on the airport surface. This conflict detection model is based on elliptical protected zones around the aircraft and follow-me cars using the positions of these vehicles, which is visualized in Figure 6.2a.

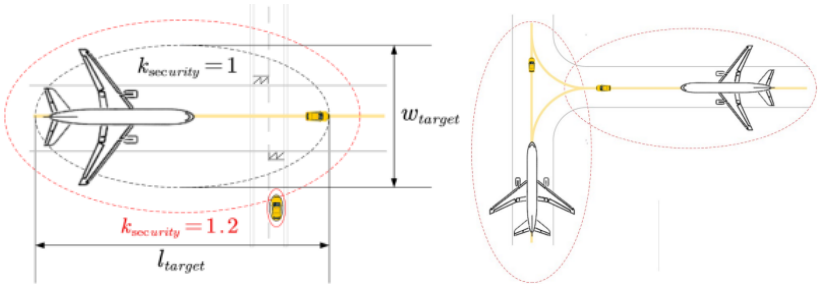

(a) Structure of protected zone (b) Situation of conflict

Figure 6.2: Elliptical protected zones [62]

In Figure 6.2a, l_{target} and w_{target} are the length and width of the UFMC or GU, respectively. The GU is the "Guidance Unit", and refers to the combination of the UFMC and the aircraft being guided by it. If the aircraft is guided, then GU is used, else UFMC. Furthermore, $k_{security}$ is the safety factor that is determined based on iteration such that the probability of detecting a collision is high, but that the number of false alarms is reduced. This protected zone is elliptical, and the semi-major axis "a" and the semi-minor axis "b" of this elliptical protected zone are defined in Equation 6.1.

$$a = (\frac{l_{target}}{2} + \frac{v^2}{2a_d}) * k_{security} \qquad b = (\frac{w_{target}}{2}) * k_{security} \tag{6.1}$$

In Equation 6.1, v and a_d are the speed and deceleration of the vehicle, respectively. This means that the protected zone is dependent on the speed and deceleration of the vehicle.
In Figure 6.2b, it is shown how a conflict is specified between two protected zones. In this case, a conflict is defined as the overlapping of both protected zones.

6.1.2. This Research

In this research, a protected zone around the aircraft is present that detects collisions between aircraft. A collision is defined when the separation requirement between aircraft is violated, which translates to the overlapping of the different protected zones. Based on previous researches presented in section 6.1, it can be concluded that this protected zone is dependent on the weight class, edge-relations, speed of the aircraft and aircraft dimensions. Furthermore, Ground Control experts suggested that the protected zone is small along the wings of the aircraft, and large in front of and behind the aircraft. Also, the experts stated that the size of the protection zones, for modeling purposes, increase linearly with the increase in speed of the aircraft. Based on discussions with operational experts and previous researches

presented in subsection 6.1.1, it is determined that the protected zone is elliptical. Therefore, the semi-major axis "a" and semi-minor axis "b" of the elliptical protected zone can be defined. For these expressions, it is assumed that the center of the aircraft is the center of the ellipse, and that the major axis runs along the length of the aircraft. The expressions for the semi-major axis "a" and semi-minor axis "b" are given in Equation 6.2.

$$a = \frac{l_{aircraft} * k_{weight} + v_{aircraft} * c}{2} \qquad b = \frac{w_{aircraft}}{2} \tag{6.2}$$

In Equation 6.2, $l_{aircraft}$ is the length of the aircraft in meters, $w_{aircraft}$ is the wingspan of the aircraft in meters, $v_{aircraft}$ is the speed of the aircraft in meters per second, and k_{weight} is a parameter that is dependent on the separation distances defined by Van Oosterom et al. (2023) [58]. This k_{weight} parameter is equal to the minimum separation defined for the weight class of the concerning aircraft, divided by the minimum separation defined for narrow-body aircraft. This means that the k_{weight} parameter is equal to $40/40 = 1$ for narrow-body aircraft, $50/40 = 1.25$ for wide-body aircraft and $60/40 = 1.5$ for heavy-wide-body aircraft. Furthermore, the factor c is introduced, which is equal to 1 second to make sure the addition in the expression for the semi-major axis can be performed.

In this case, the semi-major axis "a" is defined by taking into account the horizontal separation between two aircraft traveling along the same path defined by Malte von der Burg and Alexei Sharpanskykh presented in subsection 6.1.1. However, in this case, dependencies on the aircraft speed and weight class are also taken into account. This does not not hold for semi-minor axis "b", where this axis is only dependent on the wingspan because aircraft themselves are responsible for keeping minimum distance along the wings. For both axes, the speed of the aircraft is added up to create the linear relation between aircraft speed and separation, which was advised by Ground Control experts. It may be noticed that when the speed is low, aircraft are able to move closer along and behind each other, which relates to the ground movement operations on the apron.

6.2. Detection of Violations

To detect whether ellipses overlap with each other, an algorithm made to determine the relative position between two ellipses is hereby adopted. This algorithm is created by G.B. Hughes and M. Chraibi [26], and is given in Algorithm 1 in Appendix 1. This algorithm first determines the symmetric matrix of each of the two protected zones, which are symmetric matrix A and B. The inputs of each symmetric matrix are the parameters that determine the dimensions of the protected zone given in subsection 6.1.2, namely the length, width, speed and k_{weight} parameter. Furthermore, the coordinates of the center of the protected zone and the heading of the protected zone are used as input for the symmetric matrix of the protected zone. Using both symmetric matrices, the characteristic polynomial of the pencil $\lambda \cdot A + B$ is determined and is given in Equation 6.3.

$$f(\lambda) = det(\lambda \cdot A + B) = \lambda^3 + a \cdot \lambda^2 + b \cdot \lambda + c \tag{6.3}$$

After the polynomial given in Equation 6.3 is turned monic, the coefficients a, b and c are interpreted. Based on the values of these coefficients, in combination with the associated outcomes of s_1, s_2, s_3 and s_4 using these coefficients, the algorithm outputs the relative position between the two protected zones [26].

7

Multi-Agent Path Finding

In this chapter, different single-agent path finding algorithms are discussed. Before these are discussed, in section 7.1, the main principle of multi-agent path finding is discussed. Then, three single-agent path finding algorithms are discussed, which are A^* in section 7.2, SIPP in section 7.3 and SIMP in section 7.4. Consequently, in section 7.5, the multi-agent path finding model created at the TU Delft by Von der Burg & Sharpanskykh [59] is explained. Then, in section 7.6, the single-agent path planning algorithms are evaluated, and one of these algorithms is chosen for further use.

7.1. Main Principle

In a multi-agent path finding problem (MAPF), multiple agents need to find their collision-free paths from their start to their goal locations that minimizes some objective. This objective could be a makespan objective, where the goal is to minimize the latest arrival time of an agent at its goal location. However, this objective could also be a flowtime objective, where the goal is to minimize the sum of the arrival times of all agents at their goal locations [31]. In this case, an agent is an autonomous entity that can be computed. Furthermore, this entity can perceive its environment through its sensors and acts upon its environment through its effectors [55]. At each timestep in the MAPF model, the agent takes an action. There are two types of actions; wait and move. A move action means that the agent moves from its current node to an adjacent node, and a wait action means that the agent stays at its current node for another time step. From this, it can be obtained that a solution consists of collision free paths if multiple agents are not at the same node at the same time [56].

The MAPF problem has already been applied in many different disciplines. For example, MAPF is applied in studies to re-plan paths for robots in warehouses so that these robots can pick-up and deliver packages, such that no collisions occur with other robots [27]. Also, MAPF has already been applied in the field of aviation. For example, MAPF has been applied in studies to implement autonomous towing vehicles for taxiing aircraft at the airport, such that no collisions occur with other vehicles [36] [10].

In the literature, Stern et al. [56] has set-up a general description for the MAPF problem, which is adopted in this subsection. As was already mentioned in the beginning of this section, the optimal solution of a MAPF problem does not contain any collisions. When modelling, these collisions can be specified as conflicts. In this case, five different types of conflicts are specified, which are shown in Figure 7.1. In this case, an edge conflict arises when two agents move along the same edge in the same direction simultaneously. When the agents are planned to be at the same vertex at the same time, a vertex conflict occurs. The third visualization in Figure 7.1 shows a following conflict, which happens when an agent is planned to be at the vertex at which another agent, travelling in the same direction, was in the previous time step. A cycle conflict occurs when multiple agents are planned to move in a cycle and for each time step, the previous position of an agent is occupied by another agent. The last to be specified conflict is the swapping conflict, which occurs when two agents are planned to traverse the same edge at the same time in the opposite direction.

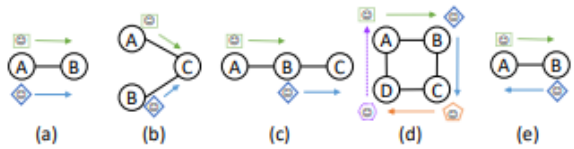

Figure 7.1: Different types of conflicts: a) an edge conflict, b) a vertex conflict, c) a following conflict, d) a cycle conflict, e) a swapping conflict [56]

Before the different conflicts can be solved, individual paths need to be generated for all the different agents. These individual paths can be generated using the A^* Algorithm, discussed in section 7.2, the SIPP algorithm, which is discussed in section 7.3, or the SIMP algorithm, which is discussed in section 7.4. To make use of these algorithms, the environment, which is the airport layout, is modeled as a graph layout with edges representing runways, aprons and taxiways, and nodes representing intersections, gates, runway entries and exits.

7.2. A^* Algorithm

The A^* algorithm is an algorithm that computes shortest paths from a given initial node to a given goal node [22]. This algorithm makes use of a graph layout represented as a function G(V,E) with edges (E) and nodes (V). The edges connect the nodes, and have a certain weight. Furthermore, the algorithm considers three different parameters. At the start of computing the shortest path, the node with the lowest f-score is taken out of an open set, and saves this node as the current node. Hereafter, given that the node is not the goal node, the algorithm explores the nearby nodes of the current node. To do this exploration, two parameters need to be defined. The first parameter is g(n), which is the cost of moving from the start node to a neighbouring node n, and the second parameter is h(n), which is an estimation of the shortest path from the neighbor n to the goal node. This estimation is also called a heuristic value. This heuristic value may never be an overestimate of the actual cost to reach the goal node. A commonly used heuristic is the Euclidean distance, which is the absolute distance between the neighbouring node and the goal node. Therefore, this heuristic never overestimates the cost. To use these parameters, the function f(n) = g(n) + h(n) is set up and updated for each neighbouring node. This function is called the f-score, or the evaluation function. The neighbouring node containing the lowest f-score is then considered the current node. This process is repeated until the goal node is reached [24].

7.3. SIPP Algorithm

The Safe Interval Path Planning (SIPP) algorithm, as defined by Phillips & Likhachev [40], is a single-agent path planning algorithm that uses safe time intervals to compute the optimal path for an agent. A safe time interval is defined as an interval in time in which an concerning agent does not conflict with other agents. Using these safe time intervals, SIPP searches in a state space that consists of configuration and interval pairs rather than location and time step pairs. Therefore, the search space used by SIPP is smaller compared to the search space used by algorithms using location and time step pairs, leading to smaller memory requirements and faster planning.

Like was mentioned before, SIPP makes use of configurations. In this case, a configuration is specified as a combination of the agent's location and other relevant information about the state of the agent, such as heading and velocity. This means that SIPP specifies a state as a configuration interval pair. For each state 's', the variables g(s), h(s), parent(s) and time(s) are saved. These variables represent the g-score (same as in A^*), the heuristic (same as in A^*), the parent state of state 's' and the earliest possible arrival time of the agent in the configuration respectively. As in A^*, SIPP chooses to generate successors for the state with the lowest f-value. However, the approach on generating successors is different between A^* and SIPP. The difference is that SIPP takes into account a set of motions that are possible from the concerning state. From these possible motions, the resulting configurations are checked for their safe time intervals. In each of these intervals, the earliest arrival time is determined and it is checked if conflicts occur. If a feasible motion is found to a new state, consisting of a configuration and a safe time interval, this state is added to the successors. Based on these successors, a node

with the lowest f-score is expanded next, which is a similar approach as with A^*. This process of state expansion continues until the goal node is reached.

To give an example of a state expansion using SIPP, the scenario specified in Figure 7.2 is considered. This example is specified by Phillips & Likhachev in [40].

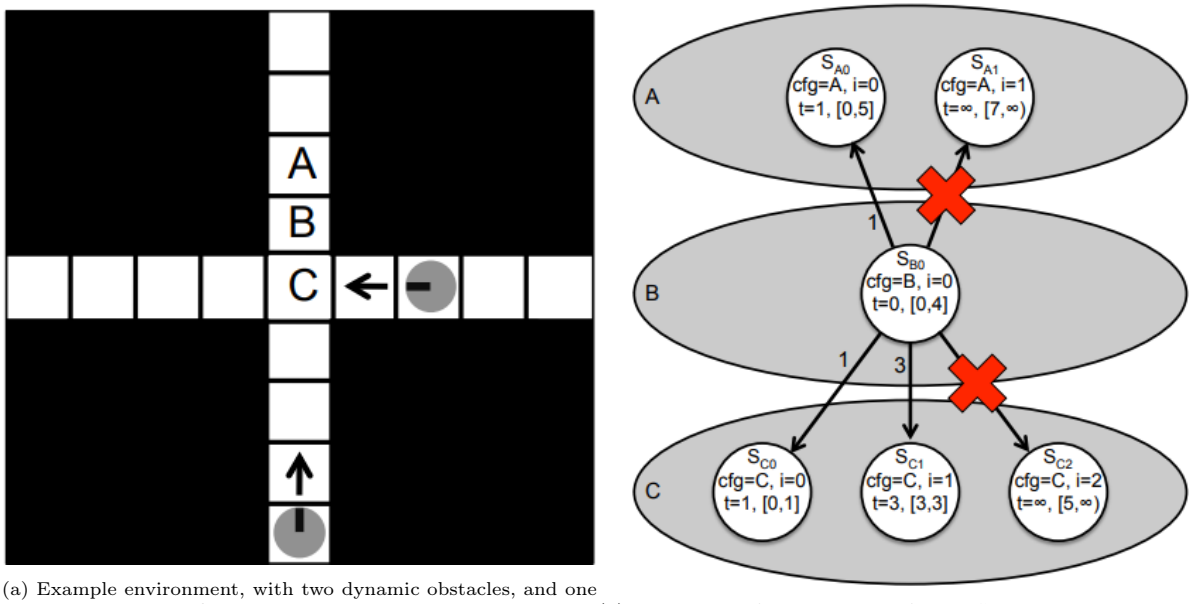

(a) Example environment, with two dynamic obstacles, and one agent starting at configuration B

(b) Illustration of an expansion of state S_{B0}

Figure 7.2: Example application of SIPP [40]

In Figure 7.2a, three configurations are specified for the agent, which are A, B and C. The agent that is planned using SIPP is in this case located at configuration B. Through the environment, two dynamic obstacles move in the indicated direction, and should be avoided by the agent starting at B.
In the initialization step of the algorithm, the safe intervals are determined for each configuration. Given that the dynamic obstacles move one cell per time step, the safe intervals for A are [0,5] and [7,∞]. This is because at time step 6, configuration A is occupied by the dynamic obstacle moving upwards, so time step 6 can not be part of the safe interval. Time step 6 is part of the collision interval, which is the opposite of the safe interval. The save intervals for configuration C are [0,1], [3,3], [5,∞]. This is because at time step 2, configuration C is taken by the dynamic obstacle moving to the left, and at time step 4, configuration C is taken by the dynamic obstacle moving upwards. The safe interval for configuration B is [0,4] because the agent can at maximum wait until time step 4 at B, or else a conflict with the upward moving agent occurs [40].
In the following step, the state S_{B0} is expanded, where the direct neighbors of B are the potential successors. There are different ways on how to arrive in these successors, which is visualized in Figure 7.2b. In this figure, each white circle represents a state. The first line in the circle is the state name, in the second row the configuration (cfg) and its safe interval (i) are specified. The third row specifies the earliest arrival time at that state (t) and the safe interval [a,b]. The gray ovals group states by their configuration, and the arrows indicate transitions from one state to another, labeled with their cost. When considering state S_{A0}, the agent can directly move to configuration A, and arrives the earliest at A on time step 1. This arrival time is within the first save interval of the configuration. Therefore, the move to state S_{A0} is feasible. For state S_{A1}, the agent needs to wait till time step 6 at configuration B, and then move to configuration A to arrive at time step 7. However, it is not possible to wait longer than time step 4 because the safe interval at B ends then. Therefore, expansion to state S_{A1} is unfeasible. There are two feasible options to go from B to C. For state S_{C0}, moving directly to C would result in an earliest arrival at C at time step 1, which is within the concerning safe interval. Furthermore, for state S_{C1}, waiting at B till time step 2 and then move to C with an earliest arrival at time step 3 falls within the concerning safe interval. The last state, S_{C2}, results in waiting at time step B until time

step 4 and then move to configuration C, which results in a conflict with the upward moving obstacle. Therefore, the move to state S_{C2} is unfeasible [40].
As a last step, the successors are evaluated. In this case, the feasible successors from state S_{B0} are S_{A0}, S_{C0} and S_{C1}. The g-score is updated for these states with the earliest arrival time at these states. Furthermore, the f-score is updated by adding the heuristic and the g-score. Then, the state with the lowest f-score is expanded next. This process continues till the goal state is reached [40].

7.4. SIMP Algorithm

The Safe-Interval Motion Planning (SIMP) algorithm is an algorithm developed at the TU Delft, and is an augmented version of the SIPP algorithm. SIMP builds further on the SIPP algorithm by taking into account heterogeneous, non-holonomic agent properties, including their dimensions, into account. This algorithm uses motions in continuous time and space along a graph representing the taxiway network of an airport [60]. Its application for the layout of Schiphol airport is presented in [59].

7.5. Multi-Agent Planning Model of Amsterdam Airport Schiphol

At the TU Delft, Von der Burg & Sharpanskykh [59] have created a multi-agent planning model for autonomous airport surface movement operations at Amsterdam Airport Schiphol, named the Multi-Agent Airport Surface Movement Operations simulator (MAASMO-sim). This model makes use of a multi-agent system (MAS) that plans conflict-free routes for all aircraft on the ground and controls their execution. In subsection 7.5.1, it is explained how the airport taxiing infrastructure is build-up. Then, in subsection 7.5.2, it is explained what the different agents are and what their function in the model is.

7.5.1. Airport Taxiing Infrastructure

The airport taxiing infrastructure is represented by a graph G = (V, E). This graph comprises vertices V and directional edges E. The lay-out of Amsterdam Airport Schiphol is presented in Figure 7.3.

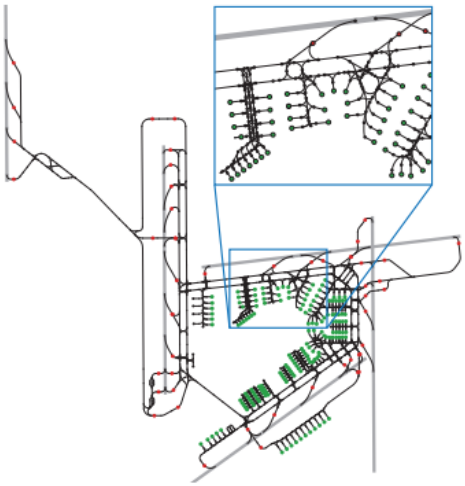

Figure 7.3: Graph of layout of Amsterdam Airport Schiphol [59]

In Figure 7.3, the vertices that denote aircraft stands are green, the taxiway intersections are black, and the stopbars in front of the runway entries are red. Furthermore, the edges that denote taxiways are black, and the runways are grey. The bidirectional taxiway segments between two vertices are constructed from two unidirectional edges that connect the vertices [59].

7.5.2. Agents

The multi-agent system (MAS) comprises a distributed-hierarchical structure, that includes both centralized and distributed agents. This system is shown in Figure 7.4.

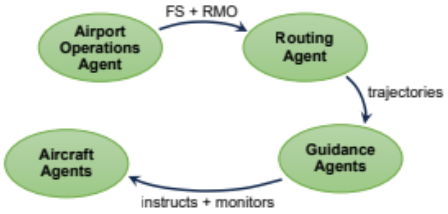

Figure 7.4: Multi-agent system [59]

The centralized Airport Operations Agent defines and updates the runways in use, which is in the model expressed as the runway mode of operation (RMO). To make sure active runways and the resulting flight paths of departing and/or arriving aircraft are not crossed, the Airport Operations Agent sets layout constraints on these taxiway segments that need to be blocked. This can also be done for taxiway segments that are unavailable, due to maintenance for example. Also, the Airport Operations Agent schedules all the flights, and updates them based on new predictions of the underlying A-CDM milestones. These milestones are explained in subsection 3.1.3. The flight schedule and constraints are sent to the Routing Agent, and this agent computes conflict-free routes for all taxiing aircraft within the upcoming planning window w_{plng}. The routing plans are re-computed when the Routing Agent receives updates from the Airport Operations Agent, or latest after the re-planning period h_{plng} has passed. These routing plans are sent to the Guidance Agents, which are located at each intersection in the taxiway system. Each Guidance Agent only controls the Aircraft Agents that are moving towards the location of the concerning Guidance Agent. The Guidance Agents instruct the Aircraft Agents to execute the next part of the planned trajectories, and monitors these actions. This is done by making use of the airport radar by the Guidance Agents that reports the position, speed and heading of all the Aircraft Agents during their movements over the airport. Furthermore, the Guidance Agents locally adjust the trajectories of the Aircraft Agents that deviate from their planned routes. This is done to minimize deviations from the planned trajectories. However, the Guidance Agent requests central re-planning from the Routing Agent when the impact becomes too extensive. The guidance responsibility for aircraft passing the location of the concerning Guidance Agent is passed to the next Guidance Agent that is located along the paths of the aircraft [59].

7.6. Evaluation of Single-Agent Path Planning Algorithms

In this subsection, the low-level multi-agent path planning algorithms A^*, SIPP and SIMP are evaluated. The A^* algorithm has proven to be optimal and complete, meaning that it is certain that the algorithm finds a shortest path from the start node to the goal node [24]. This algorithm is seen as efficient because a heuristic from the neighbouring node to the goal node is taken into account, which means that A^* only takes into account the area in the direction of the destination [22].
Because SIPP makes use of intervals, these intervals are considered suitable for efficient application in continuous time. Furthermore, this algorithm can also handle waiting actions in continuous time efficiently, based on the start and end times of the intervals. This makes the SIPP algorithm more efficient then the A^* algorithm [15]. Also, SIPP defines states based on feasible motions and the resulting configurations. Therefore, the possibility exists to include agent kinematics, such as acceleration and deceleration, during planning of the path of the agent [30]. This makes this algorithm more interesting to use for ground operations at airports then A^* because the kinematics of the aircraft can be taken into account. Regarding SIMP, this algorithm builds further on SIPP by taking into account more agent properties [60]. Therefore, SIMP is chosen as the single-agent path planning solver in this project.

8

Research Proposal

In this final chapter, the research proposal is discussed. In section 8.1, a recap of the literature study is presented. Then, in section 8.2, the research objective and research questions are given. Lastly, in section 8.3, the research methodology is presented.

8.1. Recap Literature Study

In chapter 2, the different aspects of runway and taxiway maintenance are discussed. From this chapter, it became clear that the different steps in the process of the construction of the runway maintenance strategy leads to different insights in planning runway maintenance, depending on operational, but also non-operational aspects. Therefore, analyzing these aspects well results in a more integral and accepted runway maintenance planning. This approach is also used for taxiway maintenance planning, where MovingDot made different analyses to support the planning decision making. Furthermore, it was obtained that heavy maintenance is the most restricting type of maintenance, as aircraft movement operations are impacted the longest. In general, this maintenance type is also called large-scale maintenance. From both the runway and taxiway maintenance analyses, it is obtained that there is limited insight in the impact on Ground Control workload. The impact of taxiway maintenance on the workload of ground controllers is characterized by differences in airside airport operations, which is discussed in chapter 3. In this chapter, the concept of airside airport operations at Schiphol Airport is explained using different principles. It is clear from this chapter that these airport operations are complex and dynamic in nature, and are influenced by a significant number of factors that are difficult to estimate. Therefore, aircraft operations change continue using different runway configurations, meaning that studying the workload of ground controllers per runway configuration is most valuable. The Ground Control unit located at Schiphol Airport was discussed in chapter 4. From this chapter, it became clear that ground controllers have a large set of responsibilities, where they have to communicate a lot with different colleagues and use different screens and equipment. Then, the workload of these ground controllers were discussed in chapter 5. From this chapter, it can be obtained that workload has many different interpretations throughout the literature. In this study, the focus is on task load, which is part of workload, and is defined as the number of re-plannings by ground controllers and Dynamic Density. The re-planning metric is taken into account by quantifying the number of separation violations when using a shortest path algorithm. This shortest path algorithm is also used by the Dynamic Density model, which is used to predict the R/T load for the given individual routes. From chapter 6, it can be obtained that the violations are determined based on the violation of protected zones, which are elliptical and expressed based on the speed and dimensions of the aircraft. These violations are detected by an algorithm that determines the relative position of two ellipses. The shortest paths are determined using a single-agent path planning algorithm, discussed in chapter 7. In this chapter, the different single-agent path planning algorithms that were discussed where A^*, SIPP and SIMP. From these algorithms, SIMP has been chosen to be the single-agent path planning algorithm in this research, as this algorithm is an extension on the SIPP algorithm by including more agent properties, and is more efficient than the A^* algorithm.

8.2. Research Objective & Research Questions

In this section, the research objective and research questions are given. In subsection 8.2.1, the research objective is presented. Then, in subsection 8.2.2, the research questions are presented.

8.2.1. Research Objective

Based on the recap of the literature study given in section 8.1, the following research objective is defined:

"To model and evaluate the impact of large-scale taxiway maintenance on the task load of ground controllers for different runway configurations"

This research objective tackles the gab from practice to establish a relationship between large-scale taxiway maintenance and task load of ground controllers at Schiphol Airport. Furthermore, by modeling the task load for nominal and maintenance scenarios with different metrics, this project aims to fill the gab by providing better insight into the impact of large-scale taxiway maintenance on the task load of ground controllers. To tackle this research objective, a main research question and sub-questions are defined, and are presented in subsection 8.2.2.

8.2.2. Research Questions

In this subsection, the main research question and sub-questions are defined based on the research objective presented in subsection 8.2.1.

Main Research Question

Given the research objective, the following main research question is established:

"How does large-scale taxiway maintenance impact the task load of ground controllers for different runway configurations?"

Sub-Questions

Based on this main research question, the following sub-questions are set-up:

1. How is task load defined?
2. Which metrics are used to describe task load?
3. Which factors are included to determine task load?
   (a) Which factors are most relevant to determine task load for taxiway maintenance scenarios?
   (b) How are these factors included?
4. What data is used to model task load?
5. Which parts of the taxiway infrastructure are considered for modeling?
6. How are the different runway configurations included?
   (a) Which runway configurations are included?
   (b) What are the flows for these runway configurations for the nominal case?
   (c) What are the flows for these runway configurations for the maintenance case?
7. What are the changes between the nominal and maintenance scenarios?
   (a) How do traffic flows change because of large-scale taxiway maintenance?
   (b) What is the change in task load?
8. What is the reason for these changes in task load?

8.3. Research Methodology

In this section, the research methodology is presented. This is done by first specifying an overview of the methods used in subsection 8.3.1. Hereafter, the work packages of these methods are presented in subsection 8.3.2. Lastly, the research scope is presented in subsection 8.3.3.

8.3.1. Overview

In this research, a single-agent path planning algorithm is used to plan individual paths for the different aircraft. From the literature study, it can be obtained that the SIMP algorithm is most suitable. Therefore, this algorithm is used, which is already implemented in the MAASMO-sim described in section 7.5. To make sure the paths generated by SIMP correspond to flows representative for the given runway configuration, for both the nominal and maintenance case, the SIMP algorithm is calibrated using weights and constraints. Then, the resulting paths and simulation properties of the MAASMO-sim are used by the Dynamic Density model. Furthermore, these biased paths and simulation properties are used by an analysis tool, which quantifies the number of times the minimum separation between aircraft are violated based on the overlaps of protected zones around aircraft described in chapter 6. In this research, this tool will be called the Violation Tool. Before simulating, two validation steps are conducted. The first validation step is to compare the paths generated by the SIMP algorithm to the paths from ASTRA data. When both paths are similar, the SIMP paths are used by the Dynamic Density and Violation Tool to compare these two metrics with each other. This is done to see if there are similarities between the two metrics. Then, simulations are run for flight schedules from the year 2019, as this year was a demanding year and the runway configurations described in subsection 3.4.4 where frequently used in that year for the maintenance case described in section 2.4. The results of these simulations are analyzed, and then evaluated.

8.3.2. Work Packages

In this subsection, the activities required to conduct the research are sub-divided into different work packages. These different work packages are given in the following parts.

Work Package 1: Calibrate the SIMP Algorithm

The main goal of this work package is to calibrate the SIMP algorithm, which is implemented in the MAASMO-sim. The key activities that need to be conducted to reach this goal are:

1. Familiarize with the MAASMO-sim
2. Run scenarios to better understand the behaviour of the MAASMO-sim
3. Include constraints to model the maintenance scenario and required flows
4. Adopt the weights of the SIMP algorithm to make sure certain taxiway segments are used more often

Work Package 2: Implement and Optimize the Dynamic Density Model

The main goal of this work package is to make sure the Dynamic Density model is implemented and optimized in the MAASMO-sim. The following key activities are hereby done:

1. Implement the Dynamic Density model in Python
2. Run the Dynamic Density model only using ASTRA data
3. Optimize the Dynamic Density model by using SIMP route data and the flight schedules
4. Test model using different test samples

Work Package 3: Implement the Violation Tool

The main goal of this work package is to implement the Violation Tool in the MAASMO-sim. Hereby, the following key activities are done:

1. Determine where in the simulator this tool fits best
2. Implement the Violation Tool in the simulator
3. Test the Violation Tool using different test samples

Work Package 4: Conduct Path Validation

The main goal of this work package is to validate the paths of the SIMP algorithm. This is done using the following key activities:

1. Prepare the flight schedules used for validation
2. Conduct path validation
3. Analyze results
4. If paths of SIMP are not similar with paths of ASTRA data: change weights and constraints for SIMP algorithm to make sure these paths are similar to the paths of the ASTRA data, and re-do path validation

Work Package 5: Conduct Metric Validation

The main goal of this work package is to validate both metrics used in this research. This is done using the following key activities:

1. Conduct metric validation
2. Analyze results

Work Package 6: Run Simulations

The main goal of this work package is to simulate task load per runway configuration. This is done using the following key activities:

1. Clean and prepare flight schedules for simulation
2. Run the simulations for both metrics and per runway configuration

Work Package 7: Analyze Results

The main goal of this work package is to analyze the results of the simulations. This is done using the following key activities:

1. Analyze the numerical outcomes of the metrics
2. Analyze the differences in routes and other notable differences between the nominal and maintenance case

Work Package 8: Evaluate Results

The main goal of this work package is to evaluate the obtained results. This is done using the following key activities:

1. Create general statements for the given scenarios based on the results from work package 7
2. Create general statements for different scenarios based on the results from work package 7

8.3.3. Research Scope

In this section, the research scope is presented. This scope covers the assumptions that are made in this research.

1. The model is a fast-time model because this model needs to be able to advise Schiphol on a strategic level
2. The model takes into account current operations, so no taxibots are implemented for example
3. The aircraft follow preferred routing as much as possible
4. The flight schedules used as input for the model are assumed to support the maintenance scenarios sufficiently

5. The validation for one scenario is assumed to be sufficient to represent validation for the other maintenance scenarios
6. Non-nominal operations, including de-icing operations and low visibility conditions, are not considered
7. Making certain vertices and edges inactive represents the closing of infrastructure at that position accurately
8. The already implemented model properties (push-back procedure, taxiing procedure and infrastructure properties for example) accurately represent the current properties implemented at Schiphol Airport

III

Supporting work

1

Appendix 1: Relative Position of Two Protected Zones

Algorithm 1 Relative position of two protected zones. In this algorithm, h_1 and k_1 are the translation coordinates of the center of the ellipse of aircraft 1 with respect to the origin of the given coordinate system. The same holds for h_2 and k_2, which are the coordinates of the center of the ellipse of aircraft 2. Furthermore, l_{ac1} and l_{ac2} are the lengths of aircraft 1 and aircraft 2, w_{ac1} and w_{ac2} are the widths of aircraft 1 and aircraft 2, $k_{weightac1}$ and $k_{weightac2}$ are the weight factors of aircraft 1 and aircraft 2, v_{ac1} and v_{ac2} are the speeds of aircraft 1 and aircraft 2, and φ_1 and φ_2 are the headings of aircraft 1 and aircraft 2 [26].

Input: h_1, h_2, k_1, k_2, l_{ac1}, l_{ac2}, w_{ac1}, w_{ac2}, $k_{weightac1}$, $k_{weightac2}$, v_{ac1}, v_{ac2}, φ_1, φ_2

$A_1 \leftarrow l_{ac1} \cdot k_{weightac1} + v_{ac1}$
$A_2 \leftarrow l_{ac2} \cdot k_{weightac2} + v_{ac2}$
$B_1 \leftarrow \frac{w_{ac1}}{2} \cdot k_{weightac1} + v_{ac1}$
$B_2 \leftarrow \frac{w_{ac2}}{2} \cdot k_{weightac2} + v_{ac2}$

Determine coefficients of symmetric matrix A

$a_{1,1} \leftarrow \frac{cos^2(\varphi_1)}{A_1^2} + \frac{sin^2(\varphi_1)}{B_1^2}$
$a_{1,2} \leftarrow \frac{sin(\varphi_1)\cdot cos(\varphi_1)}{A_1^2} - \frac{sin(\varphi_1)\cdot cos(\varphi_1)}{B_1^2}$
$a_{2,2} \leftarrow \frac{sin^2(\varphi_1)}{A_1^2} + \frac{cos^2(\varphi_1)}{B_1^2}$
$a_{1,3} \leftarrow \frac{-cos(\varphi_1)\cdot(h_1\cdot cos(\varphi_1)+k_1\cdot sin(\varphi_1))}{A_1^2} + \frac{sin(\varphi_1)\cdot(k_1\cdot cos(\varphi_1)-h_1\cdot sin(\varphi_1))}{B_1^2}$
$a_{2,3} \leftarrow \frac{-sin(\varphi_1)\cdot(h_1\cdot cos(\varphi_1)+k_1\cdot sin(\varphi_1))}{A_1^2} + \frac{cos(\varphi_1)\cdot(h_1\cdot sin(\varphi_1)-k_1\cdot cos(\varphi_1))}{B_1^2}$
$a_{3,3} \leftarrow \frac{(h_1\cdot cos(\varphi_1)+k_1\cdot sin(\varphi_1))^2}{A_1^2} + \frac{(h_1\cdot sin(\varphi_1)-k_1\cdot cos(\varphi_1))^2}{B_1^2} - 1$

Determine coefficients of symmetric matrix B

$b_{1,1} \leftarrow \frac{cos^2(\varphi_2)}{A_2^2} + \frac{sin^2(\varphi_2)}{B_2^2}$
$b_{1,2} \leftarrow \frac{sin(\varphi_2)\cdot cos(\varphi_2)}{A_2^2} - \frac{sin(\varphi_2)\cdot cos(\varphi_2)}{B_2^2}$
$b_{2,2} \leftarrow \frac{sin^2(\varphi_2)}{A_2^2} + \frac{cos^2(\varphi_2)}{B_2^2}$
$b_{1,3} \leftarrow \frac{-cos(\varphi_2)\cdot(h_2\cdot cos(\varphi_2)+k_2\cdot sin(\varphi_2))}{A_2^2} + \frac{sin(\varphi_2)\cdot(k_2\cdot cos(\varphi_2)-h_2\cdot sin(\varphi_2))}{B_2^2}$
$b_{2,3} \leftarrow \frac{-sin(\varphi_2)\cdot(h_2\cdot cos(\varphi_2)+k_2\cdot sin(\varphi_2))}{A_2^2} + \frac{cos(\varphi_2)\cdot(h_2\cdot sin(\varphi_2)-k_2\cdot cos(\varphi_2))}{B_2^2}$
$b_{3,3} \leftarrow \frac{(h\cdot cos(\varphi_2)+k\cdot sin(\varphi_2))^2}{A_2^2} + \frac{(h\cdot sin(\varphi_2)-k\cdot cos(\varphi_2))^2}{B_2^2} - 1$

Calculate coefficients of det($\lambda \cdot$ [A] + [B]) = $\lambda^3 + \mathbf{a} \cdot \lambda^2 + \mathbf{b} \cdot \lambda + \mathbf{c}$
Interpret coefficients of $\lambda^3 + \mathbf{a} \cdot \lambda^2 + \mathbf{b} \cdot \lambda + \mathbf{c}$ (once turned monic)

$s_4 \leftarrow -27 \cdot c^2 + 18 \cdot c \cdot a \cdot b + a^2 \cdot b^2 - 4 \cdot a^3 \cdot c - 4 \cdot b^3$
$s_1 = a, s_2 = a^2 - 3 \cdot b, s_3 = 3 \cdot a \cdot c + b \cdot a^2 - 4 \cdot b^2$
if $s_4 < 0$ **then**
  Return: Relative location 2
else if $s_4 > 0$ **then**
  if $s_1 > 0$ & $s_2 > 0$ & $s_3 \geq 0$ **then**
    $u = \frac{-a-\sqrt{s_2}}{3}$, $v = \frac{-a+\sqrt{s_2}}{3}$
    $[M] = u \cdot [A] + [B], [N] = v \cdot [A] + [B]$
    if $(m_{2,2} \cdot det(M) > 0$ & $det(M_{1,1}) > 0)$ OR $(n_{2,2} \cdot det(N) > 0$ & $det(N_{1,1}) > 0)$ **then**
      Return: Relative location 4
    else
      Return: Relative location 7
    end if
  else
    Return: Relative location 5
  end if
else
  "See next page"

if $s_2 > 0$ & $s_3 < 0$ **then**
  Return: Relative location 1
else if $s_1 > 0$ & $s_2 > 0$ & $s_3 > 0$ **then**
  $\beta = \frac{9 \cdot c - a \cdot b}{2 \cdot s_2}, \alpha = \frac{4 \cdot a \cdot b - a^3 - 9 \cdot c}{s_2}$
  $[M] = \beta \cdot [A] + [B], [N] = \alpha \cdot [A] + [B]$
  if $det(M_{3,3}) > 0$ **then**
    if $det(N_{3,3}) > 0$ **then**
      Return: Relative location 6
    else
      Return: Relative location 3
    end if
  else if $det(M_{1,1}) + det(M_{2,2}) > 0$ **then**
    Return: Relative location 4
  else
    Return: Relative location 9
  end if
else
  $\alpha = \frac{-a}{3}$
  $[M] = \alpha \cdot [A] + [B]$
  if $(det(M) = 0$ & $det(M_{3,3}) \leq 0) OR (det(M) \neq 0$ & $det(M_{3,3}) \leq 0$ & $(\frac{det(M)}{(m_{1,1} + m_{2,2})} < 0))$ **then**
    Return: Relative position 10
  else if $det(M) \neq 0$ & $det(M_{3,3}) > 0$ **then**
    Return: Relative position 8
  else
    Return: Relative position 3
  end if
end if=0

Bibliography

[1] Air Traffic Control The Netherlands. Manoeuvring area samenvatting maarten, 2018. Internal document.

[2] Air Traffic Control The Netherlands. Conops schiphol ground control, 2022. Internal document.

[3] Air Traffic Control The Netherlands. Werkboek ut spl gnd, 2023. Internal document.

[4] Air Traffic Control The Netherlands. Storyboard elearning baancombinaties, 2023. Internal document.

[5] Air Traffic Control The Netherlands. Documentation, 2024. Internal environment.

[6] Air Traffic Control The Netherlands. Gebruik start- en landingsbanen schiphol (runway use schiphol), 2024. URL https://www.lvnl.nl/omgeving/gebruik-start-en-landingsbanen-schiphol.

[7] Air Traffic Control The Netherlands (LVNL). Amsterdam/schiphol aerodrome ground movement chart - ad 2.eham-gmc.1, 2024.

[8] Australian Government. Advisory circular: Wake turbulence, 2023.

[9] J. Avery and H. Balakrishnan. Predicting airport runway configuration: A discrete-choice modeling approach. Thirteenth USA/Europe Air Traffic Management Research and Development Seminar (ATM2015), page 5, 2015.

[10] B. Benda. Agent-Based Modelling and Analysis of Non-Autonomous Airport Ground Surface Operations. TU Delft, 2020.

[11] A. Bombelli. AE4446: Airport and Cargo Operations - Airside. TU Delft, 2023.

[12] K.A. Brookhuis, C.J.G. van Driel, T. Hof, B. van Arem, and M. Hoedemaeker. Driving with a congestion assistant; mental workload and acceptance. Applied Ergonomics, 40(6):1019–1025, 2008. DOI: 10.1016/j.apergo.2008.06.010.

[13] M. Brouwer, E. van Calck, J. Knoester, T. Joustra, N. Schmidt, and S. Heblij. Baan beschikbaarheid strategie 2015, 2016. Internal document.

[14] S. Brunia. Task load estimation for atc ground control: A dynamic density-based analysis (master of science thesis). TU Delft, 2023.

[15] L. Cohen, T. Uras, T.K.S. Kumar, and S. Koenig. Optimal and bounded-suboptimal multi-agent motion planning. Proceedings of the Twelfth International Symposium on Combinatorial Search (SoCS 2019), pages 44–51, 2019. DOI: https://doi.org/10.1609/socs.v10i1.18501.

[16] R. Curran, K. Dinh, P. Roling, and E. van Calck. Simulation of airport taxiway flows for maintenance planning using value operations methodology. 12th AIAA Aviation Technology, Integration, and Operations (ATIO) Conference and 14th AIAA/ISSMO Multidisciplinary Analysis and Optimization Conference Online Proceedings, pages 1–18, 2012. ISBN = 978-1-60086-930-3.

[17] A. de Leege and C. Janssen. Probabilistic runway and capacity forecasting using machine learning to support decision making. 6th SESAR Innovation Days, 2016.

[18] R. de Neufville and A.R. Odoni. Airport Systems: Planning, Design, and Management. McGraw-Hill Education, United States of America, 2nd ed. edition, 2013.

[19] D. de Waard. The measurement of drivers' mental workload. 1996. Thesis, University of Groningen.

[20] Eurocontrol. The manual: Airport cdm implementation, 2017.

[21] K. Fines. Decentralized control for resilient airport surface movement operations: Literature study, 2018.

[22] A. Goyal, P. Mogha, R. Luthra, and N. Sangwan. Path finding: A* or dijkstra's? IJITE, 2(1), 2014.

[23] Royal Schiphol Group. Noise and runway combinations: Path to reduced noise nuisance, 2024. URL https://www.schiphol.nl/en/schiphol-as-a-neighbour/page/noise-and-runway-combinations/.

[24] P.E. Hart, N.J. Nilsson, and B. Raphael. A formal basis for the heuristic determination of minimum cost paths. IEEE TRANSACTIONS OF SYSTEMS SCIENCE AND CYBERNETICS, 4(2):100–107, 1998. DOI: https://doi-org.tudelft.idm.oclc.org/10.1109/TSSC.1968.300136.

[25] S.G. Hart and L.E. Staveland. Development of nasa-tlx (task load index): Results of empirical and theoretical research. Advances in Psychology, 52:139–183, 1988. DOI: https://doi.org/10.1016/S0166-4115(08)62386-9.

[26] G.B. Hughes and M. Chraibi. Calculating ellipse overlap areas. Computing and Visualization in Science, 15(5):291–301, 2012. DOI: 10.1007/s00791-013-0214-3.

[27] W. Hönig, S. Kiesel, A. Tinka, J.W. Durham, and N. Ayanian. Persistent and robust execution of mapf schedules in warehouses. IEEE ROBOTICS AND AUTOMATION LETTERS, 4(2):1125–1131, 2019. DOI: 10.1109/LRA.2019.2894217.

[28] International Civil Aviation Organization. Amofsg/10-sn no. 14: Aerodrome meteorological observation and forecast study group (amofsg), 2024. URL https://www.icao.int/safety/meteorology/amofsg/AMOFSG%20Meeting%20Material/AMOFSG.10.SN.014.5.en.pdf.

[29] Y. Jiang, Z. Liao, and H. Zhang. A collaborative optimization model for ground taxi based on aircraft priority. Mathematical Problems in Engineering, 2013:3, 2013. Article ID 854364.

[30] J.G. Kamphof. Design and analysis of tug-enabled engine-off taxiing operation using hierarchical multi-agent planning (master of science thesis). TU Delft, 2022.

[31] S. Koenig. Multi-Agent Path Finding. USC Viterbi: School of Engineering, 2017.

[32] Koninklijk Nederlands Meteorologisch Weer. Windrozen van de nederlandse hoofdstations, 2024. URL https://www.knmi.nl/nederland-nu/klimatologie/grafieken/maand/windrozen.

[33] R.H. Mogford, J.A. Guttman, S.L. Morrow, and P. Kopardekar. The complexity construct in air traffic control: A review and synthesis of the literature. CTA INCORPORATE, 1995. Report no.: DOT/FAA/CT-TN9S/22.

[34] F. Mooren, A. Dubero, and R. Brans. Benchmark workshop: Maintenance and rehabilitation strategies of taxiway systems, 2022. Internal document.

[35] F.P. Moreno. Dynamic methodology for atc sector characterisation through predictions based on machine learning techniques. UNIVERSIDAD POLITÉCNICA DE MADRID, 2023.

[36] R. Morris, C.S. Pasareanu, K. Luckow, W. Malik, H. Ma, T.K. Satish Kumar, and S. Koenig. Planning, scheduling and monitoring for airport surface operations. The Workshops of the Thirtieth AAAI Conference on Artificial Intelligence, pages 608–614, 2016.

[37] MovingDot. Functional analysis of schiphol twr-c. Knowledge and Development Centre Mainport Schiphol, 2017.

[38] MovingDot. Verkenning operationele impact onderhoud rijbanen schiphol: Begeleidende documentatie, 2021.

[39] T.E.H. Noortman. Agent-based modelling of airport's ground surface movement: Literaturestudy, 2018.

[40] M. Phillips and M. Likhachev. Sipp: Safe interval path planning for dynamic environments. Proceedings - IEEE International Conference on Robotics and Automation, page 5628–5635, 2011. DOI: 10.1109/ICRA.2011.5980306.

[41] M.A. Recarte and L.M. Nunes. Mental workload while driving: Effects on visual search, discrimination, and decision making. Journal of Experimental Psychology, 9(2):119–137, 2003. DOI: 10.1037/1076-898X.9.2.119.

[42] W. Rouse, J.M. Hammer, and S.L. Edwards. Modeling the dynamics of mental workload and human performance in complex systems. IEEE Transactions on Systems Man and Cybernetics, pages 1–27, 1993. DOI: 10.1109/21.257761.

[43] Royal Schiphol Group. Chronologie bos.

[44] Royal Schiphol Group. Baanonderhoudsstrategie 2017: Vervolgonderzoek fase 1 - resultaten kwantitatieve analyse -, 2018. Internal document.

[45] Royal Schiphol Group. Aircraft type table, 2019.

[46] Royal Schiphol Group. Baanonderhoudsstrategie 2019: Vervolgonderzoek fase 2 - implementatiestrategie -, 2019. Internal document.

[47] Royal Schiphol Group. Cobra complan mjop goh rijbaan a a13-a15 fase 5: Ova 35753, 2021. Internal document.

[48] Royal Schiphol Group. Traffic review 2023, 2023.

[49] Royal Schiphol Group. Aircraft stand table, 2023.

[50] Royal Schiphol Group. Kwartaalmonitor nnhs q2, 2023.

[51] Royal Schiphol Group. A-cdm manual schiphol airport, 2024.

[52] Royal Schiphol Group. Asas, 2024.

[53] W. Sardjono. Study of runway crosswind and tailwind potential for airport sustainability: A study of soekarno hatta airport, cengkareng, indonesia. IOP Conference Series: Earth and Environmental Science, page 3, 2020.

[54] C.E. Schot. Schiphol: Gebruiksprognose 2024, 2024.

[55] A. Sharpanskykh. Agent-based Modelling and Simulation in Air Transport. TU Delft, 2022.

[56] R. Stern, N.R. Sturtevant, A. Felner, S. Koenig, H. Ma, T.T. Walker, J. Li, D. Atzom, L. Cohen, T.K.S. Kumar, E. Boyarski, and R. Barták. Multi-agent pathfinding: Definitions, variants, and benchmarks. Proceedings of the Symposium on Combinatorial Search (SoCS), 2019.

[57] J. The. Optimizing ground movements considering taxiway renovation, 2020.

[58] S. van Oosterom, M. Mitici, and J. Hoekstra. Dispatching a fleet of electric towing vehicles for aircraft taxiing with conflict avoidance and efficient battery charging. Transportation Research Part C, 147:1–21, 2023. DOI: https://doi.org/10.1016/j.trc.2022.103995.

[59] M. von der Burg and A. Sharpanskykh. Multi-agent planning for autonomous airport surface movement operations: Explorative case study at amsterdam airport schiphol. SESAR, pages 1–9, 2023.

[60] M. von der Burg, J. Kamphof, J. Soomers, and A. Sharpanskykh. Towards autonomous airport surface movement operations using hierarchical multi-agent planning, 2024. Available at SSRN: https://ssrn.com/abstract=4916874.

[61] E.S. Wilschut. The impact of in-vehicle information systems on simulated driving performance: Effects of age, timing and display characteristics. 2009. Thesis, University of Groningen.

[62] D. Yuan, X. Zhu, Y. Zou, and Q. Zhao. Integrated optimization of scheduling for unmanned follow-me cars on airport surface. Scientific Reports, pages 1–23, 2024. DOI: https://doi.org/10.1038/s41598-024-58918-7.